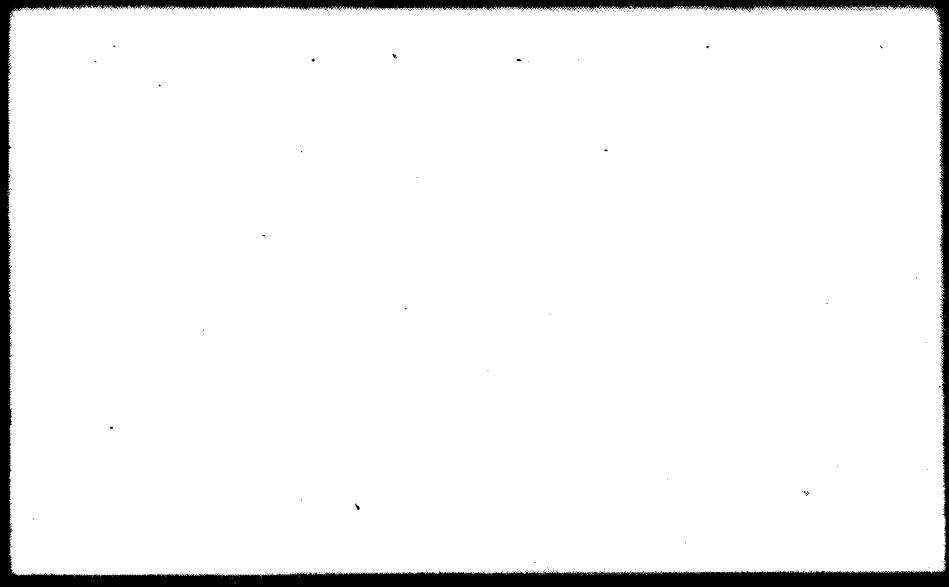

FINAL REPORT

NAG2-146

~~NAS2-6658~~

AMES GRANT 7N-91-CR 183411

PIONEER F/G DATA ANALYSIS OF THE ULTRAVIOLET EXPERIMENT

(1971 - 1981)

1630

Submitted by

Darrell L. Judge - Principal Investigator
Space Sciences Center and Department of Physics
University Park
Los Angeles, California 90089-1341

VOLUME I

FINAL REPORT

NAS2-6658

PIONEER F/G DATA ANALYSIS OF THE ULTRAVIOLET EXPERIMENT

(1971 - 1981)

Submitted by

Darrell L. Judge - Principal Investigator
Space Sciences Center and Department of Physics
University of Southern California
University Park
Los Angeles, California 90089-1341

Robert W. Carlson - Co-Principal Investigator
Earth and Space Science Division
Jet Propulsion Laboratory
California Institute of Technology
4800 Oak Grove Drive
Pasadena, California 91109

Current Co-Investigators:

Joseph A. Kunc
Fun-Min Wu*
Space Sciences Center
University of Southern California
University Park
Los Angeles, California 90089-1341

Sponsoring Agency Official:

Beverly Robertson
Administrator
Department of Contracts and Grants
Stonier Hall, Room 325
University of Southern California
University Park
Los Angeles, California 90089-1141

* Also at
TECOS Computing, Inc.
1800 Broadview Drive
Glendale, California 91208

FOREWORD

The following final report is in response to NASA correspondence AC: 241-25 requesting same for the Pioneer 10/11 Ultraviolet Experiment through termination of the contract phase (1971 - 1981).

In this report, we have included an overview of the mission objectives in the introduction, a description of the instrumentation, and in the main body, we have included all significant papers, abstracts, and internal reports produced in the course of this contract. This report is thus intended to be a complete reference to the Pioneer 10/11 Experiment from its inception through 1981.

CONTENTS

VOLUME I FINAL REPORT

1.0 INTRODUCTION

This volume presents a detailed description of the Pioneer 10/11 Extreme Ultraviolet (XUV) Filter Photometer Experiment, which is also referred to as the USC/XUV Filter Photometer. The following section (Section 2) briefly describes the scientific objectives, and then discusses the overall instrument from a functional aspect and provides all of the technical details required to understand the operation of the instrument and to perform routine troubleshooting. Detailed circuit descriptions are given in Section 3. This section also includes a description of the data output format and procedures for data reconstruction. The mechanical characteristics are discussed in Section 4, and Section 5 is devoted to the ground-support equipment. Troubleshooting procedures are defined in Section 6. Section 7 outlines the current scientific objectives and Section 8 includes the hardware description of the instrument from the subcontractor.

Volume II contains all of the scientific reports that have been published or have been submitted for publication from 1974 to 1981.

2.0 EXPERIMENT DESCRIPTION

2.1 SCIENTIFIC OBJECTIVES AND BACKGROUND

The Pioneer 10/11 missions to Jupiter and beyond have presented exceptional opportunities for unique studies of the solar system and its interstellar environment. In particular, the Pioneer trajectories (Fig. 2-1) have allowed ultraviolet measurements of Jupiter, Saturn, their environments, and the interplanetary medium to be performed, which in turn have been used to study the hydrogen and helium content of these planets, their environment, the interplanetary gas, and the galaxy, thereby gaining fundamental data concerning the origin and evolution of the planets and solar system.

Hydrogen and helium are the two most abundant elements in the universe and are of great astrophysical importance. Unfortunately, these elements are often difficult to detect from ground-based astronomical observatories since their optical features are either weak or occur in the vacuum ultraviolet region of the spectrum -- a spectral region for which the atmosphere is quite opaque. Therefore, very little was known concerning the hydrogen and helium content of the interplanetary and interstellar gas or of the content of the atmospheres of the outer planets. The detection of these elements by measurement of their ultraviolet emissions during the cruise and encounter phases was one of the goals of the Pioneer 10/11 missions.

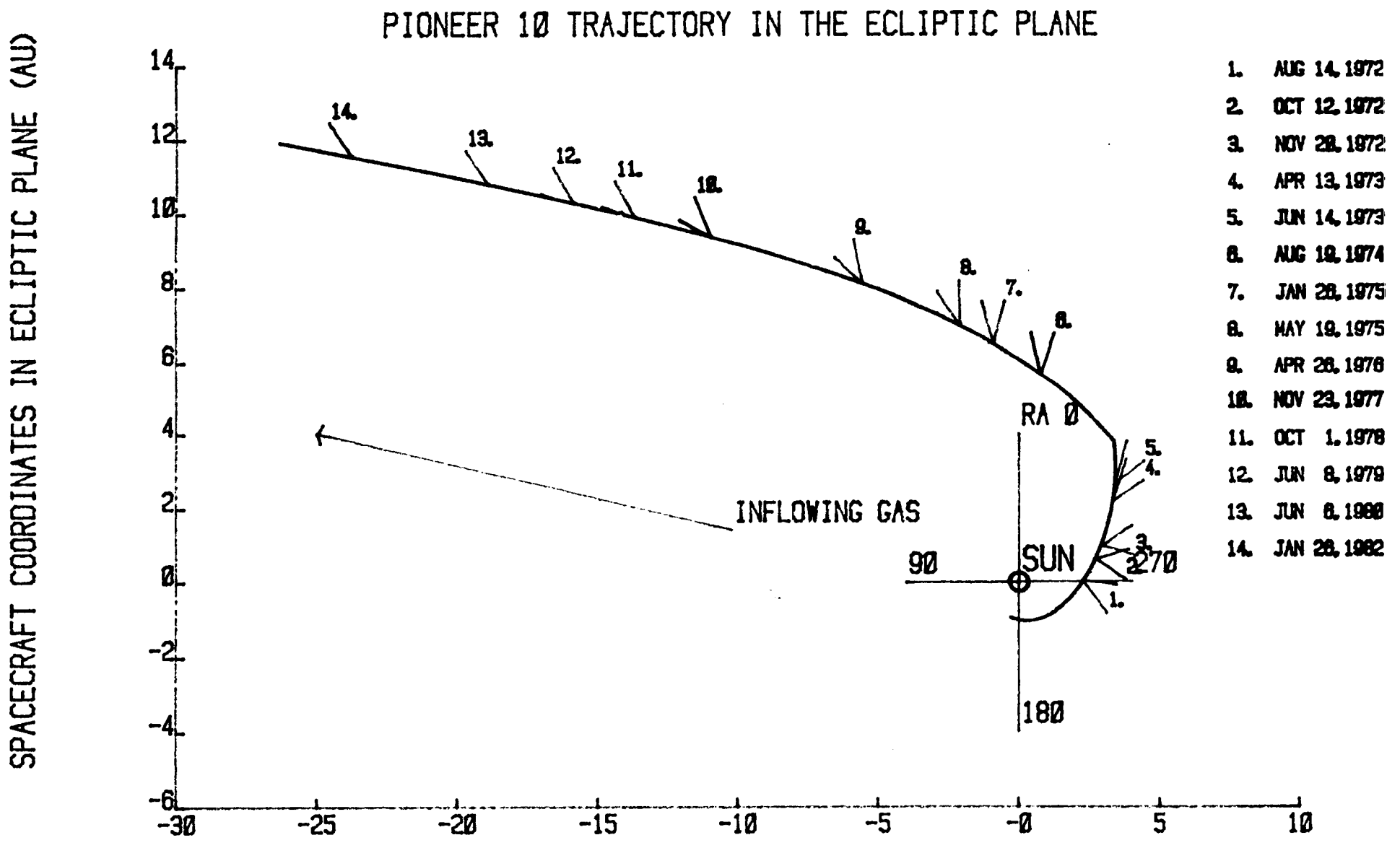

Figure 2-1 SPACECRAFT COORDINATES IN ECLIPTIC PLANE (AU)

2.0 EXPERIMENT DESCRIPTION

2.1 SCIENTIFIC OBJECTIVES AND BACKGROUND

The Pioneer 10/11 missions to Jupiter and beyond have presented exceptional opportunities for unique studies of the solar system and its interstellar environment. In particular, the Pioneer trajectories (Fig. 2-1) have allowed ultraviolet measurements of Jupiter, Saturn, their environments, and the interplanetary medium to be performed, which in turn have been used to study the hydrogen and helium content of these planets, their environment, the interplanetary gas, and the galaxy, thereby gaining fundamental data concerning the origin and evolution of the planets and solar system.

Hydrogen and helium are the two most abundant elements in the universe and are of great astrophysical importance. Unfortunately, these elements are often difficult to detect from ground-based astronomical observatories since their optical features are either weak or occur in the vacuum ultraviolet region of the spectrum -- a spectral region for which the atmosphere is quite opaque. Therefore, very little was known concerning the hydrogen and helium content of the interplanetary and interstellar gas or of the content of the atmospheres of the outer planets. The detection of these elements by measurement of their ultraviolet emissions during the cruise and encounter phases was one of the goals of the Pioneer 10/11 missions.

between the solar wind and the interstellar medium, at which point the solar wind pressure and interstellar pressures are balanced. The hot solar wind plasma is contained in this transition region for some time. This plasma, consisting largely of fast protons and electrons, eventually interacts with the inflowing cold neutral interstellar gas. One reaction that occurs is charge exchange between a fast proton and a cold hydrogen atom, producing slow protons and fast hydrogen atoms. These fast neutral hydrogen atoms can penetrate deeply into the solar system before being lost by photoionization, thereby producing an appreciable hydrogen atom density in the solar system.

This interplanetary hydrogen can be detected by observing the ultraviolet radiation which is resonantly scattered by the atoms. The sun is a bright source of the hydrogen Lyman-α line, the resonance line of hydrogen. This line is strongly scattered by hydrogen atoms and will result in a diffuse interplanetary ultraviolet glow.

The measurement of this radiation then, and in particular the intensity and radial dependence, can be used to investigate the interplanetary hydrogen atom density and thus the characteristics of the interaction of the solar wind and the interstellar medium. Indeed, one may be able to determine the heliocentric distance of the transition zone and its approximate shape and thereby investigate the fate of the solar wind as it leaves the solar system.

The hydrogen Lyman-α signal that is being observed during the cruise phase of the Pioneer 10/11 missions consists of two components: (1) the interplanetary component which has been discussed above and (2) an interstellar or galactic component. By obtaining measurements as a function of heliocentric radius in the outer solar system, one can separate these two components. Such a differentiation has not been possible previously because there have been no ultraviolet measurements obtained beyond approximately the orbit of Mars except for those of voyagers I and II.

A diffuse galactic Lyman-α glow occurs because of the multitude of stars which emit radiation at the wavelength of the hydrogen line. This radiation will be scattered by the interstellar hydrogen atoms, producing the galactic component of the Lyman-α glow. Although some of this radiation can escape the galaxy, there are so many interstellar hydrogen atoms that many scatterings take place before escape. This multiple scattering is important in two aspects. First, it increases the glow that would be observed inside the galaxy, and second, it enhances the chance of absorption by dust particles. Indeed, a major factor in the loss of the Lyman-α photon is through this absorption by interstellar dust. Therefore, a mapping of the galactic hydrogen Lyman-α glow can be used to infer such characteristics as the hydrogen atom and particulate matter densities in the nearby regions of the galaxy.

It was previously noted that the cold interstellar hydrogen gas cannot penetrate deeply into the solar system owing to the photoionization of the solar ultraviolet. The situation for helium atoms is far more favorable, however, because the energy required for photoionization of helium is much greater than that of hydrogen. Thus, interstellar helium atoms are swept up by the motion of the solar system and its gravitational attraction, with these helium atoms penetrating deep into the solar system, producing detectable quantities of interplanetary helium. As for the case of hydrogen, the helium atoms will produce an ultraviolet glow by resonance scattering of the solar He I resonance line.

The abundance of helium plays an important role in cosmological considerations. For example, in the "big-bang" theory of the formation of the universe, general relativity predicts about 7 percent (by volume) of helium for an isotropic and homogenous universe. On the other hand, the Brans-Dicke scalar tensor theory of gravitation would indicate a different relative amount of helium. At the present time, astrophysical measurements of the helium abundance are not conclusive; indeed, even the object most extensively studied, the sun, provides widely varying estimates for the helium abundance. The Pioneer 10/11 UV photometer experiment is designed to measure helium due to the nearby interstellar gas -- the gas from which the sun was formed -- thus providing data for our general understanding of the universe.

2.1.2 ENCOUNTER WITH JUPITER AND SATURN OBJECTIVES

The encounter of Jupiter, Saturn, and certain of their satellites by the Pioneer 10/11 spacecraft have presented opportunities for ultraviolet measurements of the atmospheres and environments of these outer planets. The UV photometer has viewed the discs of these planets for several hours during the encounter phases; the field of view of the instrument and the roll motion of the spacecraft results in a scanning motion across the disc of the planets. The planetary information obtained during these phases consists of measurements of the intensity of the Jovian and Saturnian ultraviolet dayglow with some spatial resolution across the discs of the planets. These data relate to two classes of scientific objectives for the Jovian and Saturnian atmospheres and environments: (1) the hydrogen and helium content of the atmosphere of Jupiter, and (2) localized excitation processes such as aurora and atmospheric excitations in the satellite atmosphere. These aspects are briefly discussed below.

The satellite observations were not primary objectives and are not discussed here but the results to date are included in volume II.

2.1.3 THE HYDROGEN/HELIUM CONTENT OF THE ATMOSPHERE OF JUPITER AND SATURN

The evolution of the planets and their atmospheres is quite different for the terrestial planets (Mercury, Earth, Venus, and Mars) and the major planets (Jupiter, Saturn, Uranus and Neptune). For the former class of planets, the primordial atmosphere which was formed near the time of formation of the planet has long since been lost, since the relatively small gravitational attraction of these planets could not retain these high temperature light gases. The present atmospheres of these planets was formed at a later time through the slow outgassing from the surface and through volcanic action. Such is not the case for the outer planets. Because these bodies are so massive and/or the temperature so low, the original atmospheres were retained and the present atmospheres of these planets is probably characteristic of the early stages of planetary evolution. Measurements of the atmosphere of Jupiter and Saturn then offers an opportunity to study the earlier history of the solar system and to gain information relating to the formation of the outer planets and the solar system. For example, one theory of the formation of the planet Jupiter suggests that the bulk of the planet was formed through hydrogen "snowing", with the subsequent accretion of a predominantly helium atmosphere. Other ideas suggest that the planets of our solar system were formed from larger

protoplanets and would possess a helium abundance similar to the solar abundance. Thus, the observation of helium in the atmospheres of Jupiter and Saturn is of considerable interest.

As we have noted, the measurement of helium is impossible from ground-based telescopes because of extinction by the earth's atmosphere. The presence of helium can be detected by the Pioneer 10/11 UV photometer by detecting the helium resonance radiation emitted in the upper atmospheres of the outer planets. This helium airglow is produced by the resonance scattering of the solar He I 584 A resonance line by those He atoms in the planetary atmospheres. Such measurements have provided the first positive indication of helium in the Jovian and Saturnian atmospheres.

Later in this section a discussion will be presented which shows how the amount of helium in the Jovian atmosphere, relative to the molecular hydrogen content, can be obtained from the Pioneer UV photometer measurements. We first discuss the measurements to be obtained with the hydrogen channel.

Most of the hydrogen in the Jovian atmosphere is in the molecular form, H_2. A fraction of this is dissociated into atomic hydrogen atoms by the action of the solar ultraviolet flux and photochemical reactions.

Theoretical calculations have shown that the rate of production is nearly independent of the relative amounts of

H_2 and He. The total amount of atomic hydrogen in the atmosphere depends upon the rate of formation and also upon the rate of recombination of H atoms back to H_2. The formation of atomic hydrogen occurs high in the Jovian atmosphere, whereas the reassociation into H_2 molecules occurs by three-body reactions in the lower regions. The rate of reforming molecules from the dissociated atoms depends upon how fast these atoms can diffuse to the lower levels. To a large extent this diffusion occurs by eddy diffusion, that is turbulant motion in the atmosphere. An observation of the hydrogen Lyman-α airglow then gives a measure of the strength of this diffusion process, or more precisely, the eddy diffusion coefficient.

Having obtained the eddy diffusion coefficient from atomic hydrogen ultraviolet emission measurements, one has information about the structure of the atmosphere. In the lower regions, where eddy diffusion occurs, there is a strong mixing of the gases and no separation of the varoius constituents. At some altitude, however, molecular diffusion becomes the more dominant process and the gas is no longer uniform; rather each constituent has a different altitude distribution depending upon its molecular mass. The transition between these lower and upper regions is determined by the strength of eddy diffusion, and this level -- the turbopause -- can therefore be estimated from the Lyman-α measurements.

The helium airglow measurements have been used to

determine the relative amounts of H_2 and He in the lower atmospheres of the outer planets. It is a measure of the ratio of He relative to H_2 because, while He scatters the radiation, molecular hydrogen absorbs this radiation through photoionization. Knowing the relative amounts in the upper atmosphere, and knowing the level of the turbopause, one can extrapolate down to the lower atmosphere to find the He/H_2 ratio in this region.

2.2 FUNCTIONAL DESCRIPTION OF THE XUV PHOTOMETER

The weight, power, and reliability constraints necessitated the choice of a simple photometric system for the ultraviolet measurements. The Pioneer 10 ultraviolet experiment is a two channel photometer which uses the transmission properties and photoelectric response of materials to measure intensities in two spectral regions. A schematic diagram of the instrument is shown in Figure 2-2. The field of view is defined by a mechanical collimator. Radiation transmitted through the collimator is incident upon a thin film filter through which short wavelength photons are transmitted. These photons strike a photocathode, producing photoelectrons which are accelerated through a 180 Volt potential into the input cone of a channel electron multiplier. The front surface of the filter is used as a photocathode with a second electron multiplier to detect the longer wavelength Lyman-α photons.

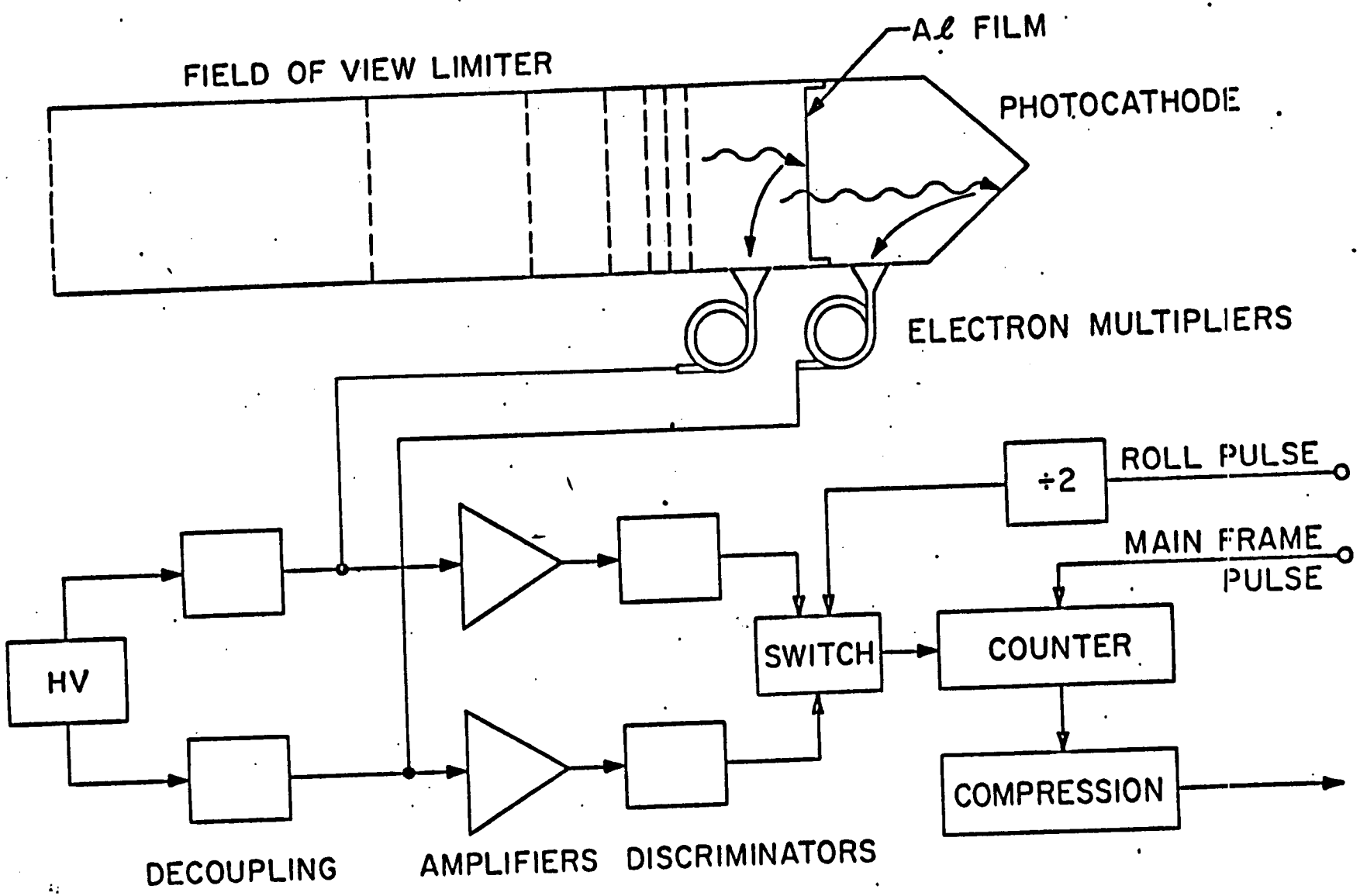
Aℓ FILM
FIELD OF VIEW LIMITER
PHOTOCATHODE
ELECTRON MULTIPLIERS
÷2
ROLL PULSE
MAIN FRAME
PULSE
HV
SWITCH
COUNTER
COMPRESSION
DECOUPLING
AMPLIFIERS
DISCRIMINATORS

Figure 2 - 2

The pulses of charge appearing at the anodes are amplified with charge sensitive amplifiers and passed to a discriminator. An electronic switch commutates between the two channels every two rolls of the spacecraft, i.e., approximately every 25 sec. The pulses are accumulated over the frame period of the spacecraft telemetry system (3/8 sec at Jupiter encounter). The accumulated counts are logarithmically compressed to 9 bits and sampled by the telemetry system for transmission.

A cover was placed over the entrance aperture to insure against dust particles entering the instrument and to protect the thin film filter from escaping air currents during launch. The cover is deployed 6 days after launch.

The instrument weighs 1.5 lb. (680 gm) and consumes 0.67 watts. The angular response characteristics, spectral response, and aspects of the electron multipliers are discussed below.

2.2.1 ANGULAR RESPONSE

The field of view of the photometer is determined by a mechanical collimator of the McGrath type. The optical axis of the collimator is oriented at an angle θ_o to the spacecraft spin axis (Figure 2-3), resulting in a scanning motion as the spacecraft rotates. The design value of θ_o is 20° while from stellar observations the actual value was found to be $\theta_o = 20.25° \pm 0.10°$.

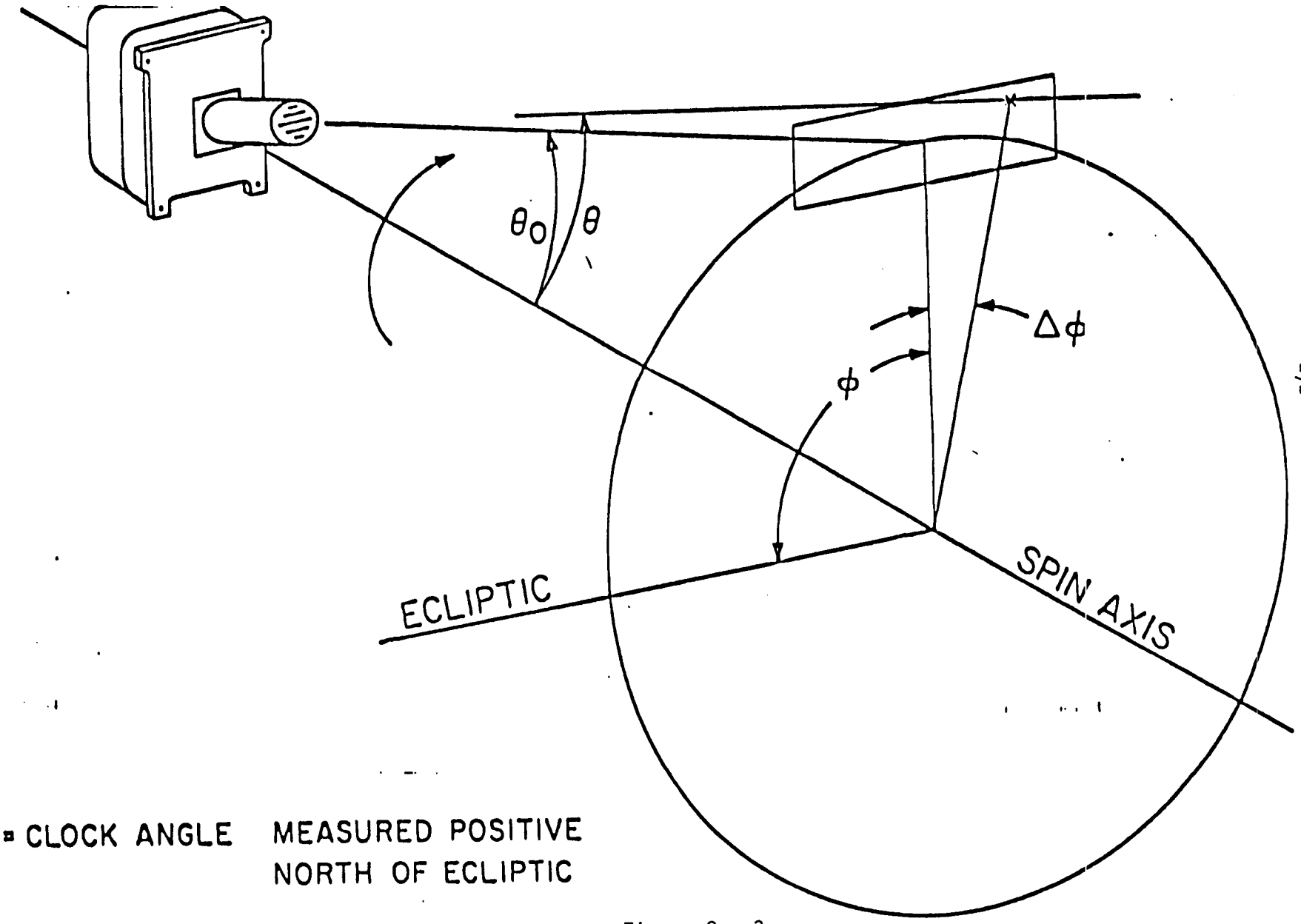

ϕ = CLOCK ANGLE MEASURED POSITIVE NORTH OF ECLIPTIC

θ = CONE ANGLE FIXED AT ~20°

Figure 2 - 3

The collimator consists of a series of seven plates arranged in the spacing suggested by McGrath (1967) and with an overall length of 10.16 cm. Each plate contains five rectangular apertures with width of 0.203 cm; the lengths (and corresponding number of baffles) are 1.92 (1),1.76 (2), and 1.36 (2) cm. The long dimension of the baffles are oriented tangentially to the cone swept out by the spacecraft revolution. The entrance area of the collimator is a = 1.66 cm^2 and the effective solid angle of acceptance $\Omega = 3.28 \times 10^{-3}$ sterad, resulting in a geometric factor of 433 photons/sec-Rayleigh for a uniform diffuse source. The angular response for a point source at angles (θ, $\Delta\psi$) as defined in Figure 2-3 is shown in Figure 2-4. The angular resolution is $\Delta\theta$ - 1°.

The response of the instrument to a finite extended source such as Jupiter is obtained by integrating over the field of the object. In addition, one must include the finite integration time and the angular velocity of the spacecraft rotation.

The plates of the collimator were coated with platinum black to reduce internal reflections. Measurements of the off-axis response in the near ultraviolet showed rejections of approximately 10^4 for $|\Delta\theta| = 5°$ and approximately 10^5 for $|\Delta\theta| > 10°$. It is expected that the off-axis rejection is even greater in the extreme ultraviolet.

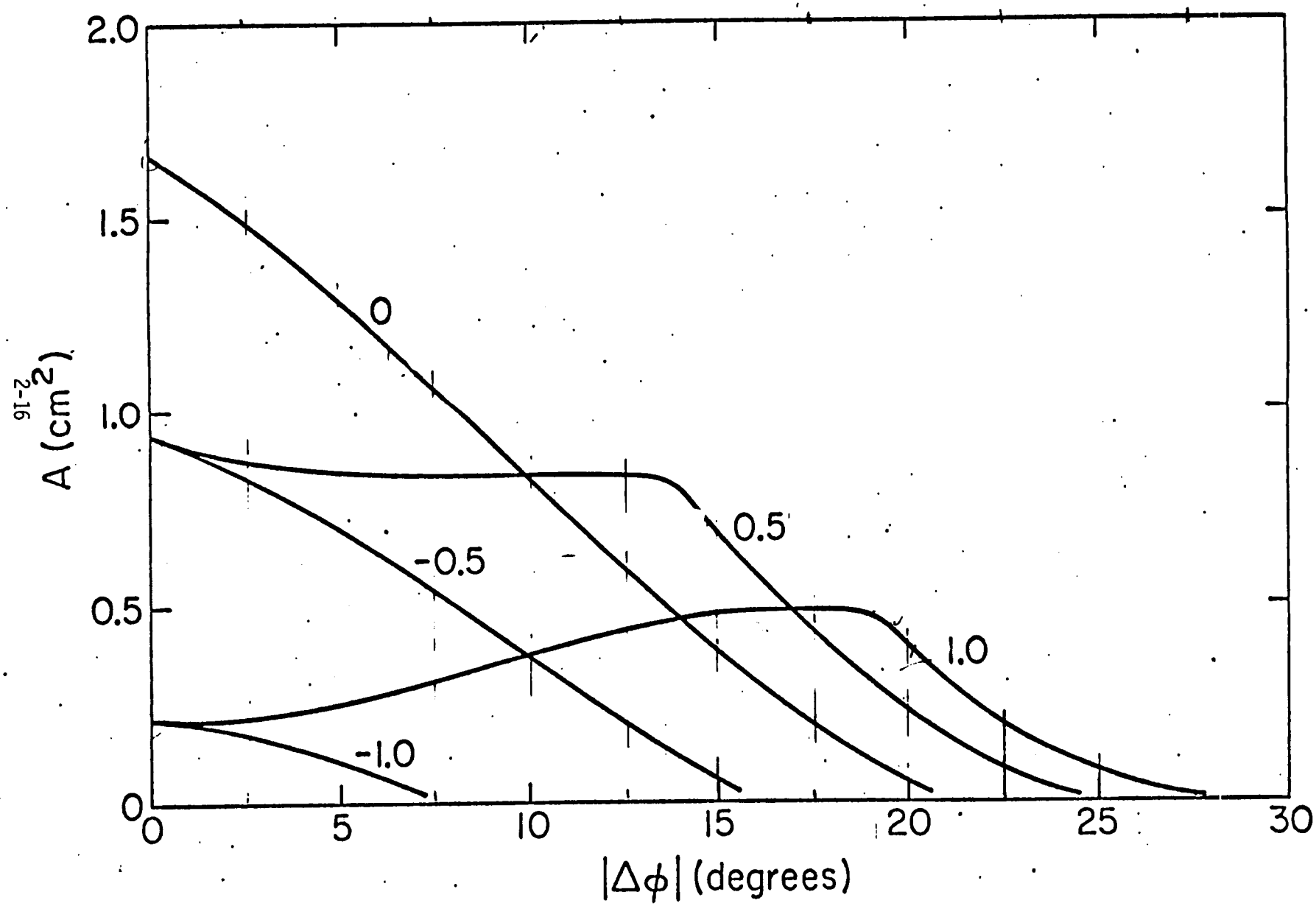

Figure 2 - 4

2.2.2 SPECTRAL RESPONSE

Since the hydrogen and helium resonance lines at λ 1216 Å and λ 584 Å respectively are expected to be the dominant features in the interplanetary and Jovian emission spectrum, only broadband isolation of these features is required. As the hydrogen intensity is much greater than the helium line, it is necessary to effectively discriminate against it in the He channel. The present photometer uses an Al thin film filter approximately 1500 Å thick coated on both sides with 100 Å, of SiO and a LiF coated photocathode to accomplish this function. The transmission properties of aluminum have been studied by Hunter et al. (1965) and others. Laboratory experience has shown it to be one of the most stable and shock resistant of the metallic filters used in the extreme ultraviolet. The photocathode material was chosen because of its large photoelectric yield at 584 Å and the relative insensitivity to H Lyman-α radiation (Samson, 1967; Bryam et al., 1961).

The spectral response of the instrument was measured relative to the response of sodium salicylate, for which the yield has been found to be constant in the spectral region of interest (Samson, 1967). The measurements were placed on an absolute scale using a rare gas double ionization chamber. The resulting efficiency as a function of wavelength is shown in Figure 2-5. For a uniform diffuse source which fills the field of view, the sensitivity of the

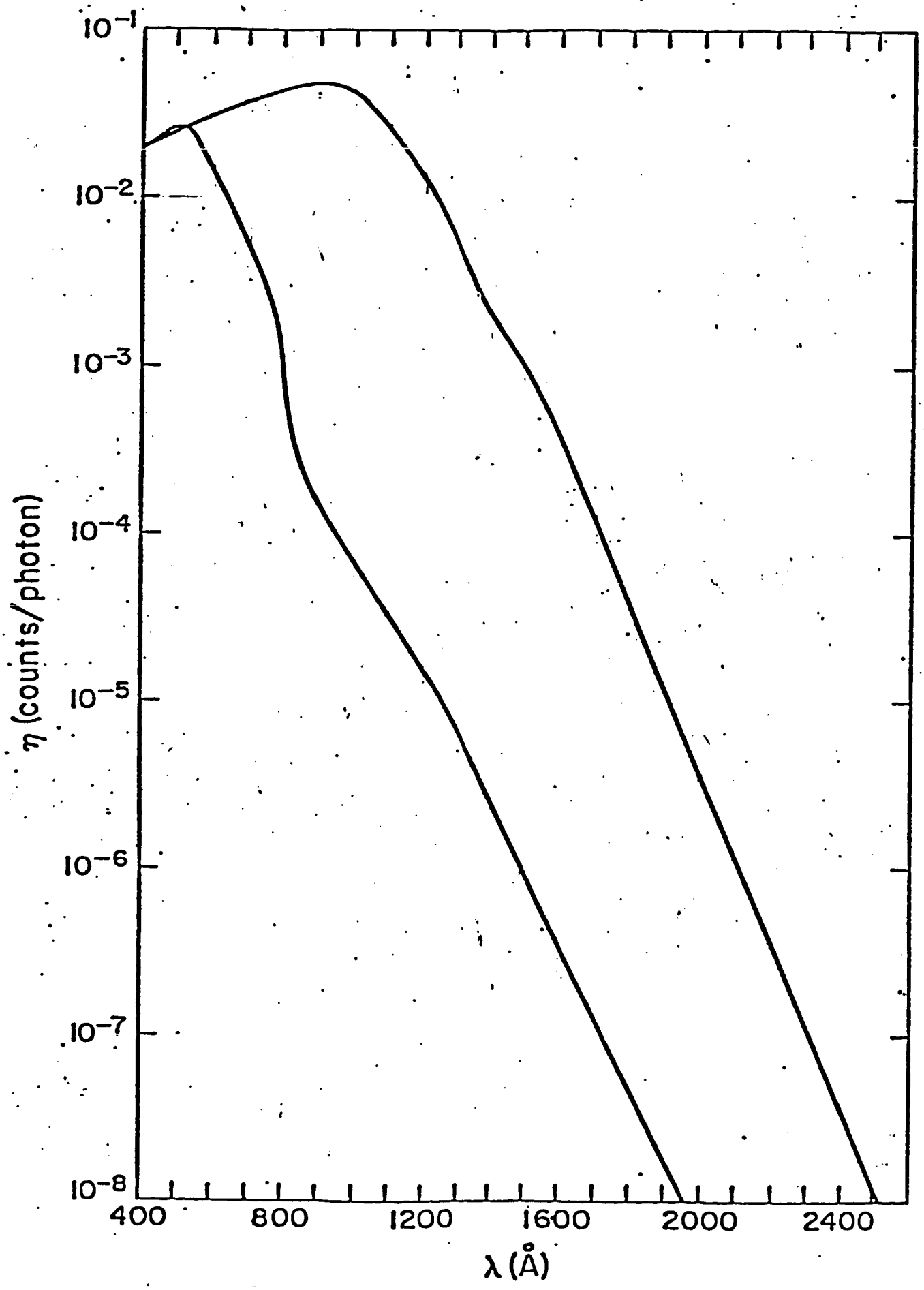
10^{-1}
10^{-2}
10^{-3}
10^{-4}
10^{-5}
10^{-6}
10^{-7}
10^{-8}
η (counts/photon)
400
800
1200
1600
2000
2400
λ (Å)

Figure 2 - 5

short wavelength channel at λ 584 A is 7.3 counts/sec-Rayleigh and 4.9 counts/sec-Rayleigh at 1216 A. This channel is also sensitive to shorter wavelength radiation but these emissions are much weaker than the H Lyman-α signal and their contribution to the long wavelength channel can be ignored.

The sensitivity of the helium channel to Lyman-α was found to be a factor of 1000 less than that of the hydrogen channel. This residual sensitivity is greater than would be expected on the bases of film transmissions and photoelectric response measurements and is due to photoelectrons liberated from the back surface of the filter.

Particular care was taken to extend the calibration to long wavelengths in order to evaluate the contribution from Rayleigh scattered radiation from the atmosphere of Jupiter. Using the albedo of Anderson et al. (1969), this contribution is found to be small, of the order of 10 counts/sec.

2.2.3 ELECTRON MULTIPLIERS AND ASSOCIATED CIRCUITRY

The electron multipliers used in the experiment are Bendix Model 4028 continuous channel multipliers and are operated with an anode to cathode voltage of 3500 volts. This results in gains of approximately 5×10^7 and places the multipliers in the gain saturation mode. The pulses

appearing at the anode are amplified with charge sensitive amplifiers followed by fixed dead-time (3 μsec) discriminators. The dynamic range of the amplifier-discriminator combination is 1000:1. The upper level is set at 10 times the nominal multiplier output to allow for any individual gain variations while the lower limit, a factor of 100 less than the nominal output, is designed to allow for any gain degradation of the multipliers during the course of the mission.

This degradation of channel multipliers with use has been of some concern. Studies in this laboratory and elsewhere have shown that if the units are properly screened before selection, then the channel multipliers can be operated to at least 2×10^{12} total accumulated counts with no serious indication of fatigue. The accumulated counts in the present instrument is 1.5×10^{11} for the hydrogen channel and much less for the other channel.

The dark counting rate for the two channels is approximately 3 counts/sec and is due to radiation from the radio-thermal isotope generators on the spacecraft.

Photographs of the XUV Filter Photometer are shown in Figure 2-6; its primary specifications are listed in Table I. A functional block diagram of the instrument is presented in Figure 2-7.

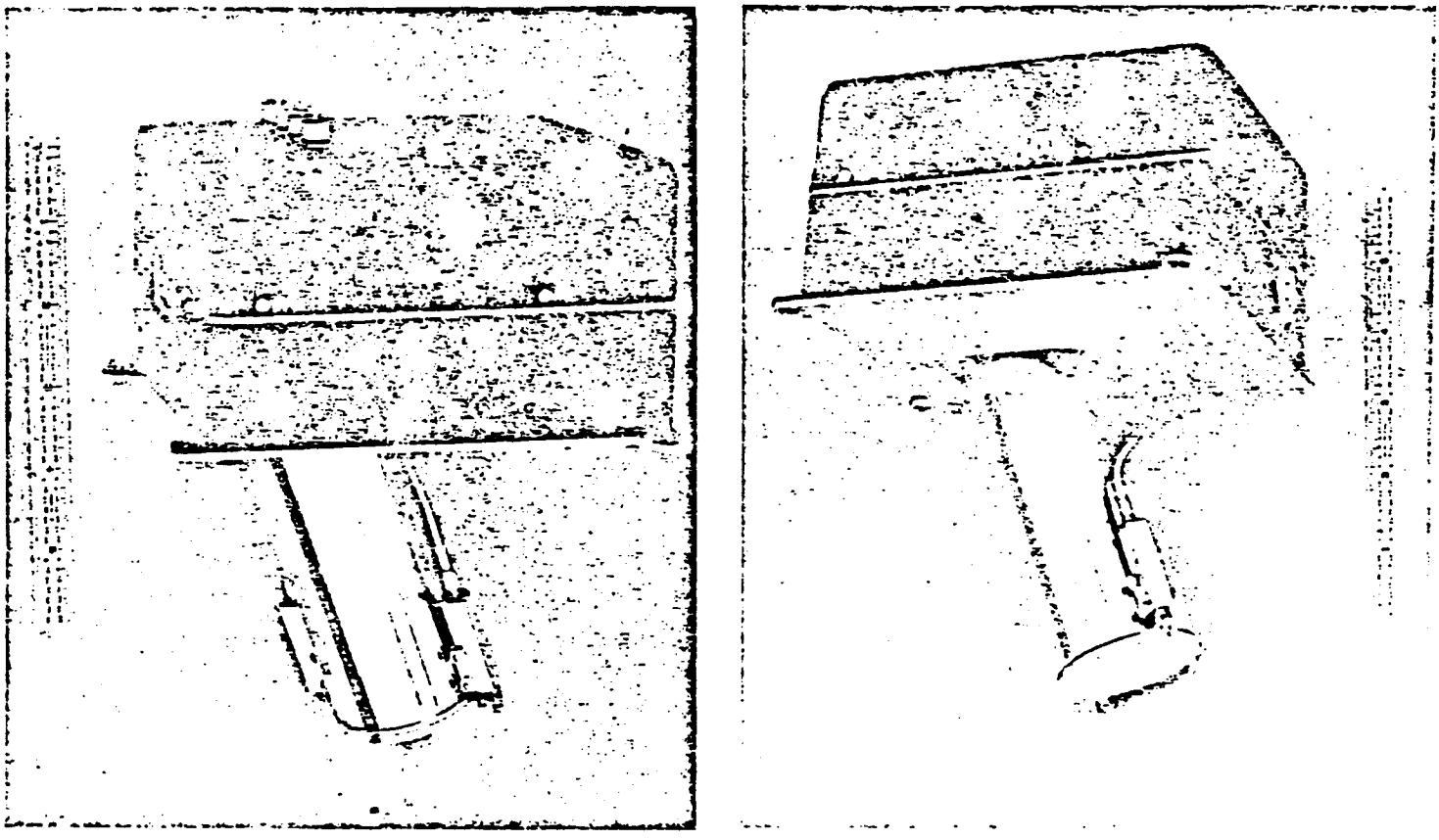

Figure 2 - 6 Pioneer F & G Extreme Ultraviolet Filter Photometer

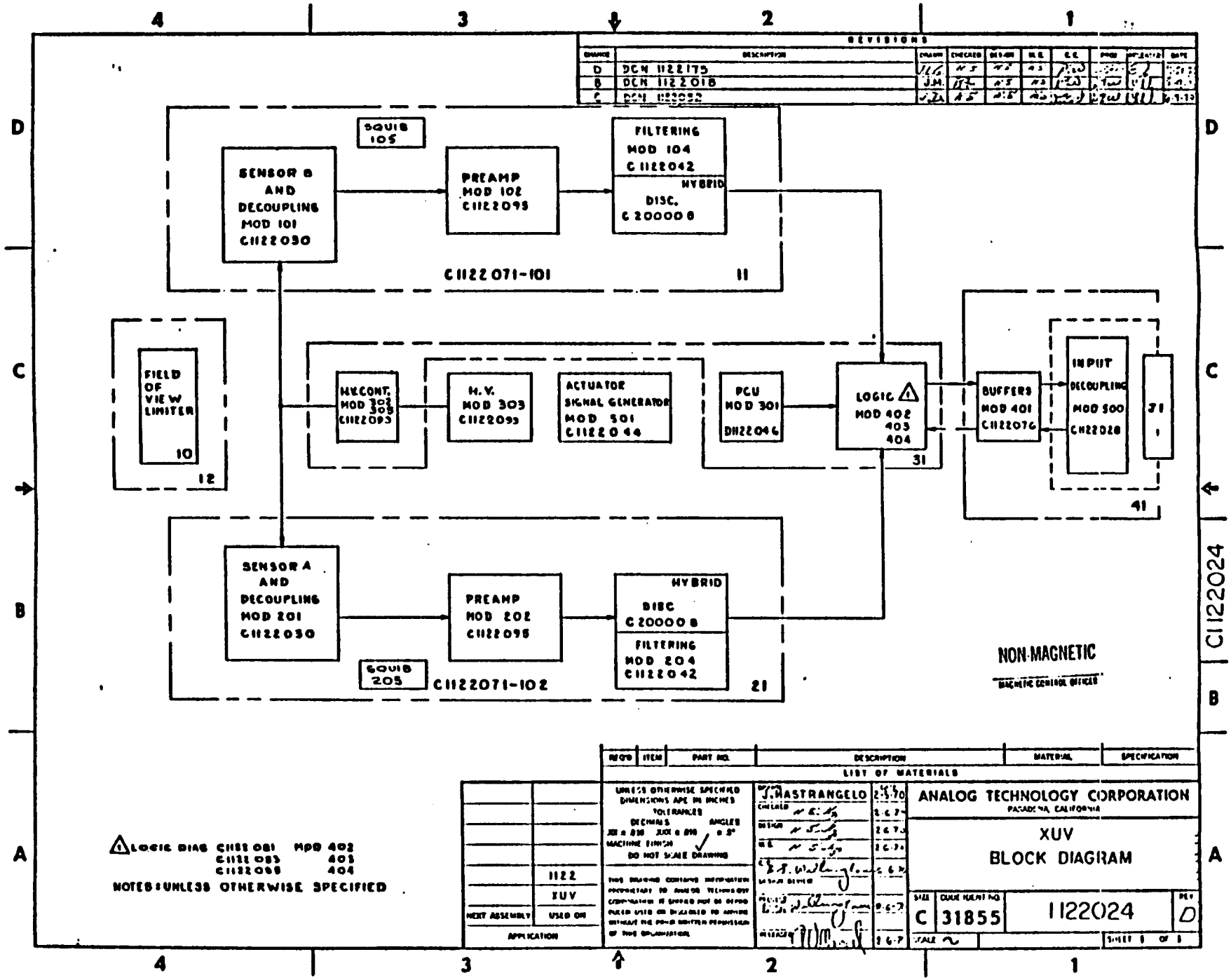
REVISIONS
SQUID 105
SENSOR B AND DECOUPLING MOD 101 C1122090
PREAMP MOD 102 C1122095
FILTERING MOD 104 C1122042
HYBRID DISC. C200008
C1122071-101
11
FIELD OF VIEW LIMITER
10
12
M.F.CONT. MOD 302 303 C1122093
H.V. MOD 303 C1122095
ACTUATOR SIGNAL GENERATOR MOD 501 C1122044
PCU MOD 301 DH22046
LOGIC MOD 402 403 404
31
BUFFERS MOD 401 C1122076
INPUT DECOUPLING MOD 500 CH22028
J1
1
41
SENSOR A AND DECOUPLING MOD 201 C1122090
PREAMP MOD 202 C1122095
HYBRID DISC C200008
FILTERING MOD 204 C1122042
SQUID 205
C1122071-102
21
NON-MAGNETIC
LOGIC DIAG C1122081 MOD 402
C1122083 403
C1122088 404
NOTES: UNLESS OTHERWISE SPECIFIED
LIST OF MATERIALS
ANALOG TECHNOLOGY CORPORATION
PASADENA, CALIFORNIA
XUV
BLOCK DIAGRAM
C 31855
1122024
D
C1122024

Figure 2 - 7

2.3 INSTRUMENT/SPACECRAFT INTERFACE

The XUV instrument provides an interface to the spacecraft as specified by the Pioneer Project and a means for achieving an internal grounding scheme that allows low-level signals to be measured. Figure 2-8 shows the complete interface circuitry for the XUV instrument, which complies except where noted with the requirements specified in PC-220*. Figure 2-9 depicts the relationship of the XUV instrument to the other components of the Pioneer spacecraft. The instrument chassis is grounded to the spacecraft.

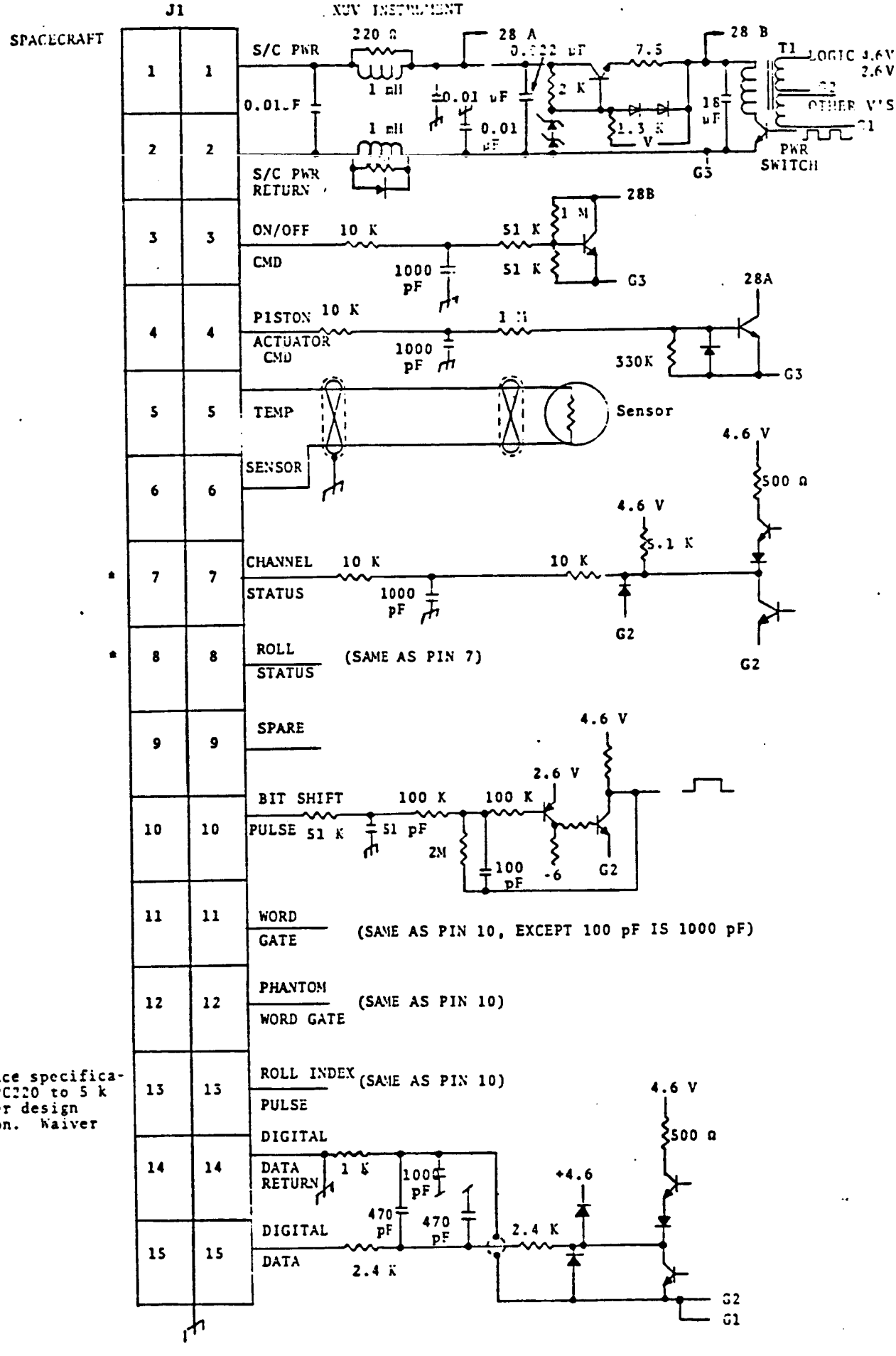

	J1		SPACECRAFT
	1	1	S/C PWR
	2	2	S/C PWR RETURN
	3	3	ON/OFF CMD
	4	4	PISTON ACTUATOR CMD
	5	5	TEMP SENSOR
	6	6	SENSOR
*	7	7	CHANNEL STATUS
*	8	8	ROLL STATUS
	9	9	SPARE
	10	10	BIT SHIFT PULSE
	11	11	WORD GATE
	12	12	PHANTOM WORD GATE
	13	13	ROLL INDEX PULSE
	14	14	DIGITAL DATA RETURN
	15	15	DIGITAL DATA

* Impedance specification in PC220 to 5 k max. after design completion. Waiver granted.

Figure 2 - 8

2.3.1 INTERFACE AND GROUNDING PHILOSOPHY

As shown in Figure 2-9, initial rf filtering is performed on each line entering the instrument. The lines are filtered and bypassed to the chassis so that noise spikes return to the main spacecraft ground point without entering the instrument. Common-mode noise on the power lines is returned in the same manner. For frequencies of interest, the instrument chassis and the preamplifier are at the same reference to prevent chassis-induced noise from propagating through the system as spurious signals. This is accomplised by tying the low-current ground, G1, to the chassis through a 0.01 μF capacitor. The dc return for the system is through the data ground, which has an isolating 1-k resistor. At the 100 ns pulse shaping frequency of the preamplifiers, the 1-k impedance dominates so that possible induced voltages due to chassis/ground currents are forced to appear across the 1-k resistor. In effect the 0.01 μF capacitor assures that G1 and the chassis are at the same

---

* Pioneer F/G Project, Specification PC-220, Spacecraft / Scientific Instrument, NASA/Ames Research Center, Rev. 16, 30 April 1971.

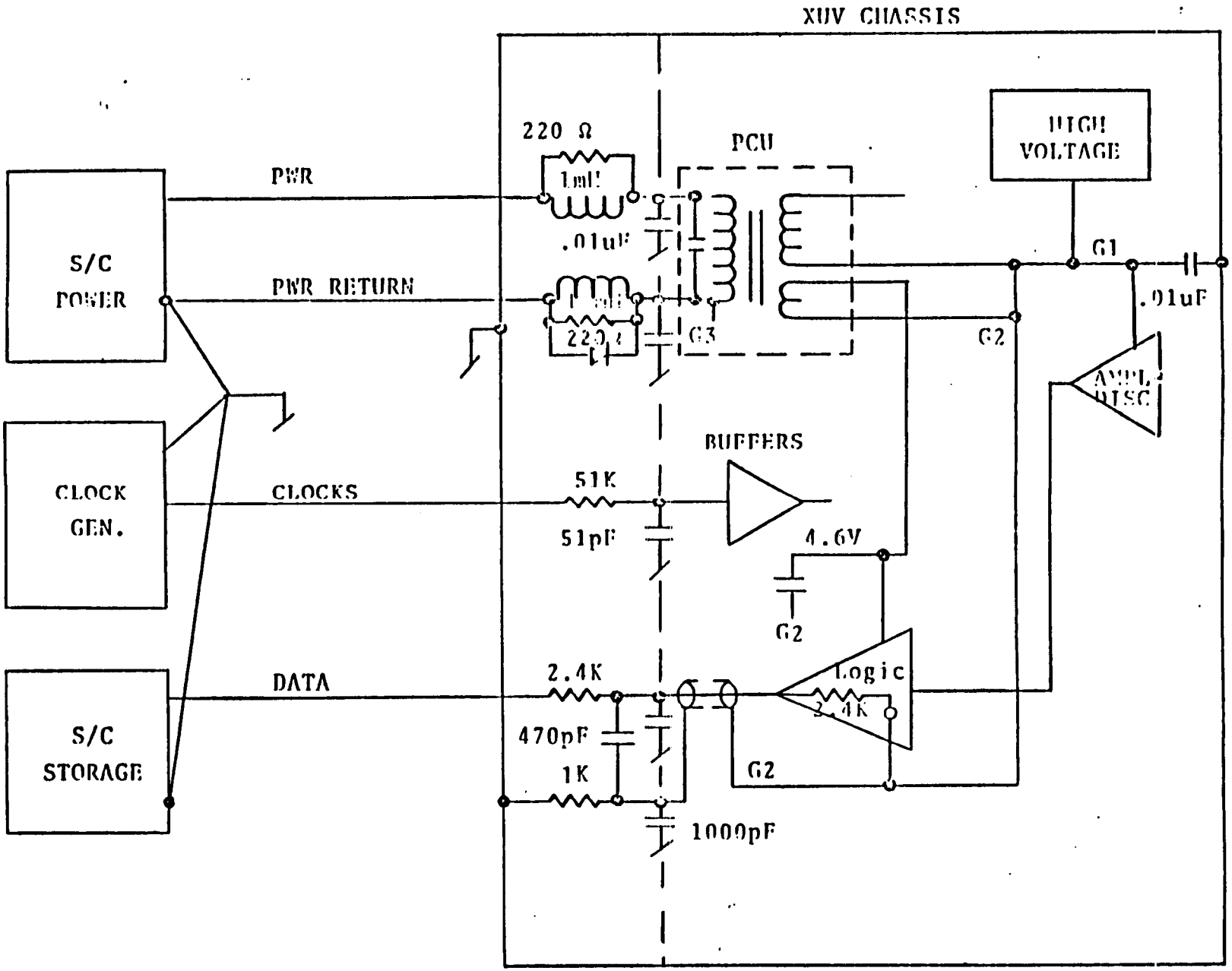

Figure 2 - 9 Grounding Analysis Diagram

potential for frequencies of interest. Thus capacitatively coupled noise signals from the chassis to the preamplifier input are eliminated.

To protect the spacecraft from rf-induced noise in the logic output switching stages, the logic data is bypassed to the logic ground, G2, prior to exiting from the instrument. The output currents are then constrained to flow in the loop comprised of the bypass capacitor of the 4.6 V bias, the shielded output data line, and the decoupling capacitor in the output filtering section. The rf decoupling scheme is shown in the input decoupling schematic of subassembly 41 presented in Section 3 (Figure 3-20).

2.3.2 SIGNAL AND GROUNDING DETAILS

The internal instrument ground and signal routing scheme is shown in Figure 2-10. The power converter unit (PCU) is constructed on three ground planes. GP1 is reserved for low-current precision grounds, GP2 for high-current logic grounds, and GP3 for the isolated instrument power.

At the preamplifier and sensor modules, all voltages are decoupled locally to the G1 ground. Ideally, the chassis should be decoupled at each of the channeltrons. This would, however, from an ac ground loop, which should be avoided. Therefore, only Channel B has been referenced to the chassis. The G1 grounds for each of the analog signal

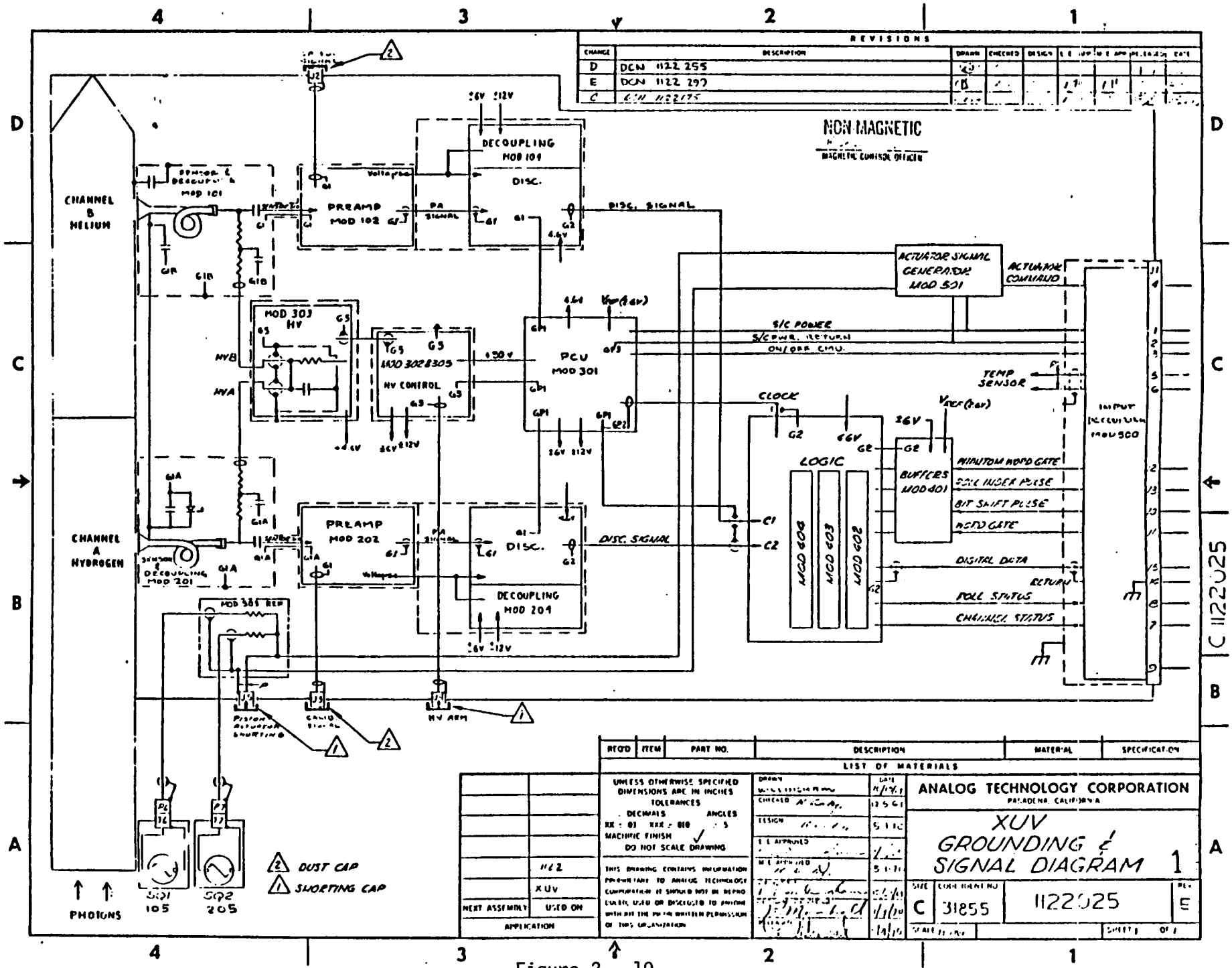
REVISIONS
NON-MAGNETIC
CHANNEL B HELIUM
CHANNEL A HYDROGEN
PREAMP MOD 102
PREAMP MOD 202
DECOUPLING MOD 104
DECOUPLING MOD 204
DISC.
DISC. SIGNAL
MOD 303 HV
HV CONTROL
PCU MOD 301
ACTUATOR SIGNAL GENERATOR MOD 501
S/C POWER
S/C PWR. RETURN
ON/OFF CMD.
TEMP SENSOR
CLOCK
LOGIC
BUFFERS MOD 401
MOD 603
MOD 602
DIGITAL DATA
RETURN
POLL STATUS
CHECKSUM STATUS
HV ARM
PHOTONS
SQ1 105
SQ2 205
2 DUST CAP
1 SHORTING CAP
LIST OF MATERIALS
ANALOG TECHNOLOGY CORPORATION
PASADENA, CALIFORNIA
XUV GROUNDING & SIGNAL DIAGRAM 1
C
31855
1122025
E

Figure 2 - 10

chains are maintained separately and are referenced to each other only at GP1. The G1 grounds are carried through the preamplifiers to the low-current elements of the discriminators and are then routed to the PCU GP1.

The high-voltage system is comprised of three modules. The controller modules have their shields referenced to G5. The multiplier section is potted in a shielding cup which is bonded to but isolated from the chassis. Heavy filtering referenced to G5 is accomplished in an output filtering section of this module. The high-voltage wire shields are maintained at the output filtering ground potential so that arcing currents (should they occur) are circulated locally. Ground G5 is subsequently tied to GP1, thus the high-current and low-current grounds are referenced to each other at one point in the PCU.

TABLE 1

USC XUV PHOTOMETER INSTRUMENT PARAMETERS

Instrument Type:	Two channel XUV Photometer
Channels:	λ_L channel for emissions with $\lambda < 1400$ A;
	λ_S channel for emissions with $\lambda < 800$ A.
Field of View (FWHM):	$1.15° \times 9.3°$ (3.26×10^{-3} sterad)
Filter:	Thin film aluminum filter
Entrance Area:	1.67 cm^2
Geometric Thruput:	434 photons sec^{-1} $Rayleigh^{-1}$
Sensitivity:	4.9 counts/sec-R (Lyman-α)
	7.2 counts/sec-R (He I λ 584 A)
Photocathode:	Aluminum (Lyman-α), LiF (He)
Sensors:	Bendix model 4028 channeltrons (2)
Weight:	650 grams
Power:	650 mW
Data Storage:	19 bits, compressed to 9 bits floating point
Electronics:	Pulse counting electronics; 3.75 kV high voltage supply; Low-voltage power conditioning unit; Compressed-storage logic; Piston actuator -- Dust cover removal system.
Dimensions:	3" x 4" x 5" (main chassis) with 1 - 3/4" diameter x 4" tubular collimator protrusion.

3.0 ELECTRONIC DESIGN

The major electronic subassemblies of the XUV Filter Photometer and their schematic drawing numbers are shown in the block diagram of Figure 2-7. Subassembly 10 is the field-of-view limiter; subassemblies 11 and 21 contain the channeltron sensors and sensor electronics; subassembly 31 is the major motherboard assembly containing the power-conditioning unit, the high-voltage control modules and the logic; subassembly 41 contains the interface circuitry; and subassembly 303 includes the high-voltage multiplier section, the piston actuator module, and miscellaneous components. Each of these subassemblies is described in the following paragraphs, with the exception of subassembly 10 which contains no electronics.

3.1 Sensor Subassemblies 11 and 21

Each sensor subassembly consists of a Bendix #4028 channeltron, a charge-sensitive preamplifier, a fixed deadtime discriminator, and bias and decoupling components. These elements are shown schematically in Figures 3-1 and 3-2.

The channeltrons are Bendix spiral units containing funnel-shaped input cups. An accelerating potential is applied to each funnel cup for purposes of electrostatically focusing photo-electrons released by the large surfaces of

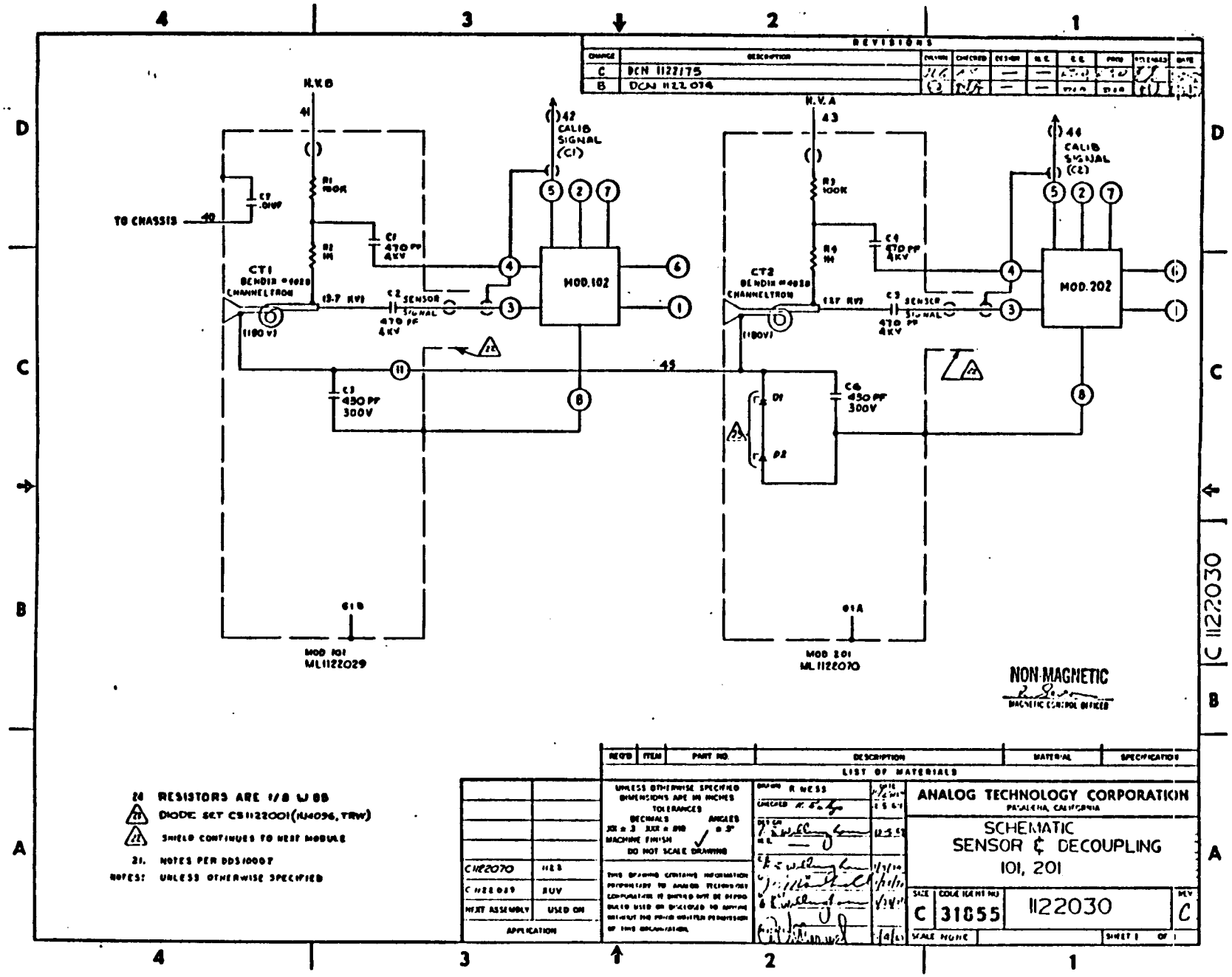

Figure 3-1 Channeltron Decoupling and Bias Circuit

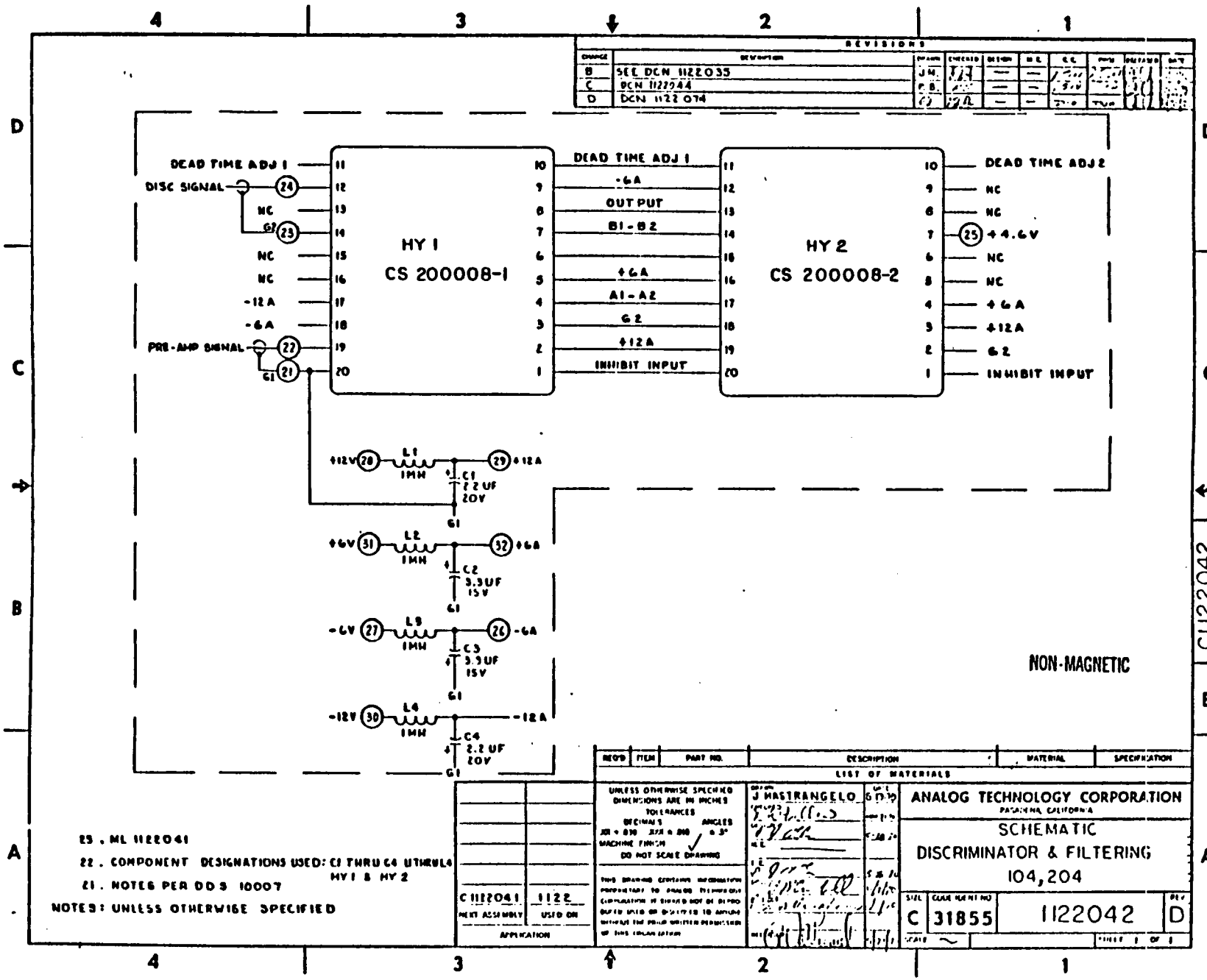
REVISIONS
B SEE DCN 1122035
C DCN 1122044
D DCN 1122074
HY 1
CS 200008-1
HY 2
CS 200008-2
DEAD TIME ADJ 1
DISC SIGNAL
NC
NC
NC
-12 A
-6 A
PRE-AMP SIGNAL
DEAD TIME ADJ 1
-6A
OUT PUT
B1-B2
+6A
A1-A2
G2
+12A
INHIBIT INPUT
DEAD TIME ADJ 2
NC
NC
+4.6V
NC
NC
+6A
+12A
G2
INHIBIT INPUT
+12V
L1
1MH
C1
2.2 UF
20V
+12A
+6V
L2
1MH
C2
3.3UF
15V
+6A
-6V
L3
1MH
C3
3.3UF
15V
-6A
-12V
L4
1MH
C4
2.2 UF
20V
-12A
G1
NON-MAGNETIC
C1122042
25. ML 1122041
22. COMPONENT DESIGNATIONS USED: C1 THRU C4 U1 THRU U4 HY1 & HY2
21. NOTES PER DDS 10007
NOTES: UNLESS OTHERWISE SPECIFIED
LIST OF MATERIALS
REQ'D ITEM PART NO. DESCRIPTION MATERIAL SPECIFICATION
ANALOG TECHNOLOGY CORPORATION
PASADENA, CALIFORNIA
SCHEMATIC
DISCRIMINATOR & FILTERING
104,204
SIZE C
CAGE IDENT NO 31855
1122042
REV D
C1122041
NEXT ASSEMBLY
1122
USED ON
APPLICATION

Figure 3-2

the field-of-view limiter photocathode or aluminum filter. This voltage is approximately 180 V and is large enough to satisfy collection and channeltron-efficiency requirements. The excitation voltage applied to each channeltron is approximately 3700 V, which places the channeltron comfortably within its gain saturation region so that average multiplication values of 10^8 are expected. The dynamic range of the associated pulse-amplifier/ discriminator circuits is 1000. The high end is a factor of 10 above the average pulse height experiences at low rates, thereby accounting for the upper half of the channeltron's pulse-height distribution (approximately Gaussian) and any upward gain variations experienced from one unit to another. The threshold level, which is set at 0.01 times the average level pulse, permits effective channeltron counting at medium rates (e.g., $<< 10^5$/sec) under conditions of long-term channeltron fatigue or gain reductions due to other causes. Normally, attenuated pulses produced at high rates due to charge-induced recovery effects in the channeltron can also be resolved with ease down to pulse spacings of 3 μs. This means that a threshold level pulse occurring 3 μs after a maximum-level pulse (1000 times larger) can successfully be resolved by the amplifier/ discriminator.

The fixed deadtime discriminator system provides accurate conversion of observed-to-actual event rates. Deadtime results in the loss of an event which follows an

analyzed event in a time less than the deadtime. The probability that a particle is actually emitted during this period results from the analysis of the Poisson distribution. The probability that no particles are lost is calculated as

$$P_o = \exp(-RT)$$

where R = average rate

T = deadtime

The average number of lost particles per discriminator triggering is given by

$$\bar{N}_{LOST} = \sum_{r=1}^{\infty} rP_r(T) = m(T) = RT$$

Although this deadtime loss may be large, accurate data corrections can be made if the deadtime itself is well known. Since the deadtime is principally determined by the discriminator pulse width and since this pulse width is independent of the rate and the triggering amplitude, only the average rate of discriminator triggering (R') need be known. This rate can then be used to find the true average rate from

$$R = \frac{R'}{1 - R'T}$$

In order to reduce the dependence of the deadtime on the pulse-height spectrum, the amplifier pulse width is made considerably less than that of the discriminator. Also, the discriminator threshold rapidly recovers to its nominal value after the output returns to its quiescent state.

The deadtime was also selected with another consideration in mind. The experimenters have indicated that rates of up to 2.5×10^5 counts/sec could be expected during planetary encounter. In the case of a 256-bps telemetry rate and an alternate spacecraft frame readout, accumulation periods of up to 1.5 sec could result. For a 3-μs deadtime discriminator, the maximum counts in 1.5 sec would be 5×10^5. The 19-bit logic register can accumulate 524,287 counts; thus, counter overflow cannot occur. Further, a true event rate of 2.5×10^5 events/sec yields a measured rate of 1.43×10^5 counts/sec with a deadtime of about 43%. A unit similar to the XUV discriminator has been shown to provide accurate data for deadtimes of greater than 75%.

3.1.1 Sensor Decoupling and Bias Circuits

The channeltron decoupling and bias circuitry is shown in Figure 3-1. Since the anode of the channeltron is at 3.7 kV, it is capacitively coupled to the amplifier input. In addition, filtering is provided to prevent the high-voltage ripple from degrading the amplifier output. These circuit

components have been selected to meet several criteria:

(1) R1 (R3) and R2 (R4) are small compared to the channeltron resistance so that variations in channeltron resistance have only a small effect on channeltron voltage drop.

(2) Since the channeltron output current is divided between R2 (R4) and C2 (C5), the R2C2 (R4C5) product is large enough to insure that almost all of the current goes to C2 (C5).

(3) The discharge of C2 (C5) after the pulse will cause the amplifier to undershoot. This discharge is made sufficiently slow to prevent the amplifier output return to zero from triggering the discriminator. In effect, this puts another limit on the minimum size of R2C2 (R4C5).

(4) Sufficient ripple filtering is provided so that the resultant noise at the discriminator is small compared to the discriminator threshold.

Considering each of these criteria in turn:

Criterion 1. R1 and R2 are set at 1 Meg each. They will drop about 0.1% of the high voltage with the lowest channeltron resistance.

Criterion 2. If we assume the impedance of C1 is small with respect to R1 and R2 at the frequencies of interest, then the fraction of the channeltron current flowing into C2 is

$$I_{C2}(s) = \frac{R2C2_p}{R2C2_p + 1}$$

$$i_{C2}(t) = e^{(-\frac{1}{R2C2}t)} \qquad \text{(step input)}.$$

For $i_{C2}(t) \geq 0.99$ at $t = 30$ ns (channeltron pulsewidth),

$$R2C2 \geq 3 \times 10^{-6}$$

or, with R2 = 1 Meg,

$$C2 \geq 3 \text{ pF}.$$

Criterion 3. The voltage at the discriminator for a unit ramp amplifier output is (see circuit details in Figures 3-3 and 3-5):

$$V_D = \frac{1}{10^7} (1 - e^{-10^7 t}).$$

For a final value of V_D of less than 10mV (10% of threshold), the rate of change of amplifier output voltage is

$$\frac{dV_A}{dt} \leq 10^5 \text{ V/sec}.$$

This implies an amplifier input of

$$\frac{di_A}{dt} \leq 0.23 \text{ A/sec}.$$

If we assume that C2 discharges through R2 to ground,

$$i_A = \frac{V}{R_2} e^{(-\frac{1}{R2C2} t)} = \frac{Q}{C2R2} e^{(-\frac{1}{R2C2} t)} ;$$

$$\frac{di_A}{dt} = \frac{-Q}{(R2C2)^2} e^{(\frac{1}{R2C2} t)},$$

where Q = channeltron charge output.

The initial value is

$$\left.\frac{di_A}{dt}\right|_{t=0} = \frac{Q}{(R2C2)^2} .$$

Thus, for

$$Q = 10^{-10} \text{ C}$$

and R2 = 1 Meg,

$$C2 \geq 20.6 \text{ pF}.$$

Criterion 4. The largest capacitance value available in the smallest case size of 4-kV capacitors is 470 pF. Considering the effects of temperature, voltage, and frequency, the effective capacitance will be about 380 pF. The use of this value for C2 more than meets the above criteria. The resulting ripple is 22 mV at the amplifier output and 500 μV at the discriminator input.

Diodes D1 and D2 are specially selected low-current 90-V zener diodes. They possess a sharp knee at currents of less than 3 μA. The leakage current of the two combined channeltrons is greater than 8 μA; thus, a 180V bias for collection of electrons at the channeltron funnels is achieved.

3.1.2 Charge-Sensitive Preamplifier Circuit

The preamplifier (Module 102 or 202) accepts the current pulses produced by the channeltrons, amplifies them, and shapes them into pulses suitable for input to the threshold discriminator. The gain has been selected so that an input pulse with a total charge of 10^{-13}C will just cause the discriminator to trigger, if it is not generating an output pulse at the time. Further, with an input pulse as large as 10^{-10}C, the amplifier output will still return to zero within the 3-μs deadtime of the discriminator. The preamplifier schematic is shown in Figure 3-3.

3.1.2.1. Pulse Shaping

The time of gain crossover is less than 20 ns, so that the output pulse shape in response to a delta-function charge input (current impulse) will be determined almost entirely by the passive feedback components. Therefore, the amplifier transfer function of interest, $V_1(p)/Q$, will be

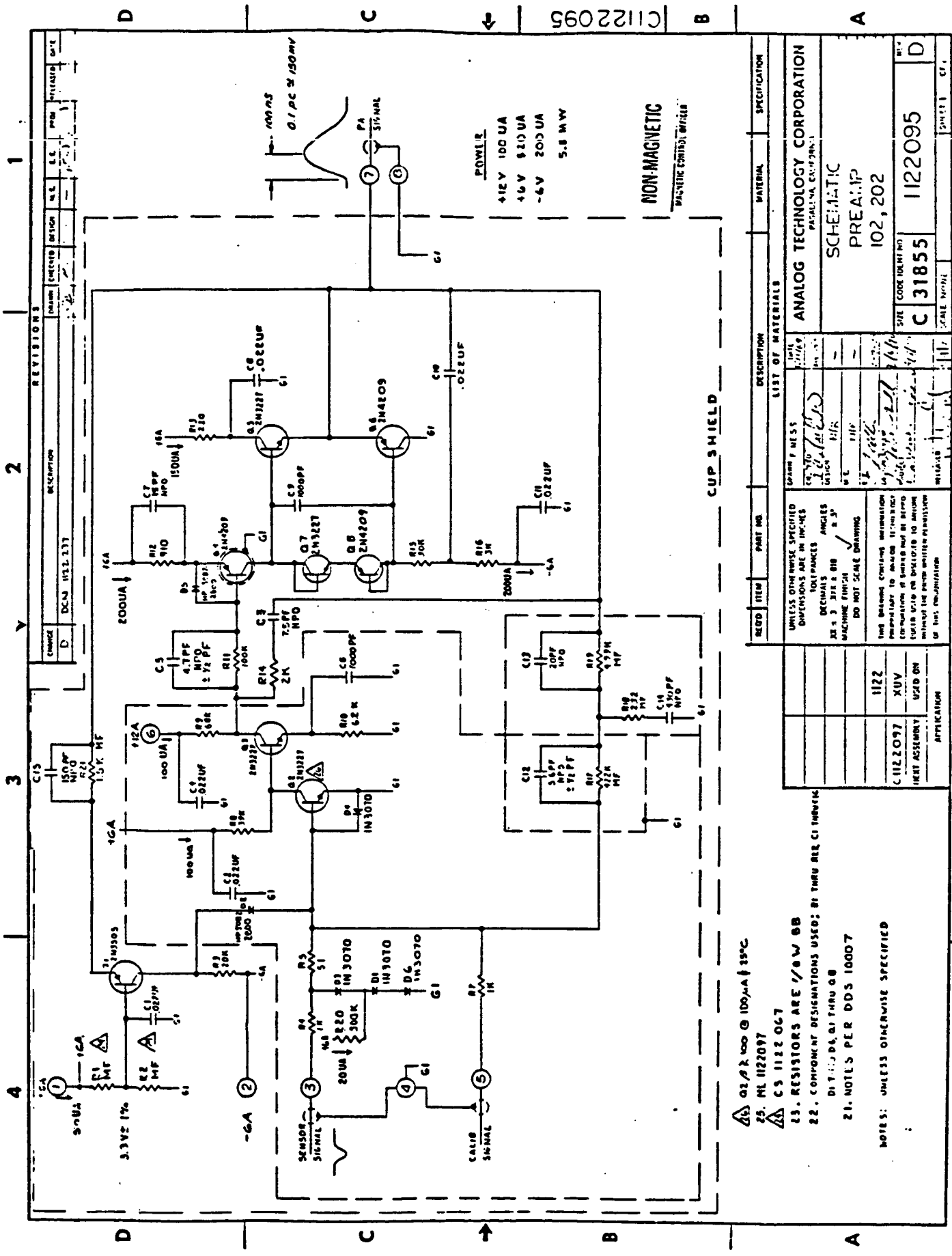
C1122095
ANALOG TECHNOLOGY CORPORATION
SCHEMATIC
PREAMP
102, 202
1122095
C 31855
NON-MAGNETIC
CUP SHIELD
POWER
+12 V 100 UA
+6 V 810 UA
-6 V 200 UA
5.8 MW
100 MA 0.1 PC @ 150 MV
P1 SIGNAL
200UA
100UA
-6A
+6A
SENSOR SIGNAL
CALIB SIGNAL
3.3V± 1%
NOTES: UNLESS OTHERWISE SPECIFIED
21. NOTES PER DDS 10007
22. COMPONENT DESIGNATIONS USED: R1 THRU R18, C1 THRU
23. RESISTORS ARE 1/8W 5%
25. ML 1122097
C5 1122 067
02 @ 2 100 @ 100μA @ 25°C

Figure 3-3

approximately equal to the feedback network transfer impedance.

$$\frac{V_1(p)}{Q} =$$

$$\frac{(R17+R19)\left[\frac{R17 \cdot R19}{R17+R19}(C12+C13)R18C14p^2+\left(\frac{R17 \cdot R19}{R17+R19}(C12+C13+C14)+R18 \cdot C14\right)p+1\right]}{(R17C12p+1)\ (R19C13p+1)\ (R18C14p+1)}$$

For the component values used, this equations reduces to

$$\frac{V_1(p)}{Q} = \frac{427k\ (1 + p \cdot 5\ ns)}{(1 + p \cdot 100ns)^2} .$$

Note that one of the factors in the numerator has been chosen to cancel (R17C12p + 1) so that the pulse shaping becomes single integration with single differentiation with equal 100-ns time constants, if we neglect the 5-ns zero. The 5-ns zero partially compensates for the nonzero width of the channeltron output pulse. The pulse after a differentiation at the input to the discriminator then becomes

$$\frac{V_2(p)}{Q} \approx \frac{427k\ (p\ 100\ ns)}{(1 + p\ 100\ ns)^3}$$

if the 5-ns zero and the nonzero channeltron pulsewidth are both neglected. The pulse shaping is then single

integration with double differentiation (τ = 100 ns), which has an inverse transform given by

$$\frac{V_2(t)}{Q} = (4.27 \times 10^{12}) \frac{(t/\tau)\,(2 - t/\tau)e^{-t/\tau}}{2}$$

The peak value of this waveform is

$$V_{2\ peak} = (0.99 \times 10^{12})Q.$$

Since the discriminator threshold is 0.1 V, the threshold charge is 0.1 pC. In 2 μs, this pulse has decayed to less than 1 part in 10^4 of its peak value and will not influence the discriminator threshold.

3.1.2.2 Amplifier

The preamplifier consists of three cascaded common-emitter stages with an emitter-follower output stage. To improve linearity, most of the third-stage load resistance is bootstrapped to the output. The amplifier is dc-coupled throughout, and feedback from the output to the base of the first stage is used to establish the quiescent operating point. The quiescent dc output is about 1 V, which is the sum of the required base-emitter voltage of Q2 (0.6 V) and the drop in the 427-k feedback resistor

resulting from the approximately 1-μA Q2 base current. The power requirement is as follows:

	+12 V	100 μA
	+ 6 V	520 μA
	- 6 V	200 μA
Total Power:		5.5 mW

An open-loop Bode plot of the uncompensated amplifier is shown in Figure 3-4. In the frequency range of interest, it is characterized by a long section of -12 dB/octave slope below the 10^7 rad/sec shaping frequency. At 10^7, a double zero from the feedback shaping network increases the slope to zero. Crossover occurs at about 3 ns with a -18 dB/octave slope. The required frequency compensation is provided by the bypassed emitter resistors and the minor loop formed by C3 and R14 enclosing the third stage and the output stages. The Q2 network is effective at frequencies below the shaping frequency and serves to reduce the slope in this region to -6 dB/octave. The minor loop and the Q4 network supply a zero at gain crossover. C15 also aids stability by rolling off gain at high frequencies, but its primary purpose, along with R11 and C5, is to improve the recovery from overload.

The amplifier must accept an input signal of 1000 times threshold. Since the output will saturate at about 35 times threshold and the input capacitors (which have been charged by the input pulse) must be discharged by the feedback

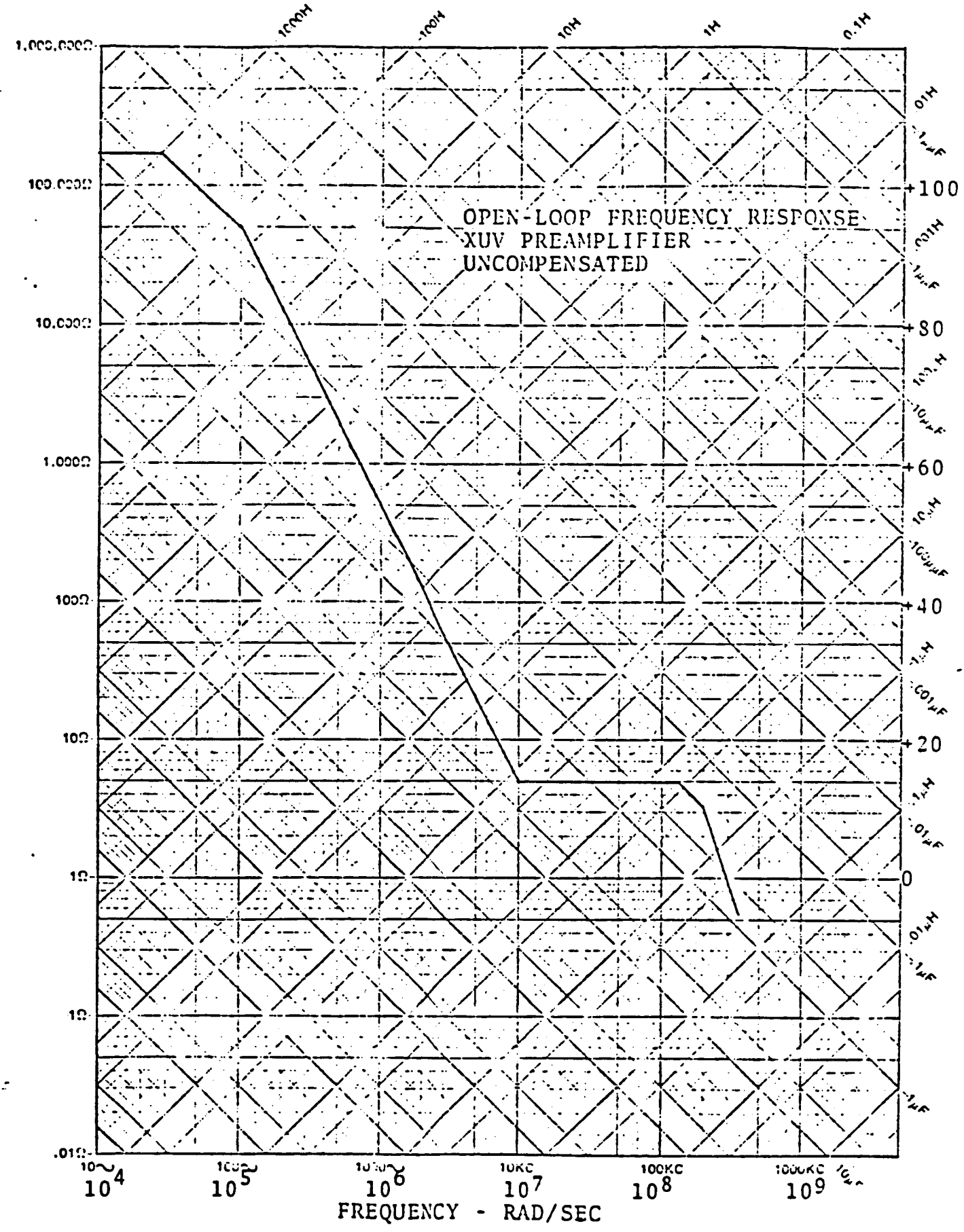
OPEN-LOOP FREQUENCY RESPONSE
XUV PREAMPLIFIER
UNCOMPENSATED
1,000,000Ω
100,000Ω
10,000Ω
1,000Ω
100Ω
10Ω
1Ω
.01Ω
1000H
100H
10H
1H
0.1H
+100
+80
+60
+40
+20
0
10KC
100KC
1000KC
10^4
10^5
10^6
10^7
10^8
10^9
FREQUENCY - RAD/SEC

Figure 3-4

network, the time for the output to come out of saturation is excessively long. Therefore, an additional high-gain feedback path is provided. This path is normally open but is closed, by turning on Q1, when the output reaches 4.2 V. With this circuit, the output returns to zero less than 2 μs after a 10^{-10}C input pulse.

Components R4, R5, D1, D3, D4 and D6 provide input base junction protection for the amplifier in case of high-voltage arcing.

3.1.3 Discriminator

The various elements of the hybrid discriminator are discussed below. The hybrid is broken into two flat packs 3/4" x 3/4". Figure 3-5 is the circuit schematic and it indicates where the circuit is broken and the lead outputs for the two flatpacks. Figure 3-2 shows the hookup of the discriminator with the analog signal filtering components.

3.1.3.1 Discriminator Input Comparator

The positive output pulses from the preamplifier are coupled to the discriminator input through an approximately 100-ns differentiating network (C6, R16). These pulses are clamped by diode D10, and the preamplifier output limit to prevent large voltage swings which could either damage Q7 or cause excessively long recovery times produced by charges in C6.

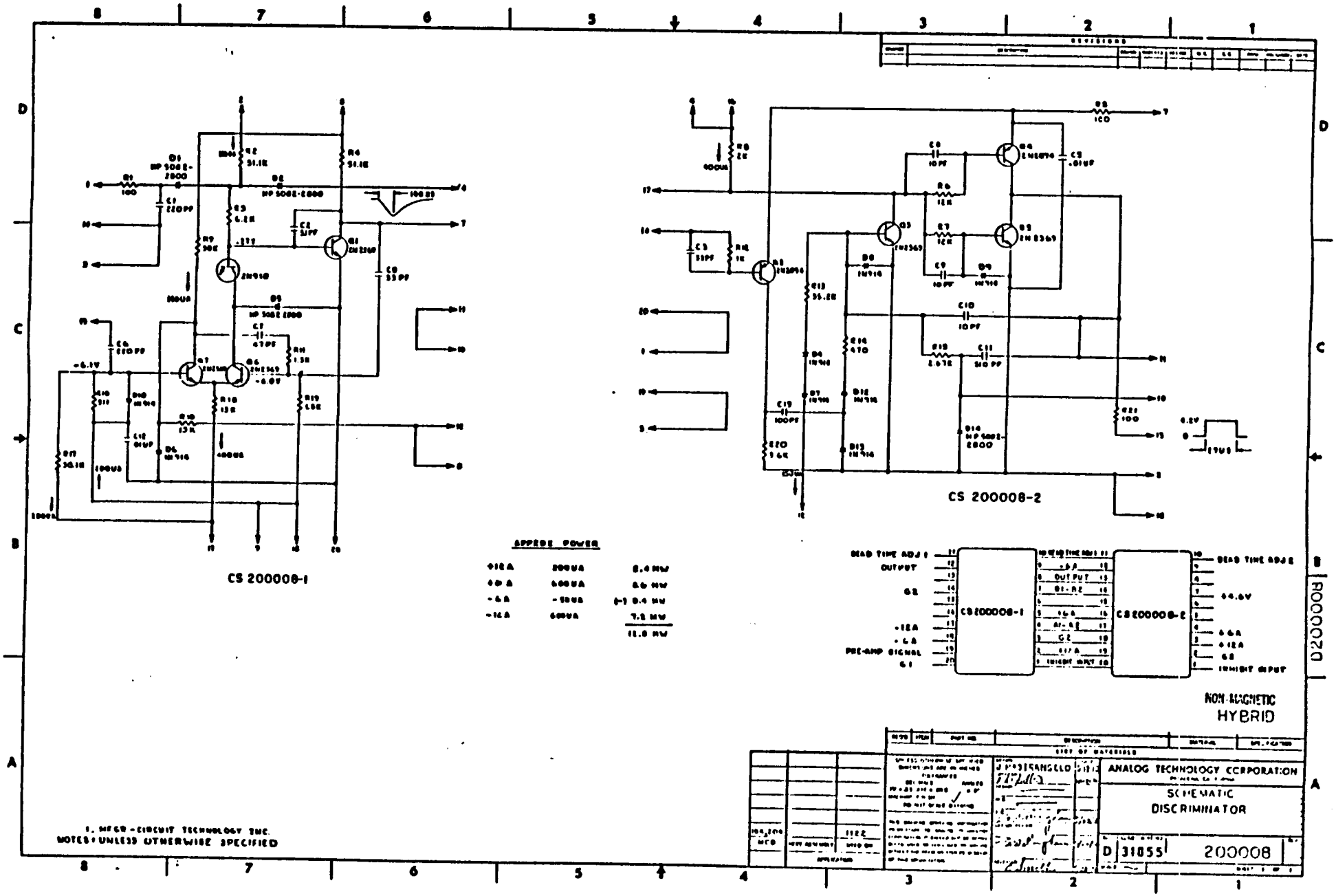
CS 200008-1
CS 200008-2
APPROX POWER
NON-MAGNETIC
HYBRID
ANALOG TECHNOLOGY CORPORATION
SCHEMATIC
DISCRIMINATOR
D 31855
200008
NOTES: UNLESS OTHERWISE SPECIFIED
1. MFGR - CIRCUIT TECHNOLOGY INC.

Figure 3-5

The remainder of the discriminator consists of a differential stage, Q6 and Q7, with a fast positive feedback provided through C7 and a slightly delayed positive loop closed through C8. The base of Q7 is biased 100 mV negative with respect to the base of Q6, so that the current in R18 all flows in the right side when no input pulse is present. As a result, Q1 is cut off, leaving Q2 also off.

When a +100-mV pulse causes the voltages on the bases of Q6 and Q7 to become equal, D6 comes out of conduction, generating a negative voltage across D6. This voltage drives Q6 further into cutoff, triggering the discriminator. This triggering can be inhibited by the current in R10. When the output pulse of the one-shot is at 4.2 V, the total current in D6 exceeds the current in R18, preventing triggering during the output pulse of the one-shot. This feature allows 2.9 μs to be used for discriminator recovery.

The positive feedback signals are sufficient to hold Q7 in the triggered state for at least 200 ns even if the input signal is removed. After the voltage on the base of Q6 decays sufficiently so that current again flows in the left side, regenerative action forces the discriminator back to its quiescent state.

3.1.3.2 Time-Delay Circuit

The time-delay circuit consists of a Miller integrator Q1, followed by an output buffer, Q2.

If the inhibit input is not grounded, the current in R2 causes Q1 to start conducting when the discriminator is triggered. Initially, this current flows in C2 and the collector-base capacitance of Q1, generating a collector voltage which decreases linearly with time from +6 V to ground. When this voltage falls to +3.2 V, Q2 saturates, generating a trigger pulse for the output one-shot. The one-shot then resets the integrator through D2 and prevents further discriminator triggering until after the end of the 2.9 µs output pulse. The time delay between the triggering of the discriminator and the saturation of Q2 is 160 ns. This delay drifts over a 100°C temperature span by about ± 20 ns, principally as a result of changes in the emitter-base voltage of Q2.

The run-up of the Miller integrator can be blocked by grounding the cathode of D2 or D1. In this case, the current in R2 flows into D2 or D1, and the base of Q1 never rises sufficiently to cause Q1 to conduct.

3.1.3.3 Output One-Shot

The output one-shot, Q3 - Q5, produces a 2.9µs pulse when triggered by the saturation of Q2.

Normally, Q3 is held cut off by the current in R13. When Q2 saturates, the positive pulse coupled through C13 and D12 causes Q3 to saturate and the output to rise to +4.2 V. The resultant current through C10 and C11 holds Q2

in saturation until the current in R15 decays to the point where it equals the current in R13. At this time, Q2 starts to come out of saturation, and positive feedback forces the output back to zero. The charge on feedback capacitor C11 is recovered through D14, so that the output pulsewidth is also 2.9 μs for a closely following trigger pulse.

The principal thermal drifts result from the voltage drifts of Q3. This drift is partially compensated by the forward voltage of D7 and D4. As a result, the 2.9-μs pulsewidth remains constant within about 10% over a 100°C temperature span.

The overall dead time of the discriminator is the sum of the 160 ns saturation time for Q2 and the 2.9 μs output pulse. The thermal drifts for these two times are in opposite directions and tend to offset each other.

3.2 Logic Subsystem, Subassembly 31

The logic system receives pulses from the two channeltron discriminators and attitude and timing information from the spacecraft. Counts are accumulated from the sensors alternately and read out as often as permitted by the spacecraft telemetry system. Each sensor is connected to the logic for approximately two rotations of the spacecraft and data is read out at a rate dependent on format and bit-rate conditions within the telemetry system. A system block diagram, Figure 3-6, illustrates the major

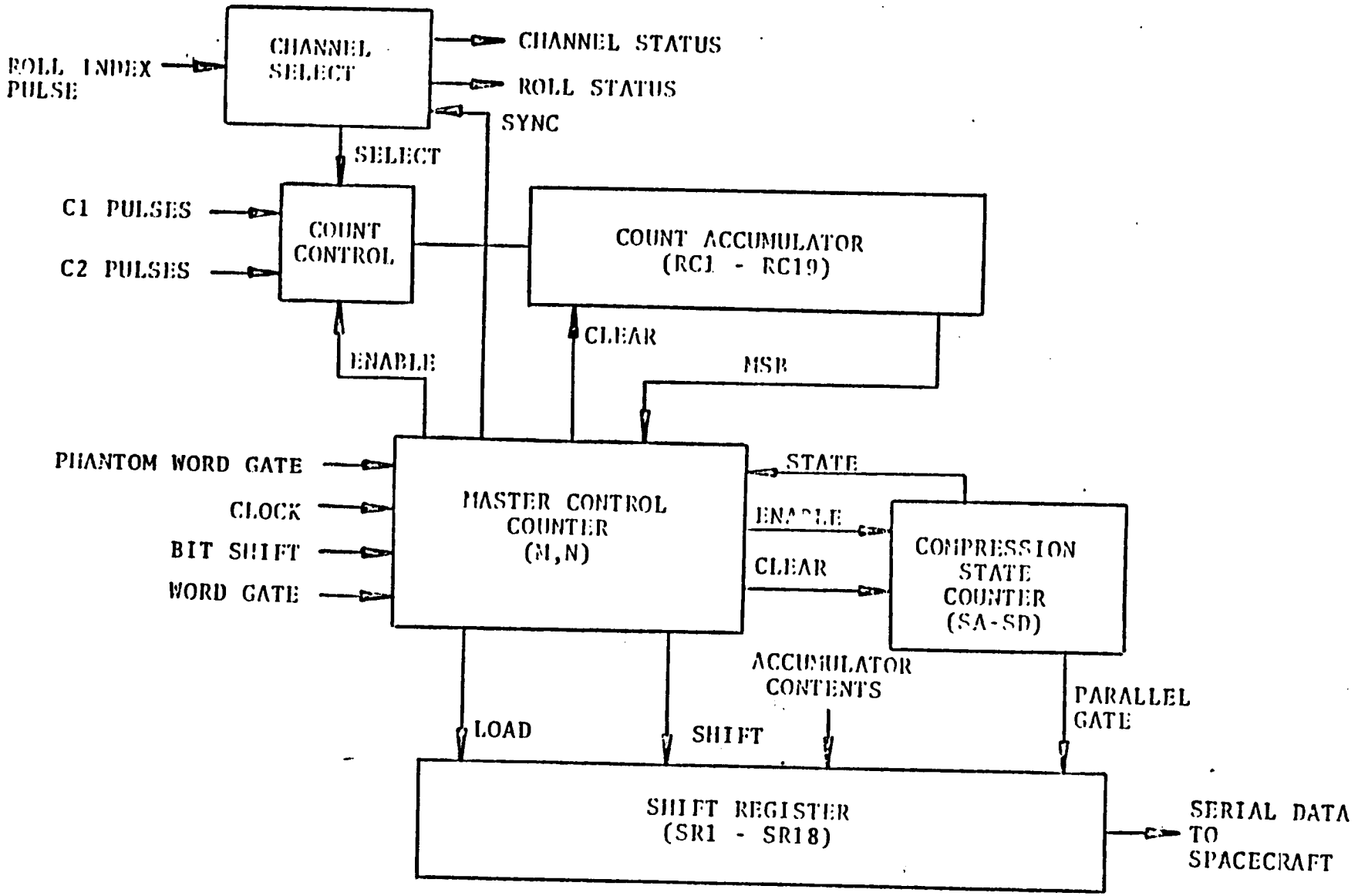

Figure 3.6 XUV Logic Subsystem Block Diagram

functional sections of the logic. The channel select logic contains a two-bit counter that counts roll index pulses and a synchronizer that permits input channels to change only at the end of an accumulation interval. The count control logic receives the synchronized channel-status signal and an enable signal to allow counts to enter the count accumulator from the selected channel, and blocks counts entirely for the brief interval while the data source can change and data transfer and accumulator clearing is taking place. The count accumulator is a 19-bit ripple counter. The capacity of this accumulator is in excess of the maximum counts that the fixed dead-time discriminators can emit in the longest sampling interval, giving immunity from count overflow ambiguities.

The master control counter provides the timing and control signals that synchronize data collection with the spacecraft telemetry system and controls the data transfer and compression functions that occur during the Phantom Word Gate (PWG) that result in the 19-bit count accumulation number being converted into a 9-bit floating-point number. This 9-bit number is read out to telemetry during the 9-bit Word Gate (WG) time by the spacecraft Bit Shift (BS) pulses. Internal operations of the compression sequence utilize a 50-kHz clock obtained from the instrument power converter.

The compression state counter and the shift register act together to provide data compression. The 19-bit count number is loaded into the shift register with the most-

significant bit at the right. The number is shifted right until a 1 is detected in the right-hand bit. It is shifted once more, and the 5 bits at the right end of the register plus a 4-bit number that describes the number of shifts required make up the transmitted word. In the case of a number less than 2^5, a special sequence is enabled that denotes this fact by causing all 0's to be transmitted as the 4-bit number-of-shifts count.

The letter designators shown within the blocks are the names given to the flip-flops that make up the various counters. They are provided to aid in followng the detailed logic discussions that follow.

3.2.1 Count Accumulation

The counts from the channeltron discriminators are accumulated by a 19-bit ripple counter in the logic, under control of: (1) spacecraft timing signals applied to the master control counter and (2) an attitude signal, the Roll Index Pulse, applied to the channel select register.

The spacecraft timing signal that initiates the counter control sequence is the Phantom Word Gate (PWG). The sequence produces a signal, S1G, to disable the counter input, transfers the counter contents to the shift register, and allows the data-source flip-flop, CIS, to change state if the roll-index-pulse count has increased enough. The counter is then reset by the Ripple Counter Clear signal,

RCC, and accumulation begins again. Details of the generation of the timing signals will be given in the master control counter discussion.

The data source that supplies pulses to the accumulator is determined by a 2-bit binary counter that counts roll index pulses and a shift register (CIS) that assumes the state of the RIP-counter most-significant-bit at each S1G pulse. This prevents the data source from changing during a readout interval, and since two roll index pulses must occur before changing data sources the probability of each data source accumulating for an entire spacecraft rotation is improved. The least-significant bit of the roll index counter is read out to telemetry as RIS, along with the state of the channel-select bit, CIS, to allow determination of the data source.

The ripple counter is made up using 5 4-bit binary counters, Texas Instruments type SN54L93, with one unused bit. A logic diagram of this logic is given in Figure 3-7.

3.2.2 Master Control Counter

The master control counter is a four-state sequence generator that controls data accumulation, compression, and readout.

The master control counter logic is illustrated in Figure 3-8 with the main logic sequence shown in the table. The sequence generator operates in conjunction with the

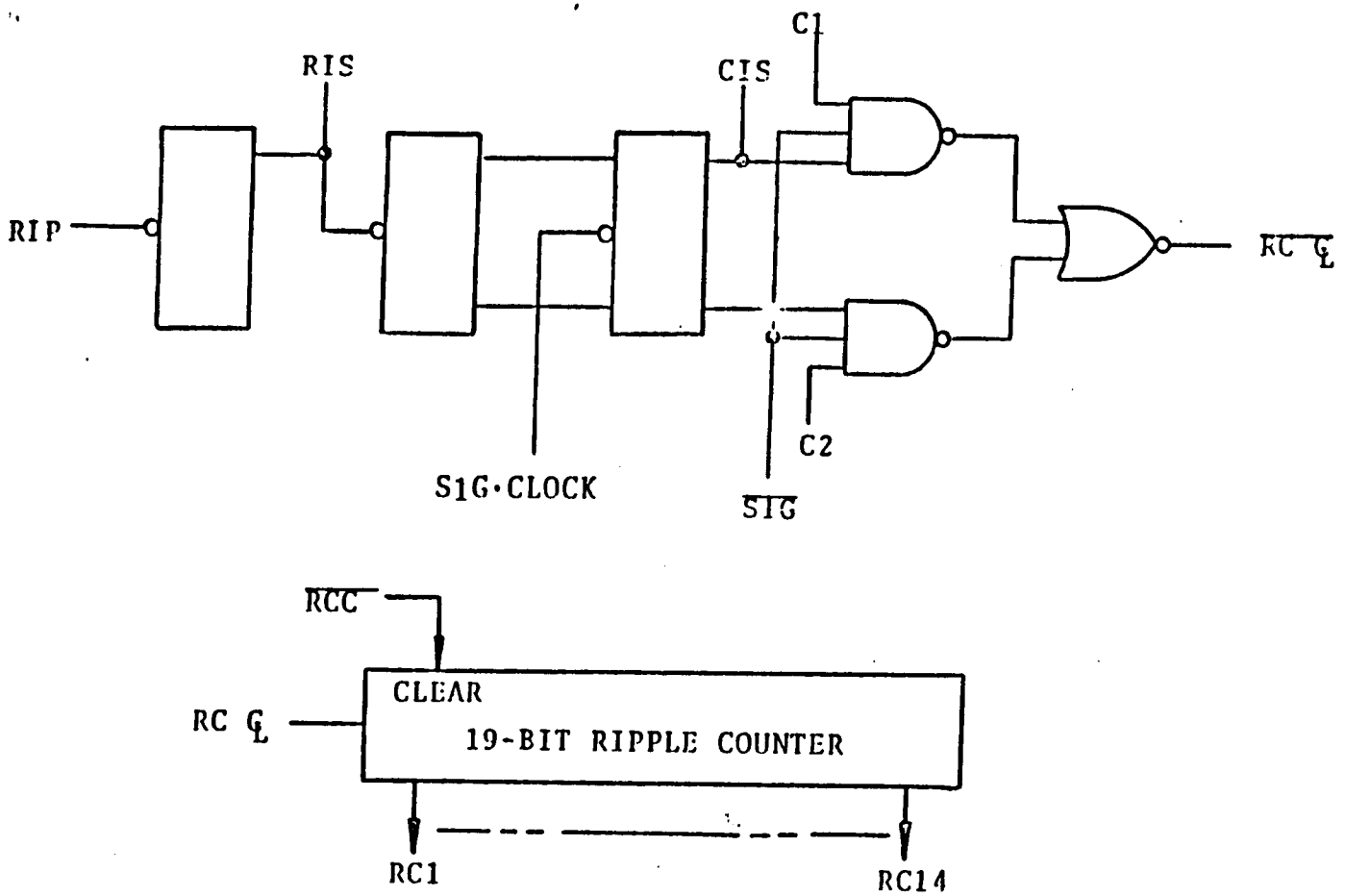

Figure 3-7. Count Accumuator Logic

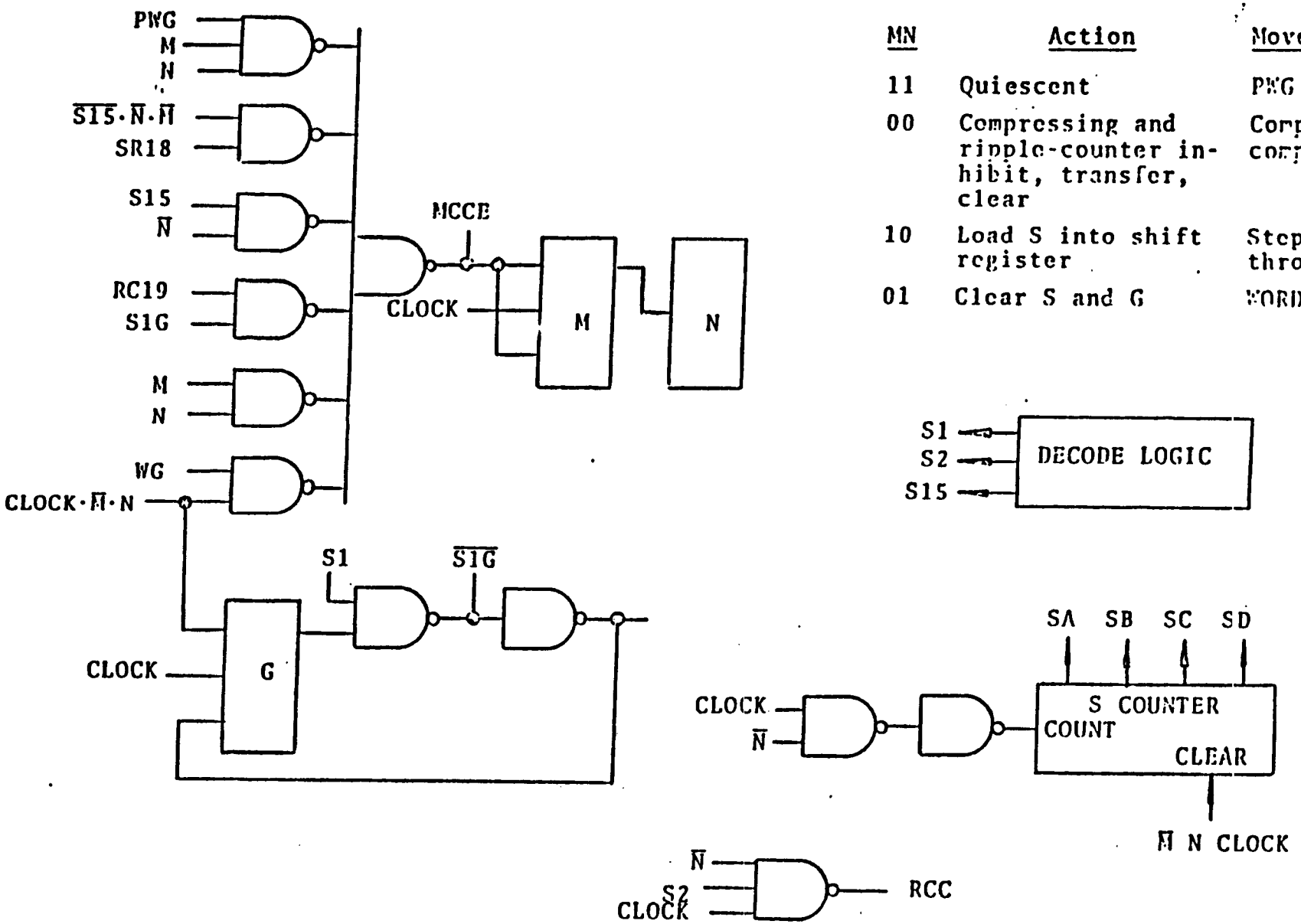

MN	Action	Moves When
11	Quiescent	PWG = 1
00	Compressing and ripple-counter inhibit, transfer, clear	Compression complete
10	Load S into shift register	Steps through
01	Clear S and G	WORD GATE =

Figure 3-8
Master Control Counter Logic

4-bit "S" counter to generate the control signals that result in a 19-bit accumulated count being available for telemetry as a 9-bit word each time the spacecraft-provided word gate is made true.

Assume the system is accumulating counts, the control counter is in the 11 state, the G flip-flop is set, and the "S" counter is in S0. At some time, PWG will become true. This causes MCCE to become true, and a clock pulse can then toggle MN to the 00 state. With MN in 00, the next clock pulse causes the S counter to advance to S1, making S1G true. This disables the ripple counter, and one-half clock pulse later enables the contents of the 18 LSB's of the ripple counter to be loaded into the shift register. The next clock pulse resets G and advances S to S2. S1G going away re-enables the ripple counter; but it is reset by S2 and clock after which counts are again accumulated. At the same time the compression logic is operating. In the usual case, where the accumulated counts are between 2^5 and $2^{18}-1$ inclusive, the S counter advances and the register shifts until a 1 is detected in SR18. The next clock pulse shifts that 1 off the end of the SR, and advances MN to 10. Two special cases must be provided for. If there were 2^{18} or greater counts in the accumulator, then the RC19 bit is true and the MN counter steps to 10, leaving the S counter in S2. If there are less than 2^5 counts, then the S counter will reach S15, and the next pulse places S in S0 when MN becomes 10. This code describes the case where the most-significant

one is not suppressed; in all other cases, the most-significant one is detected and not transmitted.

The remaining operations of the MN counter are straight-forward. The 10 state is used to copy the S counter state into the shift register in preparation to readout; the counter immediately steps into the 01 state, where the S and G registers are initialized, and awaits the arrival of WORD GATE, where it advances to the 11 state.

3.2.3 Shift Register

The shift register is 18-bits long and is connected as a parallel-in, serial-out register. Shift clock comes from the 50-kHz PCU clock for compression, and from the selectable-rate Bit Shift signal from the spacecraft.

The shift register illustrated in Figure 3-8a consists of 18 stages with nearly identical functions. Each bit of the register is capable of parallel entry of the corresponding bit of the ripple counter (when S1G is true) on command of the system clock, and of serial shift-right operation (when S1G is false) on command of the signal SRS. Extra gating provided for SR1 and SR18, and the signal SF G_L are provided only to duplicate functions performed inside the 54L95 4-bit shift register elements used for the remaining register elements.

Operation normally commences when S1G goes true, entering the RC contents into the register. When S1G

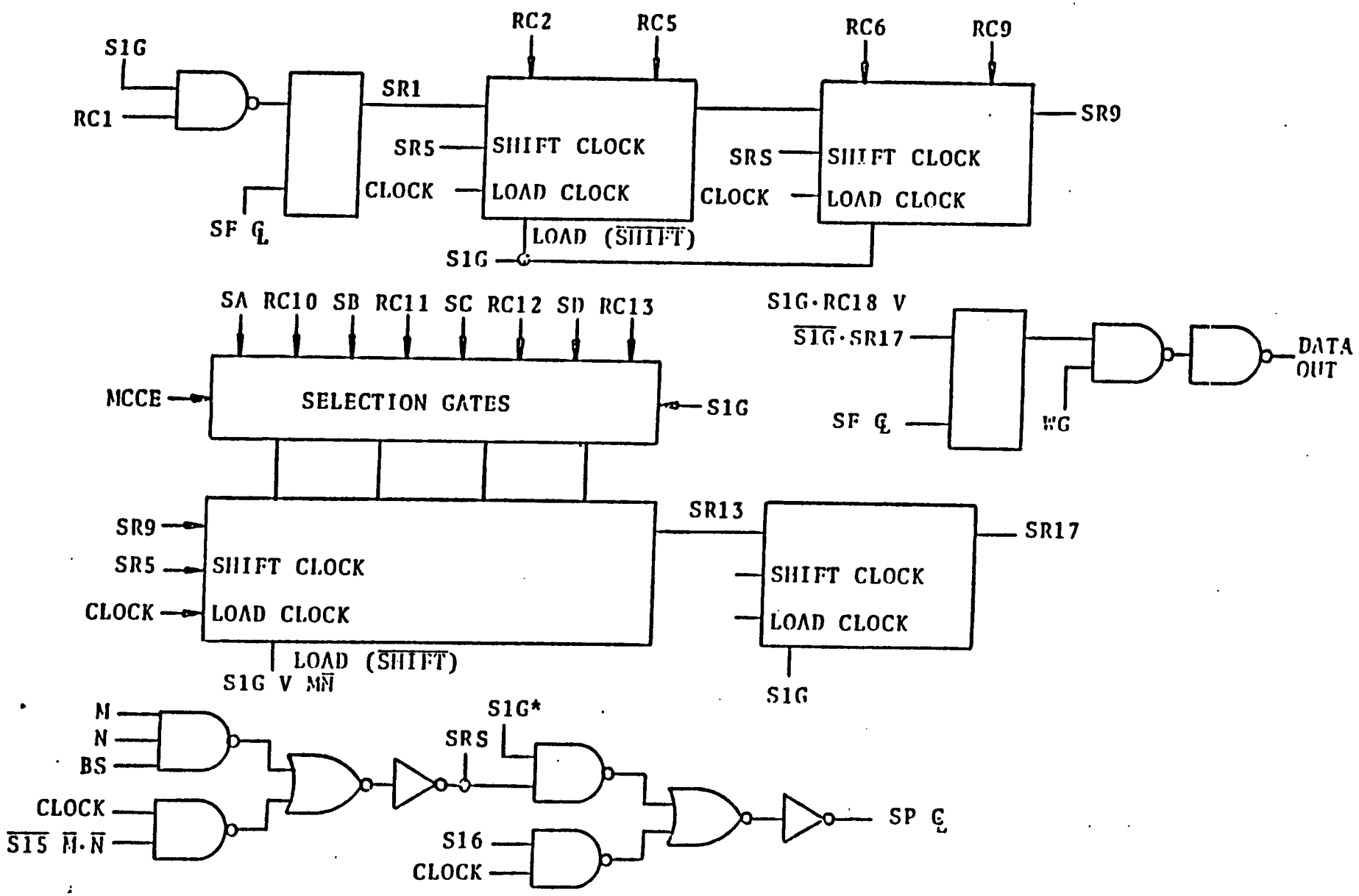

Figure 3-8a. Logic Diagram Shift Registers

becomes false, the shift-right operation is performed until a 1 appears in SR18; one more clock pulse then ends the SRS sequence because MN goes to 10. For the count less than 2^5, S15 is reached and that stops the shifting operation, leaving the 2^4 bit in SR18 ready for readout when WG comes true, causing MN to go to 11 and connecting SRS to the BS line.

Selection gates are provided to load the S-counter contents into SR9 through SR13 after compression is complete. The shift register is cleared after readout because SR1 shifts in zero's when S1G is not true, and BS is applied to the register continuously while the MN counter is in the 11 state.

3.2.4 Data Interpretation

The data from the instrument is related to the input count number by a relationship of the form $C \cdot 2^X$, where the values of C and X are determined from the last 5 and first 4 bits of the output data, respectively.

The data in the 19-bit accumulated count is compressed into a 9-bit number in a floating-point notation. Four bits of the 9 output bits describe the location of the most-significant 1 in the word, while the remaining 5 bits describe the 5 bits of lesser significance in the word. This scheme provides 16 locations for the MS-one; 14 of which are useful since 5 bits may be transmitted. One of

the 16 states is unused, and one state signifies the absence of a one in any of the 14 MSB positions of the 19-bit number. The algorithim for decoding the word is as follows.

1. The word format:

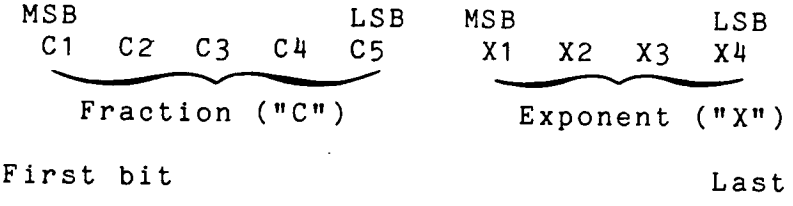

2. Convert X and C to base-10

$C1 \cdot 2^4 + C2 \cdot 2^3 + C3 \cdot 2^2 + C4 \cdot 2^1 + C5 \cdot 2^0$;

$X1 \cdot 2^3 + X2 \cdot 2^2 + X3 \cdot 2^1 + X4 \cdot 2^0$.

3. If $X_{10} = 0$, then count = C_{10} with no error.

4. If $X_{10} \neq 0$, then count = 2^{15-X} $(32 + C_{10})$ with a +1, -0 error associated with the C_{10} calculation.

5. If $X_{10} = 1$, an error has occurred.

3.2.5 Logic Schematics

The detailed logic schematics are presented in the following figures. This information duplicates that presented in the preceding discussion, but reflects the packaging details omitted from that presentation. Interfaces for signals going to the spacecraft are shown (for example, the CIS/channel status circuit on module 404). The resister-diode network will protect the driving gate from damage in the event of a misconnection during test.

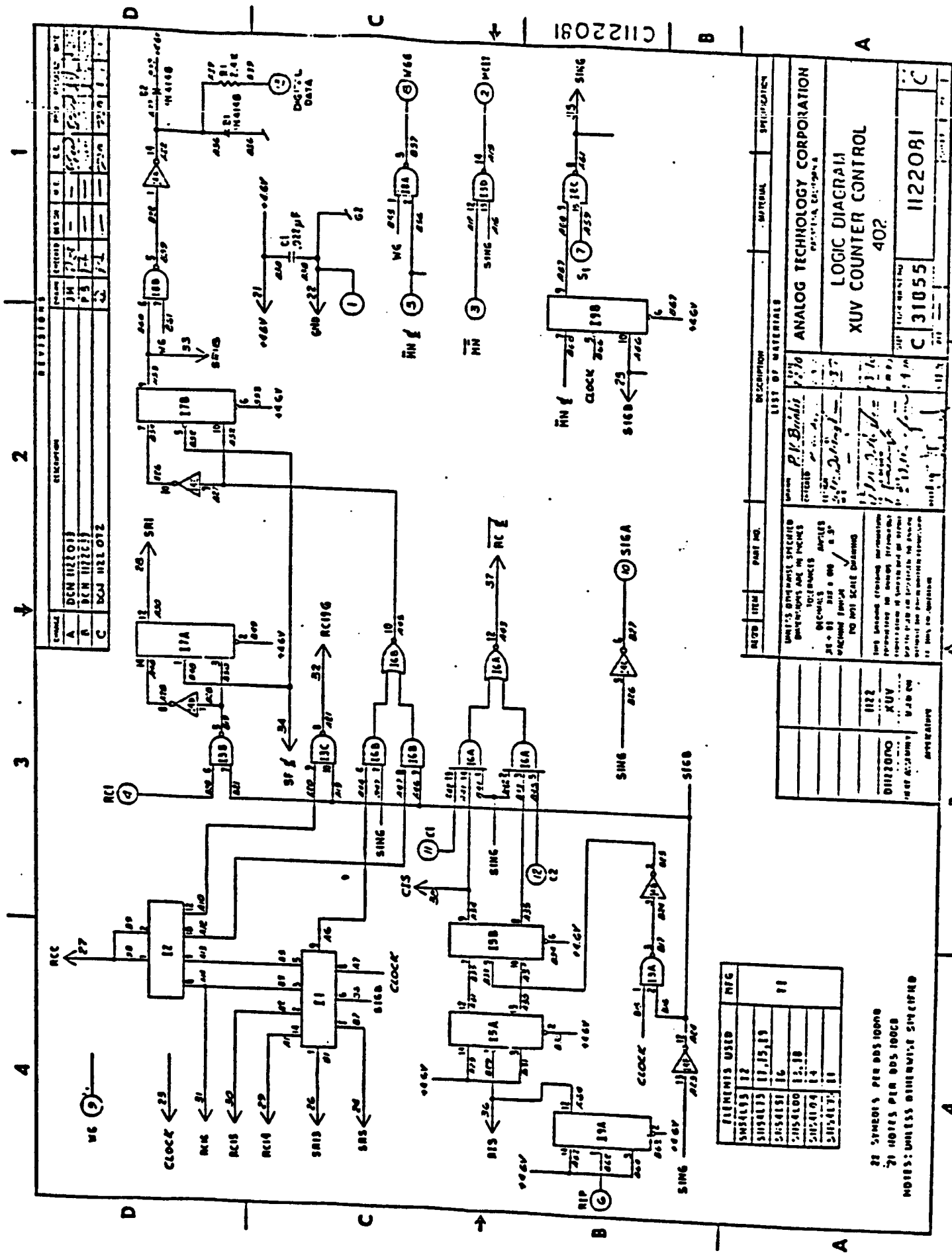
ANALOG TECHNOLOGY CORPORATION
LOGIC DIAGRAM
XUV COUNTER CONTROL
402
1122081
C 31055

Figure 3 - 9

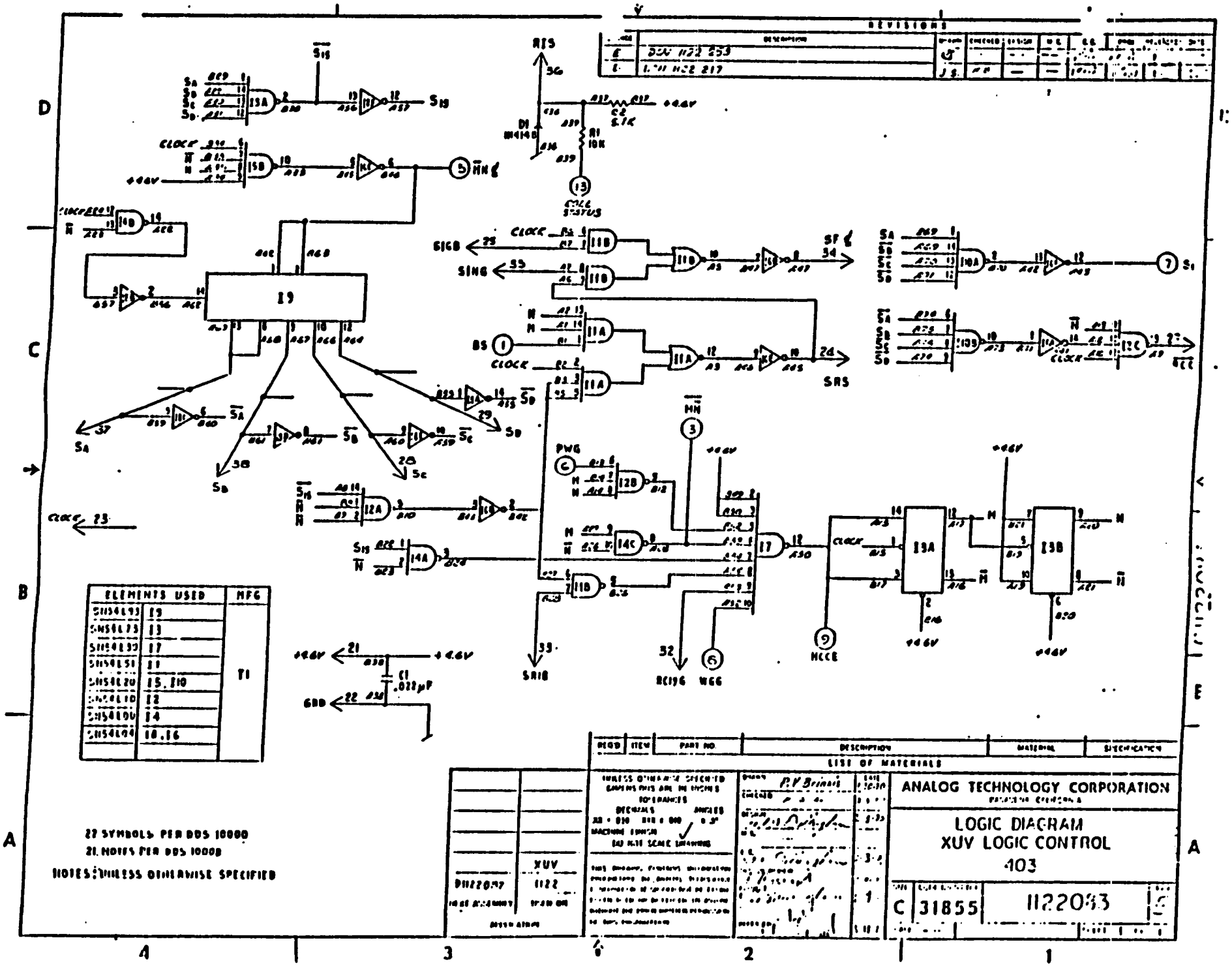
ELEMENTS USED
MFG
T1
22 SYMBOLS PER DDS 10000
21 NODES PER DDS 10000
NOTES: UNLESS OTHERWISE SPECIFIED
LIST OF MATERIALS
ANALOG TECHNOLOGY CORPORATION
LOGIC DIAGRAM
XUV LOGIC CONTROL
403
C 31855
1122083

Figure 3 - 10

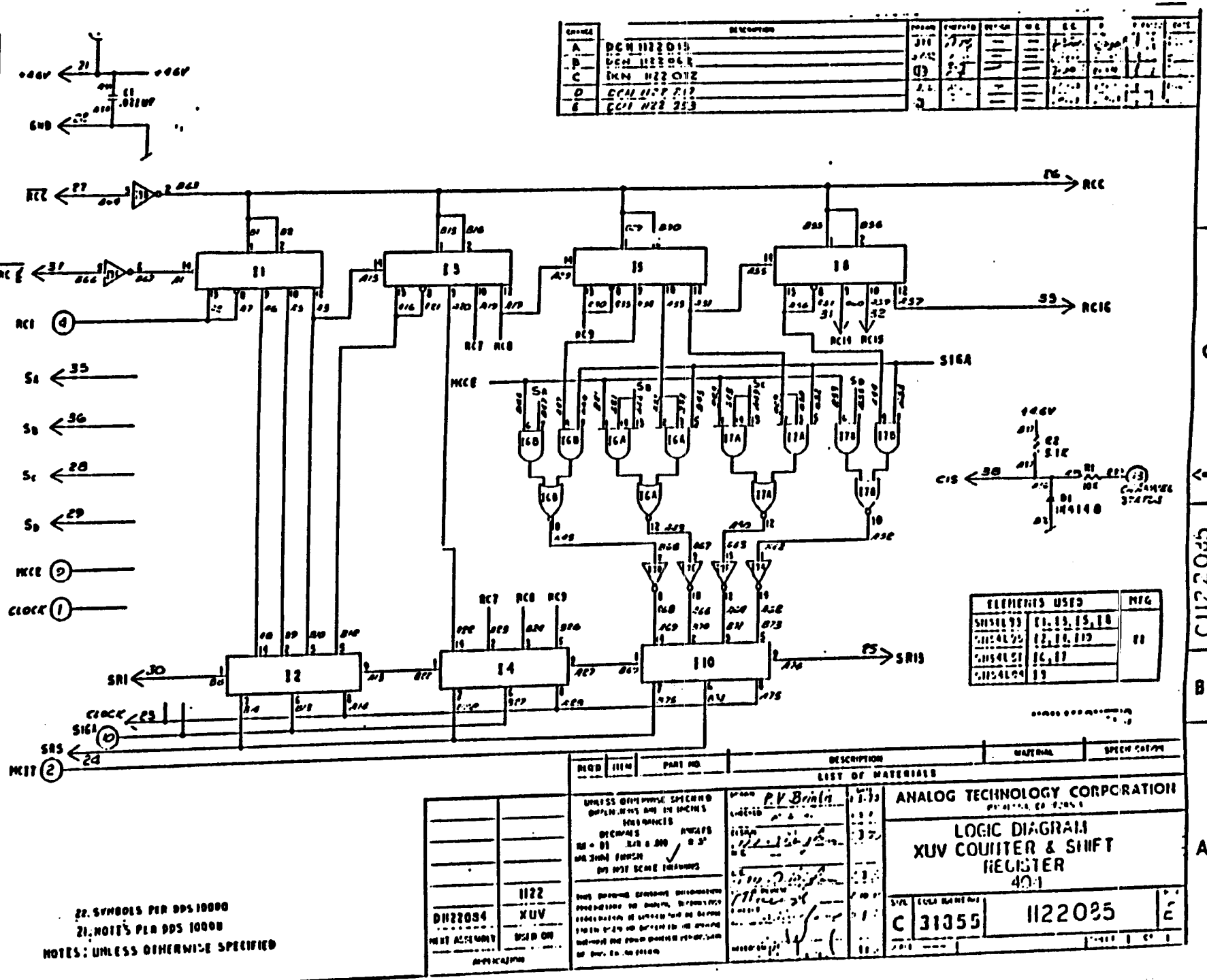
ANALOG TECHNOLOGY CORPORATION
LOGIC DIAGRAM
XUV COUNTER & SHIFT REGISTER
4011
C 31355 1122025
LIST OF MATERIALS
NOTES: UNLESS OTHERWISE SPECIFIED
22. SYMBOLS PER DDS 10000
21. NOTES PER DDS 10000
I1
I2
I3
I4
I5
I6
I7
I8
I9
I10
SRI
SRIS
RCC
RCI6
S16A
CLOCK
SIG1
SRS
MCLT
MCCE

Figure 3 - 11

3.3 Power-Conditioning Unit, Subassembly 31

The power-conditioning unit (PCU) converts the spacecraft voltage into the several voltages needed by the various parts of the instrument. A variable duty cycle, switching regulator is used for this purpose. The selection of this conversion technique was based primarily on conversion efficiency considerations. The system described below has an overall efficiency of approximately 68% at the voltage and power levels required by the XUV Instrument.

A block diagram of the PCU is shown in Figure 3-12. The clock pulse turns on a power switch that connects the primary winding of an energy-storage transformer to the spacecraft power lines. The length of time that the switch is on, and thus the amount of energy stored in the transformer, is controlled by a magnetic amplifier. When the power switch is turned off, the stored energy is distributed to the various converter loads by the secondaries of the transformer. The output of one secondary is compared against a voltage reference zener, and the resulting error signal is used by the magnetic amplifier to control the duty cycle of the power switch. The equation relating output voltages to the spacecraft voltage and the power switch duty cycle is

$$V_o = \frac{N_o}{N_{sc}} \frac{\eta}{1-\eta} V_{sc}$$

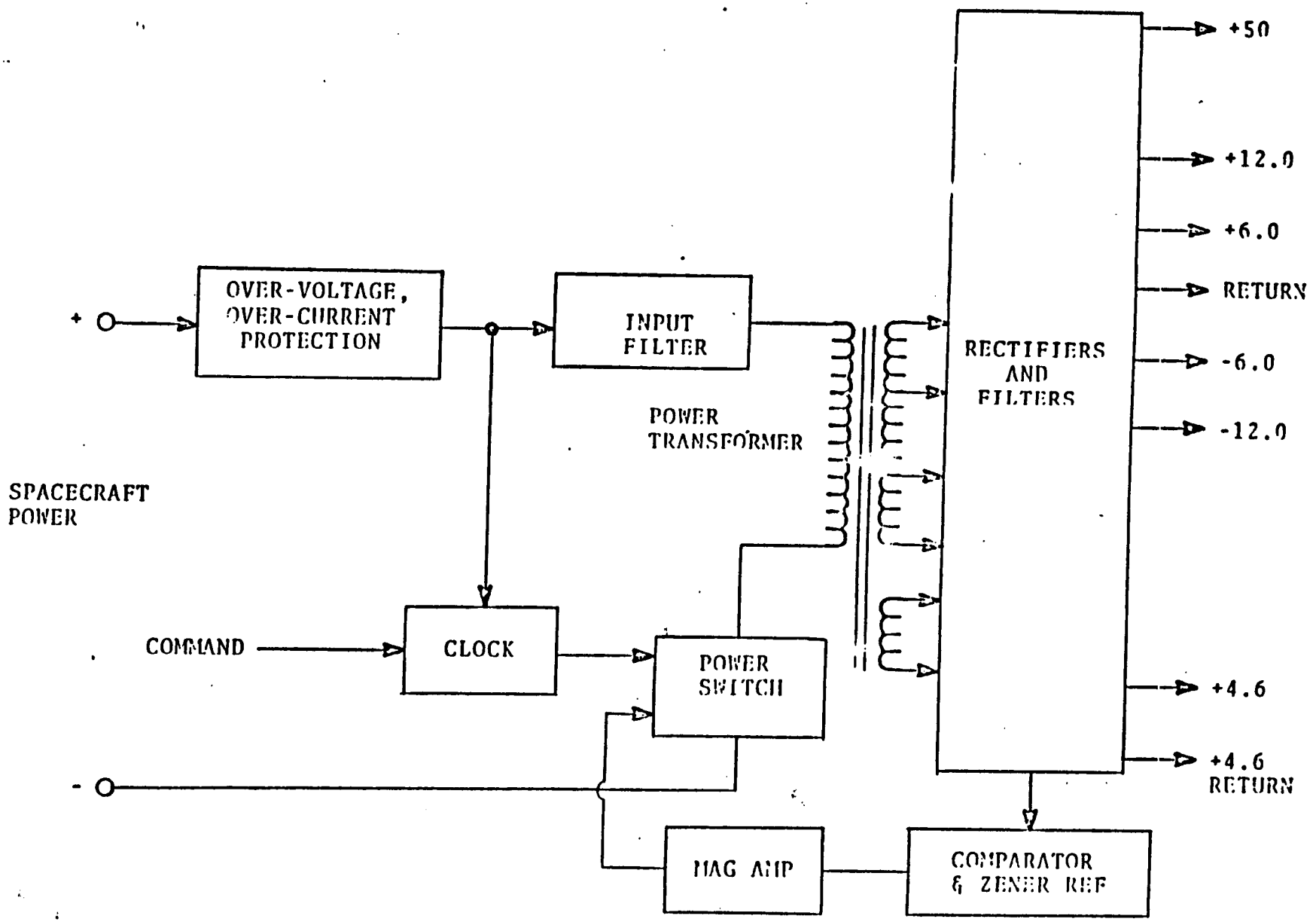

Figure 3-12 Power Conditioner Block Diagram

where V_o = an output voltage

V_{sc} = spacecraft voltage

N_o/N_{sc} = secondary/primary turns ratio

η = power switch duty cycle

The efficiency of this conversion technique depends mainly on the storage characteristics of the power transformer and the operation characteristics of the power switch. The transformer uses a gapped ferrite core, representing a choice between bulk, weight and satisfactory core loss. The air gap is internal to the core, minimizing the radiated magnetic field. The transistor is picked for low-saturation V_{ce} drop, high current gain and fast switching specifications.

Because of the extreme weight restrictions on this instrument package, the PCU clock is set at 50 kHz. This allows the use of a very lightweight transformer and minimum-sized filter capacitors. The transformer's capacitive losses are kept to a minimum by severely restricting the number and amplitudes of the transformer outputs.

Figure 3-13 is the schematic for the PCU. The discussion of the schematic will follow in greater detail the same sequence as the one for the PCU block diagram, starting with the clock/command circuits.

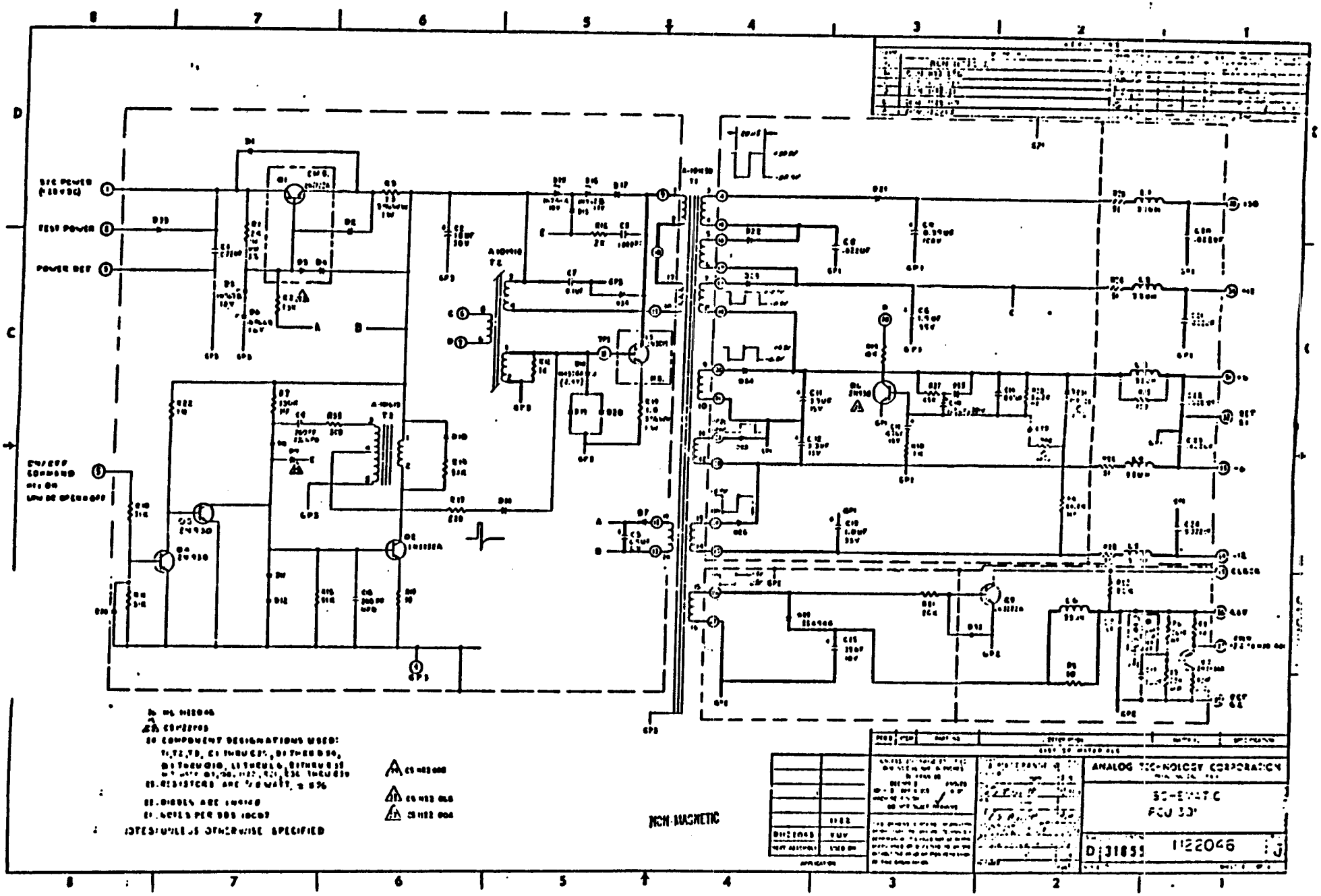
NON-MAGNETIC
ANALOG TECHNOLOGY CORPORATION
D 31855
1122046

Figure 3 - 13

3.3.1 Clock/Command

When the command line is low, Q4 is biased off. Current through R22, drawn from the spacecraft power line through R1, Q1 base-emitter and R3, saturates transistor Q5. This clamps the base of Q2 and the current through R7 to ground. With Q2 clamped off, no clock signals are generated and the PCU stays off. When the command line goes high, Q4 saturates and Q5 turns off, allowing Q2 to turn on.

As Q2 turn on, its collector voltage drops, placing a voltage across pins 1 and 2 of transformer T3. This voltage is coupled to pins 3 and 5, causing the voltage on pin 3 to rise above ground. This rise in the secondary voltage is capacitively coupled by C4 to the base of Q2, also causing the base voltage to rise. The positive feedback loop is now established; Q2 switches on in about 1.0 μs and the full voltage of C2 is applied across the transformer primary. Since the junction of Q4 and R7 can only rise three diode drops above ground, C4 acquires a charge proportional to the transformer turns ratio times the supply voltage. The clock output line goes high and turns on the power switch, an aspect that will be discussed in more detail later.

The current through R7, except for a small loss through R13, flows into the base of Q2, keeping it saturated. The

transformer primary has an inductance L. The current through it, After time t, is

$$I = \frac{E}{L} t$$

This increasing I causes an increasing IR_e drop. When this voltage drop becomes large enough, the current from R7 starts flowing through diodes D11 and D12. when the current being carried by the transistor becomes too large, the base drive is cut down and the transistor comes out of saturation and the collector voltage of Q2 rises.

This collector voltage rise represents a decrease in the voltage across the transformer primary; the secondary voltage also decreases. The decrease is capacitively coupled to the base of Q2, removing further base drive. The positive feedback is not nearly as pronounced this time since it is disconnected as soon as D8 is back-biased. After D8 is back-biased, the stored base charge in Q2 gradually dissipates, assisted somewhat by current to ground through R13.

With Q2 turned off, the primary voltage drop goes to zero and the voltage at pin 3 goes to ground. Diode D8 is back-biased by the charge placed on C4 when Q2 is turned on. This charge is dissipated by current through R7; there is an exponential rise towards +28 V. This rise is cut short when D8 becomes forward biased and Q2 turns on again. This

completes the oscillation cycle.

Some energy is stored in the inductance of the transformer primary due to the current in its primary, which can be stated as

$$E = \frac{L}{2} I^2$$

This energy is dissipated through D10 and R14 immediately after Q2 turns off and causes pin 2 of the transformer to be higher than pin 1 for a short period of time. Transistor Q2 is on for only 3% to 4% of the time. It is worth noting that C4 is charged to a voltage proportional to the supply voltage, and R7 discharges C4 at a rate also directly proportional to the supply voltage. Thus, to the first order, the frequency of this oscillator is independent of supply voltage. The required independence condition is that the voltage charge on the capacitor be large with respect to three diode drops.

3.3.2 DC-to-AC Converter

The dc-to-ac converter circuit is composed of Q3, T2 and T1. When the clock line rises, current is forced through diode D14 into terminal 8, the exact amount being limited by R17. The inductance of the drive winding (1-2) of magamp T2 is large enough so that most of the clock drive

current goes into the base of Q3, turning it on. The supply voltage is thus applied across the series combination of the primary of T1 and the feedback winding (3-4) of T2. The supply voltage will, at first pass, divide across these two windings in proportion to their inductances.

The turns ratio between the drive winding and the feedback winding of magamp T2 is 2:1. Since terminal 8 can only go positive for two diode drops at the most, the positive voltage across the feedback winding is about 0.7 V. Almost all of the supply voltage is therefore impressed across the primary of T1 and its inductance controls the flow of current.

$$I_{Q3} = \frac{V_s}{(L1)} \quad t$$

This amount of the current flows through the feedback winding of T2 and, since currents are stepped down when voltages are stepped up, one-third of this current is driven into the base of Q3 (there is substantial loss in the magamp). Transistor Q3 consequently operates under forced beta conditions, always receiving at its base approximately one-third of its collector current. The current from the clock input circuit is now extraneous; saturated operation of Q3 is established, and the clock drive can be removed.

Current flow in Q3 is now established. It will increase until some nonlinearity is reached. From previous

discussion, one can recognize the current limiter properties of R19 in the emitter lead of Q3 and the two diodes from its base to ground. This provides a basic limit on the magnitude of current which can flow. This limit will only be exercised when, for example, a secondary of T2 is shorted out, causing the primary inductance to drop and allowing Q3's collector current to rise faster than expected.

As the current flow increases, the energy stored in the magnetic fields of the two transformers is also increasing. From the discussion of the clock circuit, we have

$$E = \frac{L}{2} I^2$$

Substituting in the expression for I, we have energy stored in terms of volts x seconds:

$$E = \frac{1}{2L} (Vt)^2$$

The amount of energy that can be stored in magnetic materials is limited. The B field usually has an upper limit; the magnetic material is said to have saturated when further increases in drive cause no further increase in B. The materials in both transformers T1 and T2 can saturate, causing the inductances of their windings to decrease greatly. T1 is very carefully designed to not saturate

under all the extremes of temperature, load, and supply voltage which can be reasonably expected. T2 is very carefully designed to saturate abruptly at a specific level, independent of temperature or current levels in its windings. When it saturates, the voltage put out by the drive winding (1-2) drops to zero. This removes base drive from Q3, which turns off. Q3 will be on for 60% of a clock period unless there is current through windings 5-6 of T2.

Since Q3 operates about one-half of the time, the current pulled by it is pulsed to about twice the dc level. Capacitor C2 provides a low-impedance source for this pulse current. R3 serves to keep the ripple transferred to the spacecraft line down to a reasonable level.

3.3.3 Energy Storage Transformer

Energy was stored in transformer T1 during the on time of Q3. This energy is transferred to the loads when Q3 is turned off. This configuration gives good control of the energy being transferred through the low-voltage power supply. In particular, output shorts only deplete the energy in the transformer rather than pulling power directly from the input power line.

With the clock operating and the dc-to-ac converter cycling, the output voltages rise to a level determined by the following calculations.

The current in the primary of T1 is given by

$$I_L = Vt/L \qquad (1)$$

$$E_K = 1/2\ LI^2 \qquad (2)$$

where E_K is the energy stored in the magnetizing inductance. Substituting (1) into (2) gives

$$E_K = \frac{1}{2L} (Vt)^2 \qquad (3)$$

giving the stored energy in terms of applied voltage and length of time applied. To determine the primary/secondary voltage transformation, we assume that all energy stored in the primary is transferred to the secondary. Thus,

$$E_{KP} = \frac{1}{2L_p} (V_p T_p)^2 = E_{KS} = \frac{1}{2Ls} (V_s T_s)^2 \qquad (4)$$

The primary and secondary inductances are proportional to the number of turns in their respective coils, resulting in

$$L_p = A_L\ N_p^2,\ L_s = A_L\ N_s^2 \qquad (5)$$

where A_L is dependent on the magnetic and geometric properties of the core. Substituting (5) into (4) gives

$$\frac{(V_p T_p)^2}{2A_L N_p^2} = \frac{(V_s T_s)^2}{2A_L N_s^2} \tag{6}$$

$$\frac{V_p T_p}{N_p} = \frac{V_s T_s}{N_s} \tag{7}$$

Since the magamp/power switch combination is cycled by the arrival of the clock pulse, T_p and T_s are related to the clock period

$$T_p + T_s = P. \tag{8}$$

It is convenient to have a standardized period of 1, so that we can write

$$T_p = \tau, \quad T_s = 1 - \tau. \tag{9}$$

Substituting (9) into (7) gives

$$\frac{V_p \tau}{N_p} = \frac{V_s (1 - \tau)}{N_s} \tag{10}$$

Solving for the transformer's secondary voltage results in

$$V_s = \frac{N_s}{N_p} V_p \left(\frac{\tau}{1 - \tau}\right) \qquad (11)$$

From equation (11) we can say that, for a fixed duty cycle, the secondary voltage (V_s) is directly related to the primary voltage (V_p) and the turns ratio (N_s/N_p). If, however, the duty cycle is increased, the secondary voltage will increase in direct proportion. When the duty cycle is 0.6 and since the turns ratio to the +6.0-V line is 0.3,

$$V_s = .3 \times 28 \times \frac{.6}{1-.6} = 13 \text{ V}$$

The output voltages will therefore rise sufficiently high. A regulator is needed to prevent excessive voltage.

3.3.4 Zener Reference and Error Amplifier

Zener diode D31 and the voltage divider R20 and R40 essentially monitor the +6.0-V line; the current through R4 serves mainly to keep the zener on. When the +6.0-V line is low, the divider network output is low and transistor Q6 is off. This prevents bias current from flowing through bias winding 5 - 6 of transformer T2; the magamp gives maximum duty cycle. When the +6.0-V line gets high enough,

transistor Q6 turns on. The resulting bias current cuts down the duty cycle of the magamp as shown in Figure 3-14. The regulating loop is established in this manner. The loop gain is high enough to keep the 6.0-V output steady to 1% while the spacecraft power line moves from 22 to 34 V.

The loop gain is controlled by a variety of components. The principle pole-zero pair is formed by R40 (about 8 k), C15, and R10, giving corner frequencies of 5 Hz and 200 Hz. Capacitor C14 gives some lead compensation, with the first corner at 20 kHz. Capacitor C10 gives a strong lead compensation during turn-on as it charges through diode D35. Once the circuit is regulating, it is out of the circuit. Since it discharges through R27 and R20 when the power is turned off, the power must be left off for at least 1 second whenever it is turned off.

The necessity for C10 is as follows. When the magamp is running at 60% duty-cycle, the energy transferred per cycle is approximately twice that required during normal operation. The output voltages consequently rise fast during turn-on. While the output voltages are rising, however, capacitor C15 is being charged negatively. When the +6.0-V line reaches approximately +4.0 V, C15 starts charging positively through R20. Its voltage must move approximately 1.0 V while charging through an effective resistance of 100 k. This would take approximately 100 ms, which is a comparatively long time. The output voltages would overshoot by 50% or so. The function of C10 is, then,

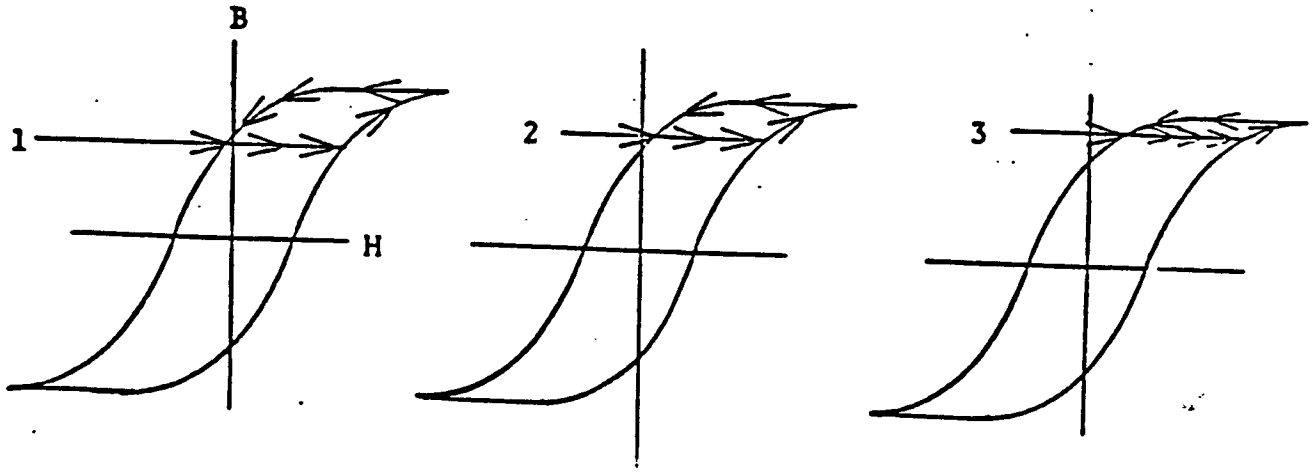

Point 1 is the initial point with no control winding current and magnetic core energy expended. When transistor switch Q3 is turned on, the operating point moves to the right across the BH loop and up to saturation. Q3 is then turned off, and the operating point moves to the left and down to point 1. The next sketch shows some control winding current and the initial point established at 2. The closed-loop locus now traces out a smaller energy product. Initial point 3 represents greater control current, thus allowing for an even smaller $\Delta\phi$, and thus less time, before saturation occurs.

Figure 3-14. Magamp B/H Loop

to fast-charge C15. Diode D30 provides a rough temperature compensation to the base-emitter diode of Q6.

3.3.5 Input Current and Over-voltage Protection

The PCU contains two protective elements: an input current limiter and an over-voltage limiter. The current limiter is composed of transistor Q1 and associated resistors and diodes. Under normal operation, the current through R2 saturates Q1. The voltage from the base of Q1 to the point labeled B is then about one base-emitter voltage plus the IR drop across R3. As the load current increases above the nominal value, the voltage from the base of Q1 to point B increases due to increased IR drop. Limiting occurs when the voltage across R3 equals the voltage across D4 (assuming that the voltage across D3 equals the base-emitter voltage Q1). In the event of a catastrophic short on the output of the current limiter, this configuration must stand full-limit current at the highest supply voltage, so Q1, D3, and D4 have a common heat sink. The current limit is set to 2.0 times the maximum running current. Limit stability over the required temperature range is about ±13%.

If the spacecraft voltage rises higher than the combined zener voltages of D5 and D6, these two diodes conduct. These zeners then define the maximum voltage that may appear at the base of Q1 and therefore the maximum voltage seen by the PCU.

3.3.6 Miscellaneous Circuits

Since the PCU generates frequencies in the 1 to 10 MHz region, regardless of the harmonics of the 50-kHz switching frequency, all output lines have rf filters.

Transistor Q9 provides the clock drive to the digital section of the instrument, protecting the digital IC's from negative transformer swings while providing a current sinking capability of approximately 30 mA. Transistor Q10 provides a low-impedance reference voltage to module 401. The PNP emitter follower provides a natural current limit of 4.6 mA.

As discussed earlier, the clock transistor Q2 turns off when its collector current becomes excessive. This is true for low (10 - 14) spacecraft voltages. The clock runs at 50 kHz with a 6-μs long output pulse. This assures long on times of Q3 before there is enough spacecraft voltage to cause sufficient current flow to cause the magamp to cycle. When the PCU is regulating, the collector of Q3 will rise 20 V above the spacecraft line and C5 will take a charge from current flowing through R16, D13, and D15. When Q3 saturates, point E will be pulled below ground and C5 will discharge through D9, turning off the clock transistor Q2 rapidly. As the spacecraft voltage rises from zero, therefore, the clock will have two operating modes, slow speed with long output pulses and fast speed with short output pulses.

3.4 High-Voltage Power Supply

The high-voltage power supply for the XUV instrument is a regulated, switching-mode supply. Regulation is achieved by feeding back a signal from the output to control the pulse width of a pair of continuously-cycling switches. The supply exhibits good output regulation and excellent efficiency.

A block diagram of the supply is shown in Figure 3-15. The local oscillator is a class-A amplifier with feedback. It starts oscillating when the input power is turned on. The output of the oscillator drives a set of switches, connecting the input of the L/C "Q" multiplier to either a supply voltage or ground. Since the L/C tank circuit has an optimum operating frequency (its self-resonant frequency) giving maximum voltage multiplication, part of the tank's output is used to slave the local oscillator. The tank drives a diode/capacitor multiplier, which develops the final output voltage. This voltage is compared to a known reference voltage and the duty cycle of the signal to the power switches is adjusted to maintain the required output voltage.

The more detailed descriptions given below are divided into two sections according to their frames of reference. The first section describes the schematic, while the second considers the theoretical aspects.

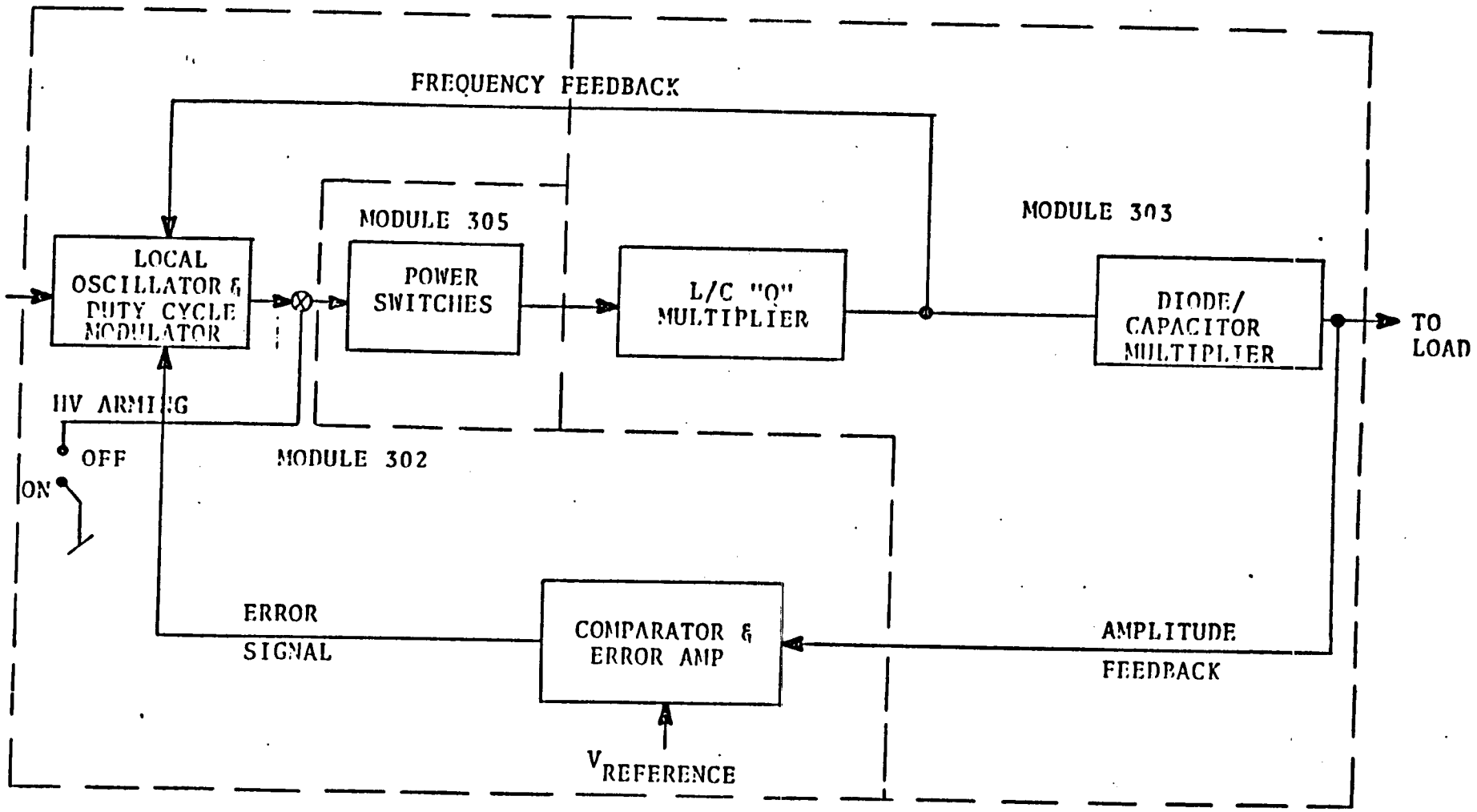

FIGURE 3-15 High-Voltage Power Supply Block Diagram

3.4.1 Detailed Circuit Description

In Figure 3-16 (module 302) transistor Q1 is the local oscillator and duty-cycle modulator. Its two bases are biased at +6.0 V, the left-hand base by resistor divider R3, R5, R6, and R7 and the right-hand base by resistor R4. If we assume that diodes D4 and D17 are not conducting, the 200 μA of current through R2 is evenly divided between the two sides of the transistor, so that their collector voltages match at approximately +0.5 V. Since the collector voltage of Q1A is fed back to its base through resistive divider R6, R5, and R3, both Q1A and Q1B are guaranteed to be conducting in spite of a ±1.0-V uncertainty in any power supply line (+12, +6, or -6). While the resistive feedback guarantees excellent dc stability, the existence of the three capacitors C2, C3 and C4 guarantees more than 180° of phase shift at some frequency. Thus, transistor Q1A is the active element in a phase-shift oscillator. The oscillation is assisted by the positive feedback from the collector of Q1A to the base of Q1B. The operating frequency is approximately three times higher than that computed from a typical (R6, C3) time constant. The operating frequency is approximately 25 kHz.

Since there is more than enough loop gain to guarantee oscillation, the 200 μA through R2 is essentially switched back and forth between Q1A and Q1B. The collector current of Q1A is integrated by capacitor C4, causing the voltage

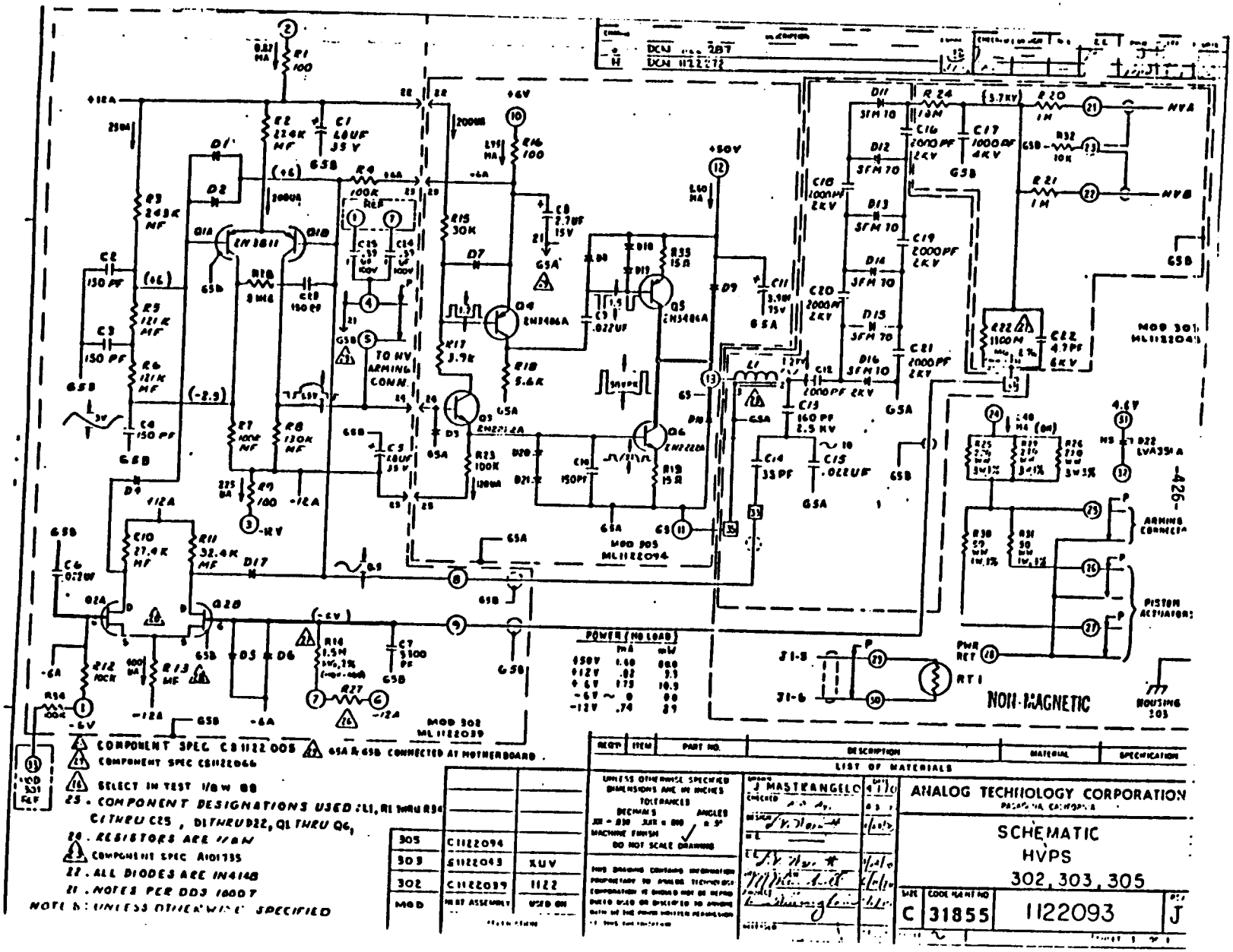
ANALOG TECHNOLOGY CORPORATION
SCHEMATIC
HVPS
302, 303, 305
C 31855 1122093 J
NON-MAGNETIC
LIST OF MATERIALS
COMPONENT SPEC C81122005
COMPONENT SPEC C81122066
SELECT IN TEST 1/8W 88
COMPONENT DESIGNATIONS USED: L1, R1 THRU R34, C1 THRU C25, D1 THRU D22, Q1 THRU Q6,
RESISTORS ARE 1/4W
COMPONENT SPEC A101735
ALL DIODES ARE IN4148
NOTES PER DD3 16007
NOTE 5: UNLESS OTHERWISE SPECIFIED
65A & 65B CONNECTED AT MOTHERBOARD
MOD 301 ML1122041
MOD 302 ML1122039
MOD 305 ML1122094
TO HV ARMING CONN
ARMING CONNECTOR
PISTON ACTUATOR
HOUSING 303
POWER (NO LOAD)
+50V 1.60 80.0
+12V .82 9.9
+6V 1.75 10.5
-6V ~ 0 0.0
-12V .74 8.9
305 C1122094
303 C1122043 XUV
302 C1122039 1122
MOD ASSEMBLY USED ON

Figure 3 - 16

signal to be approximately triangular. The collector signal of Q1B is essentially square, its excursions being limited by diode D3 (module 305) and the combined base-emitter drops of Q3 and Q6. When Q1B is on, therefore, Q3, Q4, and Q6 are also on. When Q1B is off, Q5 is on. The input to the L/C tank circuit (terminal 13) is consequently alternately switched between ground and the +50-V input whenever the high-voltage arming connector is removed. Putting this connector in place shorts the base of Q3 to ground, placing a 0.6-V back bias on the base-emitter junction of Q6 and clamping it off. With signal transmission between the oscillator and the L/C section inhibited, the supply remains off.

While the arming connector is in place, the 200 μA through R15 more than supplies the 110 μA flowing through Q3 and R23. the excess current flows through diode D7, providing back-bias to transistor Q4 which is off. Since there is no base-emitter resistor around Q5, it operates in the open-base mode. Because its leakage current will accordingly be much larger than that of Q6, the voltage at the common collector point rests at the + supply voltage (+50). Capacitor C13 will, of course, have the same voltage on it.

When the arming connector is removed, the base of Q3 will be allowed to rise. Since the rise of its emitter is inhibited by the existence of C10, it will have substantially increased conduction before Q6 starts to

conduct. This extra conduction will quickly turn on Q4. The rise in the collector voltage of Q4 is coupled by C9 to the base of Q5, turning it off before Q6 is finally turned on.

When the base of Q3 falls, Q3 and Q4 are directly turned off. Capacitor C9 charges through R18, establishing a base current for Q5 of approximately 1 mA, which decays towards zero with a time-constant of 120 µs, about eight times the length of a half-period.

With terminal 13 - the input to the L/C tank circuit - being switched between ground and the +50-V supply, the tank circuit starts absorbing energy and ringing. Part of the current through capacitor C13 is coupled by capacitor C14 to the base of Q1B. The phase of the feedback is positive; when Q5 switches on, current flow is into L1, C13, C14, and Q1B base. This causes Q1B to turn off, Q3 and Q4 to turn off, and Q5 to turn on. Thus, the circulating currents of the tank circuit serve to drive the power switches to maximize the circulating current. The result is that the amplitude of the voltage swing at the output of L1 rises.

The swing at the output of L1 is coupled by C12 to diode D16, which clamps the negative peak of the signal to ground. Diode D15 conducts at the positive peak, so the dc voltage across C21 has the same value as the peak-to-peak voltage across C13. Capacitors C19 and C16 become charged in a similar fashion through their related diodes and charging capacitors. The input to R24 therefore is at a dc

potential three times higher than the peak-to-peak voltage across C13. The signal at R24 also has an ac component that is roughly sawtooth in shape, since the combined series capacitance of C16, C19, and C21 support the output current approximately 95% of the time. The combination of R24 and C17 give approximately 40 db of attenuation to this signal.

The output of R24 is coupled by the resistive divider R22, R14, and R27 to the gate of transistor Q2B. As long as the output of R24 is low, the gate of Q2B will be low and Q2B turned off. Diodes D5 and D6 prevent the gate from going too low, which would seriously upset the bias conditions of the circuit. when Q2B is off, Q2A is on and diodes D4 and D17 are back-biased as mentioned earlier. Under this condition, the oscillator and switches are completely controlled by the synchronizing current through C14. The power switches run at 50% duty-cycle and switch at the correct time for maximum energy transfer into the L/C Multiplier.

When the output gets high enough to turn Q2B on sufficiently to cause current flow in D17, the base of Q1B is pulled down. Likewise, the base of Q1A is pulled up. This puts a dc bias on the sine-wave output of the oscillator; the base of Q3 tends to rise, as does the base of Q6. Thus, Q6 stays on longer than Q5, and the operating mode moves away from 50% duty-cycle. Under no load conditions, Q5 will be on only 10% of the time. With the reduced duty-cycle, the energy shifted per cycle into the

L/C circuit is reduced to just match the energy required to maintain the output voltage.

Even though the duty-cycle is reduced, the current in the tank curcuit remains constant in proportion to the output voltage. This current is:

$$I = \frac{V_{C13}}{Z_{C13} \text{ @ } 25 \text{ kHz}} = \frac{1.2 \times 10^3}{40 \times 10^3} = 30 \text{ mA p-p}$$

When this current is flowing out of L1 into Q6, it develops a peak voltage drop across R19 of approximately 0.22 V. Since the base voltage rise of Q6 is limited by diodes D20 and D21, there is a limit to the emitter current of Q6. When the tank current is flowing into L1 and Q5 is not on, the current actually flows through diode D10. This flow pulls the collector of Q6 to -0.7 V, and the base of Q6 to ground. There will actually be current flow in Q6 in proportion to its inverse β. which isn't very large.

When Q5 does turn on, D10 and the collector-base junction of Q6 back-bias quickly, and current flows from Q5 into L1. When Q5 turns off, diode D10 resumes conduction. Thus, the signal at terminal 13 actually is negative 0.7 V during the time when neither Q5 nor Q6 are on.

3.4.2 Theoretical Discussion

The most novel part of the high-voltage supply is the L/C voltage multiplier. A schematic of the power switches and their resonant circuit load is shown in Figure 3-17. When the drive voltage is low, transistor Q5 is saturated and capacitor C is charged through inductor L. When the drive voltage is high, transistor Q6 is saturated and the capacitor discharges through L to ground. The action of the square wave formed between the collectors of the power switch and the L/C tank circuit is best described in mathematical terms.

The voltage gain of the tank circuit is computed as follows. The transfer function for the circuit is

$$V_{out} = \frac{R_L // \frac{1}{pC}}{R_L // \frac{1}{pC} + pL} \; V_{in},$$

where p is the Laplace operator. After some algebraic manipulation we have

$$V_{out} = \frac{V_{in}}{p^2 LC + \frac{pL}{R} + 1},$$

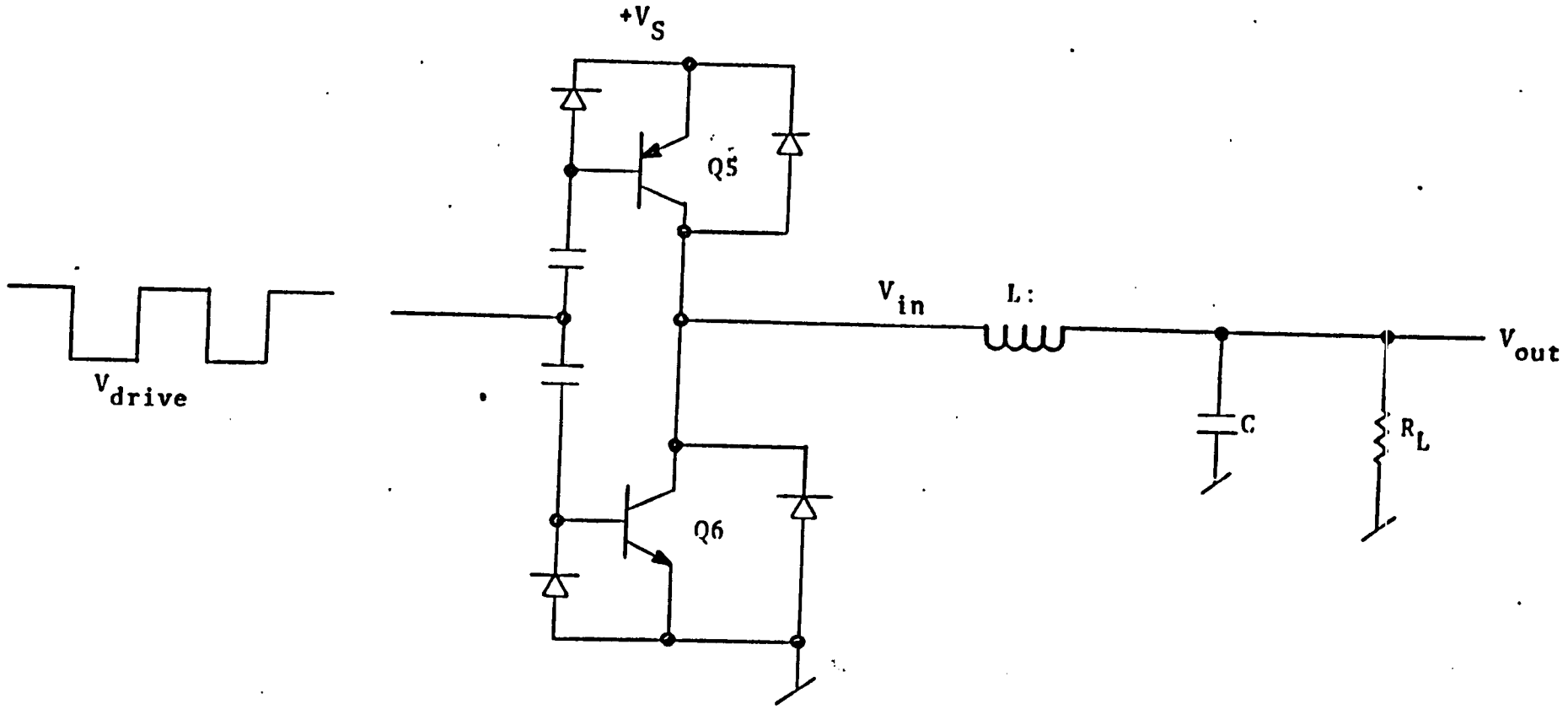

Figure 3-17 Power Switches and Q Multiplier

which is the common form for a second-order system. If $j\omega$ is substituted for p, we obtain

$$\frac{V_{out}}{V_{in}} = \frac{1}{1 - \omega^2 LC + j\omega\frac{L}{R}}$$

If the applied frequency ω is precisely

$$\omega_N = \frac{1}{\sqrt{LC}},$$

where ω_N denotes natural frequency of the tank, we have

$$\frac{V_{out}}{V_{in}} = \frac{1}{1 - \frac{1}{\sqrt{LC}}^2 LC + j\omega_N \frac{L}{R}} = -j\omega_N \frac{R}{L}$$

The term $R/\omega_N L$ is commonly called the Q of the tank circuit. Since Q's of 10 to 100 are not uncommon, significant gain can be realized at the natural resonant frequency.

The tank circuit is being driven by a variable-duty-cycle square wave:

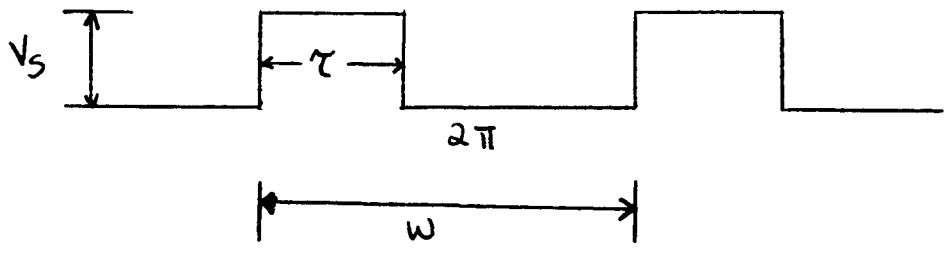

The Fourier expression for this wave is

$$V_{DR} = V_S \frac{\tau\omega}{2\pi} + \sum_{N=1}^{\infty} \frac{2V}{N\pi} \sin \frac{N\tau\omega}{2} \cos N\omega t,$$

The frequency feedback loop of the high-voltage circuit guarantees that the ω of this equation matches the ω_N of the tank circuit. Thus, the output of the tank circuit will be

$$V_{out} = V_S \frac{\tau\omega}{2\pi} + \frac{R}{\omega_N L} \frac{2V_S}{\pi} \sin \frac{\tau\omega_N}{2} \cos N\omega_N t,$$

or

$$V_{out} = V_S \frac{\tau\omega}{2\pi} + Q\frac{2V_S}{\pi} \sin \frac{\tau\omega_N}{2} \cos N\omega_N t.$$

The fundamental frequency component of the input voltage is therefore Q multiplied. Furthermore, this multiplication depends upon the duty cycle of the drive signal, varying from 0 to 1 as the duty cycle varies from 0% to 50%

Because of limits on the voltage ratings of the switching transistors and the range of Q values expected due to changing loads, the Q multiplier is followed by a diode/capacitor voltage multiplier. A schematic for such a multiplier is shown in Figure 3-18 along with the formula for computing the output ripple.

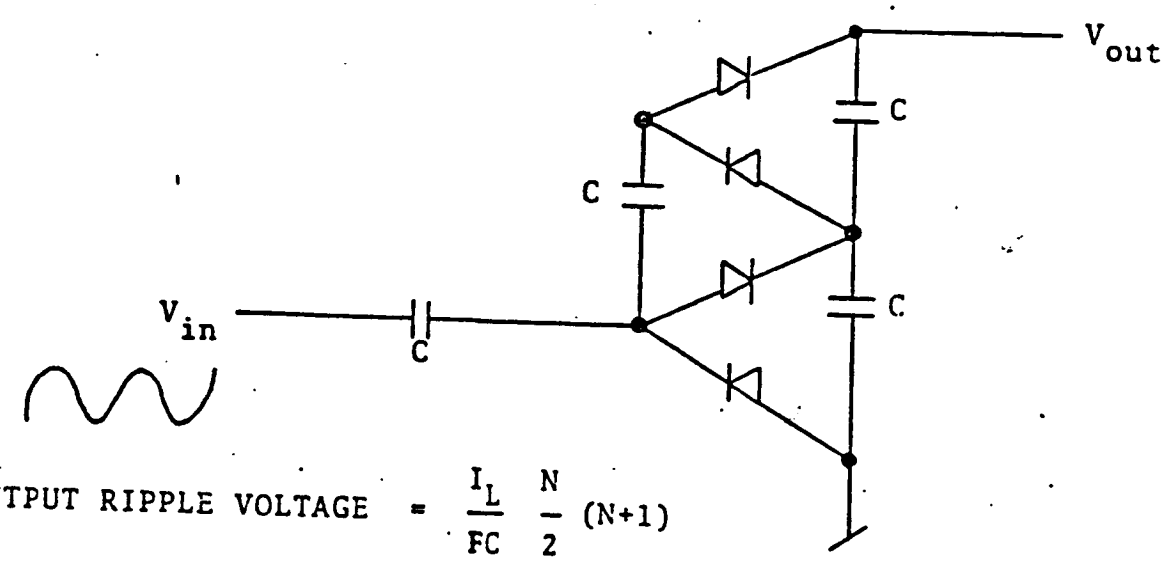

$$\text{OUTPUT RIPPLE VOLTAGE} = \frac{I_L}{FC} \frac{N}{2} (N+1)$$

I_L = average load current

F = frequency of V_{in}

C = capacitances V_{Sen}

N = number of stages

Here, N = 3;

$$V_{RIP} = \frac{6I_L}{FC}.$$

Figure 3-18

Diode - Capacitor Multiplier

3.5 Actuator Signal Generator, Subassembly 303

The actuator signal generator accepts a command signal from the spacecraft to remove the optical dust cover. This unit operates from the spacecraft's 28-Vdc power and supplies 100 mA to each of the two piston actuators. The circuit is shown in Figure 3-19. It includes an input switch, Q5, a differential stage, Q1, a switch, Q2, and a Darlington amplifier, Q3 and Q4. The input switch is activated by a positive 4-V signal which turns on the left side of Q1. The collector current runs up R6 and C1 until Q2 turns on. Q2 then pulls the Darlington pair, Q3 and Q4, on and fires the piston actuators.

The Darlington pair, which has high gain, amplifies the current to produce an output of approximately 200 mA. Current-limiting is provided in the output by R25, R26, and R29 and 50 Ω in series with each separate line feeding the two piston actuators. A shorting connector grounds the output at pin 25 to prevent current from firing the piston actuators unless desired. In this manner, the electronics can be tested after instrument assembly without destroying the actuators.

Care was required to eliminate sensitivity of the circuit to the turn on of the 28-V supply. This was achieved principally by holding Q2 off with C1 and minimizing capacitive coupling of the bus voltage to any transistors which could momentarily turn on. A long

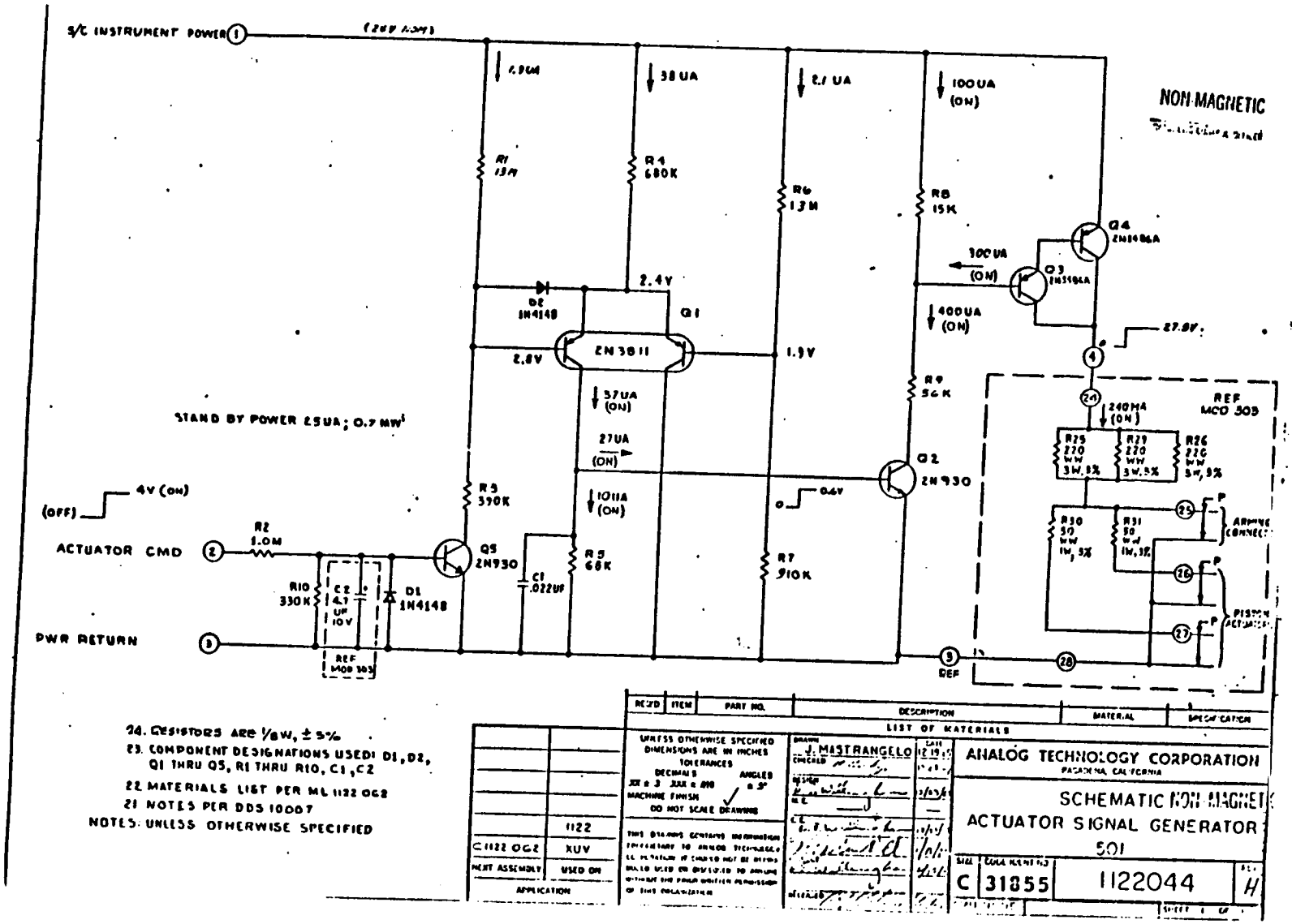
S/C INSTRUMENT POWER
NON MAGNETIC
STAND BY POWER 25UA; 0.7 MW
4V (ON)
(OFF)
ACTUATOR CMD
PWR RETURN
R1 13M
R2 1.0M
R3 390K
R4 680K
R5 68K
R6 13M
R7 910K
R8 15K
R9 56K
R10 330K
C1 .022UF
C2 4.7 UP 10V
D1 1N4148
D2 1N4148
Q1 2N3811
Q2 2N930
Q3 2N5196A
Q4 2N6486A
Q5 2N930
4.9UA
38UA
2.1 UA
100UA (ON)
100UA (ON)
400UA (ON)
2.4V
2.8V
1.9V
57UA (ON)
27UA (ON)
10UA (ON)
0.6V
27.8V
240MA (ON)
R25 270 WW 3W, 5%
R29 270 WW 3W, 5%
R26 270 WW 3W, 5%
R30 50 WW 1W, 5%
R31 50 WW 1W, 5%
REF MCO 303
REF
ARMING CONNECT
PISTON ACTUATOR
24. RESISTORS ARE 1/8W, ± 5%
23. COMPONENT DESIGNATIONS USED: D1, D2, Q1 THRU Q5, R1 THRU R10, C1, C2
22. MATERIALS LIST PER ML 1122 OC2
21 NOTES PER DDS 10007
NOTES: UNLESS OTHERWISE SPECIFIED
LIST OF MATERIALS
ANALOG TECHNOLOGY CORPORATION
PASADENA, CALIFORNIA
SCHEMATIC NON MAGNETIC
ACTUATOR SIGNAL GENERATOR
501
J. MASTRANGELO
C 31855
1122044
H
1122
XUV
USED ON

Figure 3 - 19

integration time was desired from command initiation to command execution so as to prevent accidental actuator firings. This was achieved by the capacitor at the command input circuit and provides approximately 0.6 sec integration time.

3.6 Input Decoupling and Logic Buffering, Subassembly 41

The purpose of the input decoupling was discussed in Section 2.2. In each case, the line resistance and capacitance has been set according to the guidelines given in PC-220. The input decoupling (module 500) schematic is shown in Figure 3-20.

In order to perform the shielding properly, module 500 is constructed in two sections and mounted at the instrument connector J1. The inner shield wall cuts the capacitance that occurs across each part and creates a separate filtering chamber. Lines must be kept short, as indicated, in order to eliminate loops which will pick up induced noise. The power line inductors are low-resistance (<2 Ω) 1-mH inductors designed to tolerate the large currents required when the piston actuators are fired. Damping resistors assure that ringing response does not occur during turn-on and turn-off of the high-current mode of operation. D1 assures that the reverse drop across L1B is never sufficient to retrigger the piston actuator circuit.

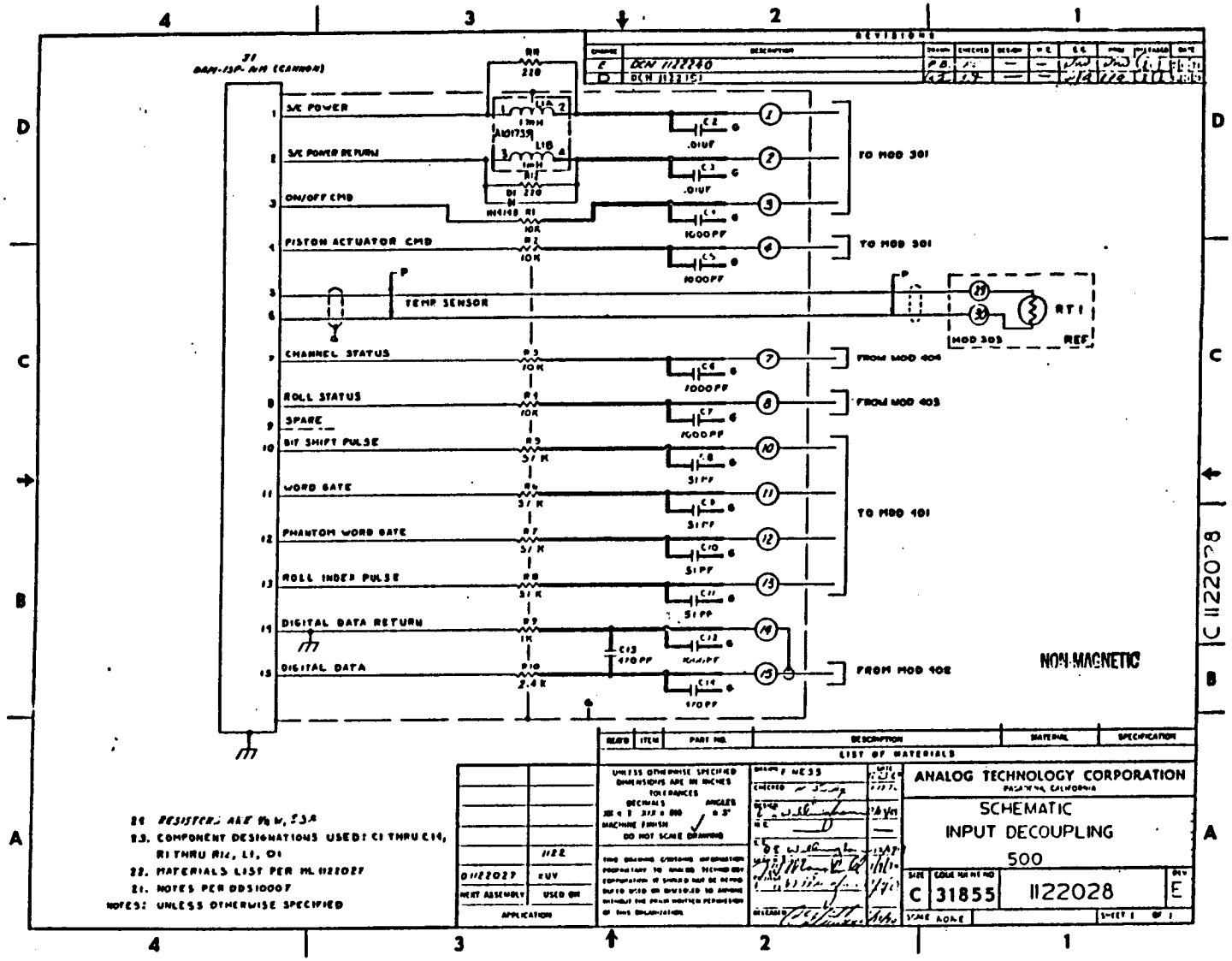
SVC POWER
SVC POWER RETURN
ON/OFF CMD
PISTON ACTUATOR CMD
TEMP SENSOR
CHANNEL STATUS
ROLL STATUS
SPARE
BIT SHIFT PULSE
WORD GATE
PHANTOM WORD GATE
ROLL INDEX PULSE
DIGITAL DATA RETURN
DIGITAL DATA
TO MOD 301
TO MOD 301
FROM MOD 404
FROM MOD 403
TO MOD 401
FROM MOD 402
RT 1
REF
MOD 303
NON-MAGNETIC
ANALOG TECHNOLOGY CORPORATION
SCHEMATIC
INPUT DECOUPLING
500
C
31855
1122028
E

Figure 3 - 20

The input buffers (module 401) shown in Figure 3-21 are hybrid versions of those which have been used several times at ATC and are essentially Schmidt triggers. These buffers are used on each spacecraft switching input signal. They are low power, have a high noise immunity and can switch states at a 2-V input signal level while providing almost 2-V of noise immunity.

The schematics for the two types of hybrid circuits indicated, are shown in Figures 3-22 and 3-23. Circuit 200010 provides more delay than circuit 200011 and assures that word gate occurs after the other spacecraft signals. Simultaneous occurrence of word gate and one of the other signals can potentially confuse the logic. The resultant buffered pulse delays are approximately 50 μs and 10 μs, respectively.

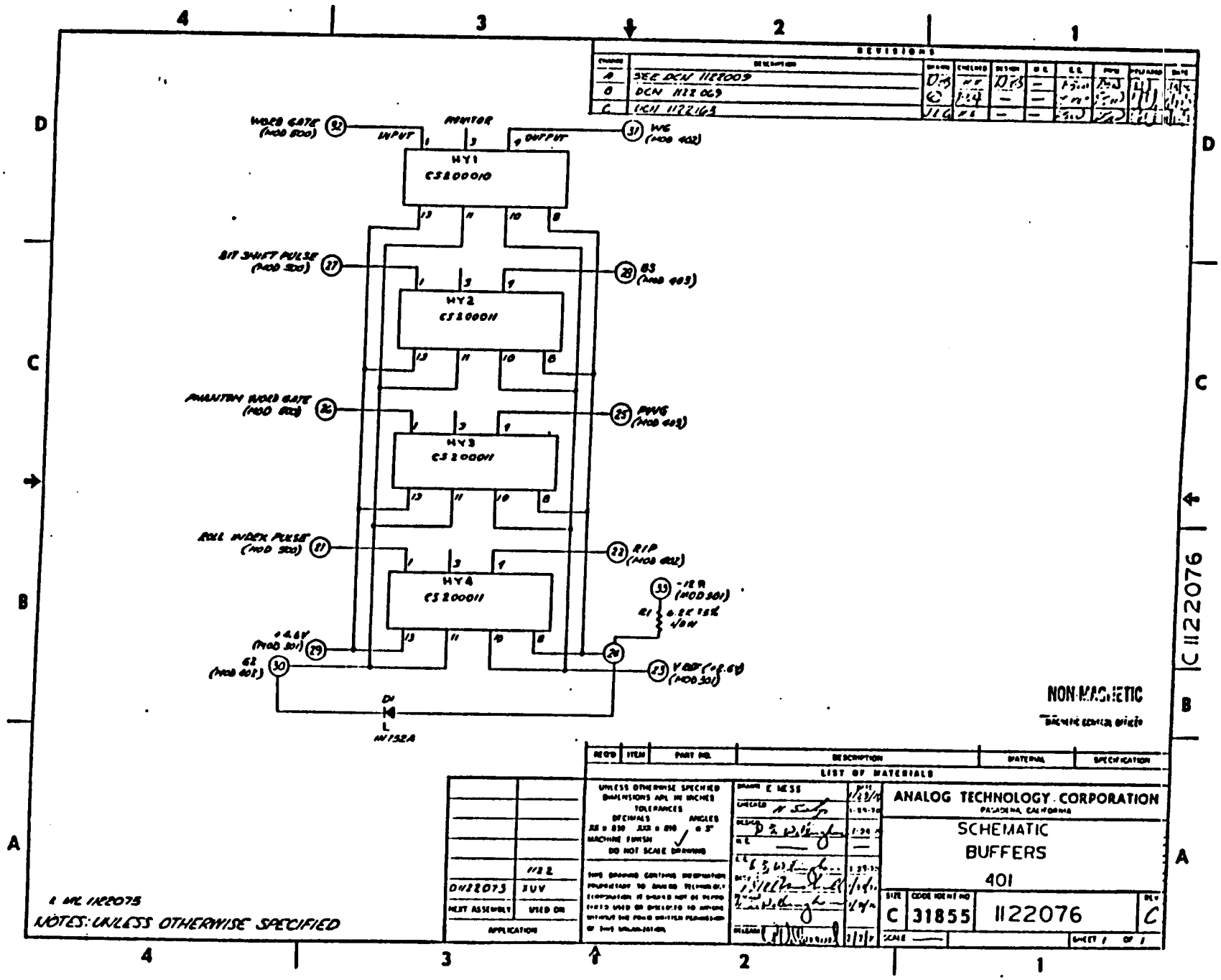
REVISIONS
A SEE DCN 1122009
B DCN 1122069
C DCN 1122163
HOLD GATE (MOD 800)
MONITOR
INPUT
OUTPUT
WE (MOD 402)
HY1
CS200010
BIT SHIFT PULSE (MOD 300)
BS (MOD 403)
HY2
CS200011
AMMUNITION HOLD GATE (MOD 800)
PWG (MOD 403)
HY3
CS200011
ROLL INDEX PULSE (MOD 300)
RIP (MOD 402)
HY4
CS200011
-12 V (MOD 301)
0.2C 1% 1/2W
+4.6V (MOD 301)
G2 (MOD 401)
V REF (+2.5V) (MOD 301)
D1
IN1524
NON-MAGNETIC
LIST OF MATERIALS
ITEM
PART NO.
DESCRIPTION
MATERIAL
SPECIFICATION
UNLESS OTHERWISE SPECIFIED
DIMENSIONS ARE IN INCHES
TOLERANCES
DECIMALS
ANGLES
MACHINE FINISH
DO NOT SCALE DRAWING
DRAWN E NESS
CHECKED
ENGR
QC
MFG
APPROVED
ANALOG TECHNOLOGY CORPORATION
PASADENA, CALIFORNIA
SCHEMATIC
BUFFERS
401
SIZE
C
CODE IDENT NO
31855
1122076
REV
C
SCALE
SHEET 1 OF 1
NEXT ASSEMBLY
USED ON
APPLICATION
NOTES: UNLESS OTHERWISE SPECIFIED
1122076

Figure 3-21

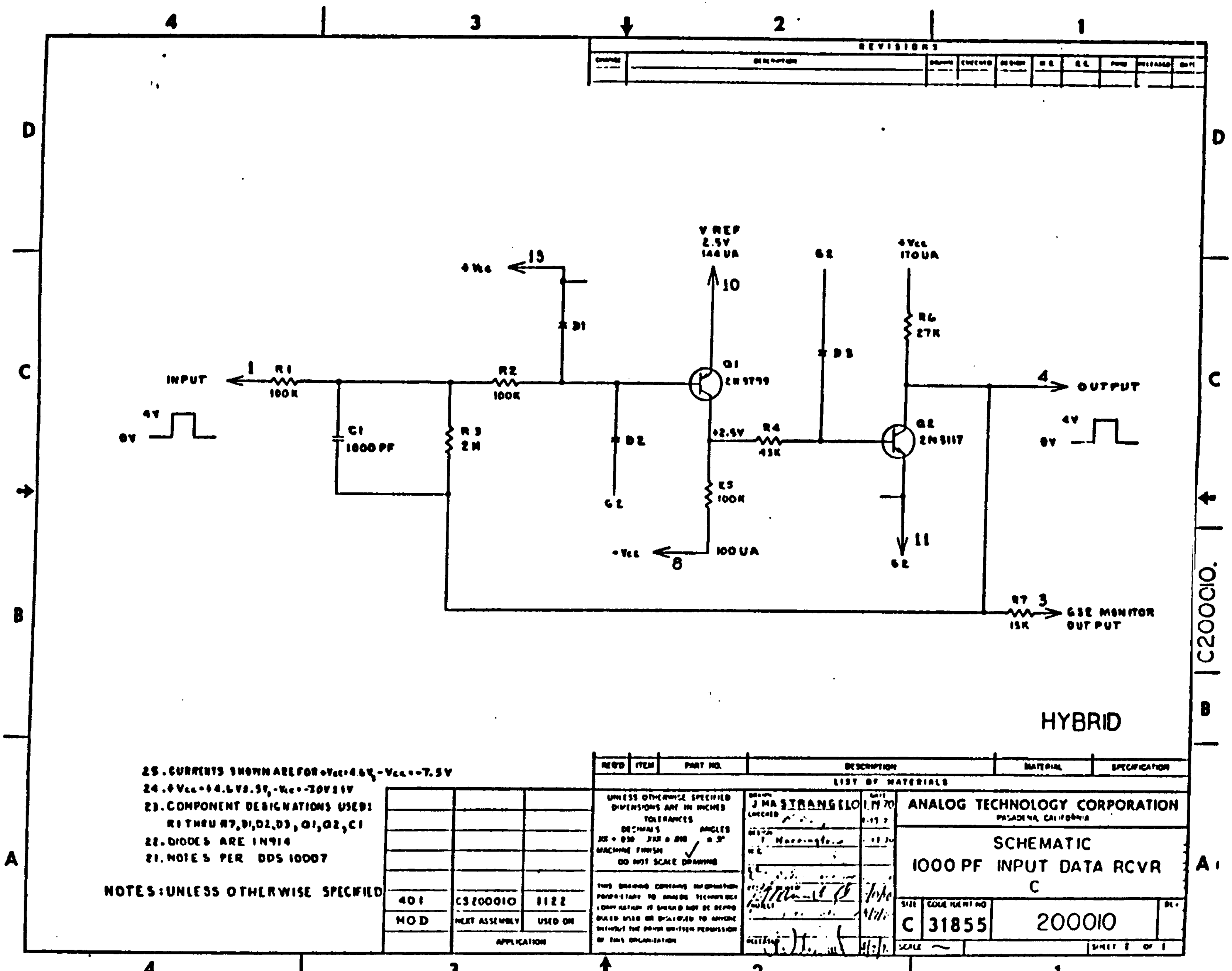

INPUT
R1 100K
C1 1000PF
R2 100K
R3 2M
D1
D2
D3
Q1 2N3799
Q2 2N3117
R4 43K
R5 100K
R6 27K
R7 15K
V REF 2.5V 144UA
+Vcc 170UA
-Vcc
100UA
+2.5V
OUTPUT
GSE MONITOR OUTPUT
HYBRID
NOTES: UNLESS OTHERWISE SPECIFIED
21. NOTES PER DDS 10007
22. DIODES ARE 1N914
23. COMPONENT DESIGNATIONS USED: R1 THRU R7, D1, D2, D3, Q1, Q2, C1
ANALOG TECHNOLOGY CORPORATION
PASADENA, CALIFORNIA
SCHEMATIC
1000 PF INPUT DATA RCVR
C
C 31855
200010
C200010

Figure 3-22

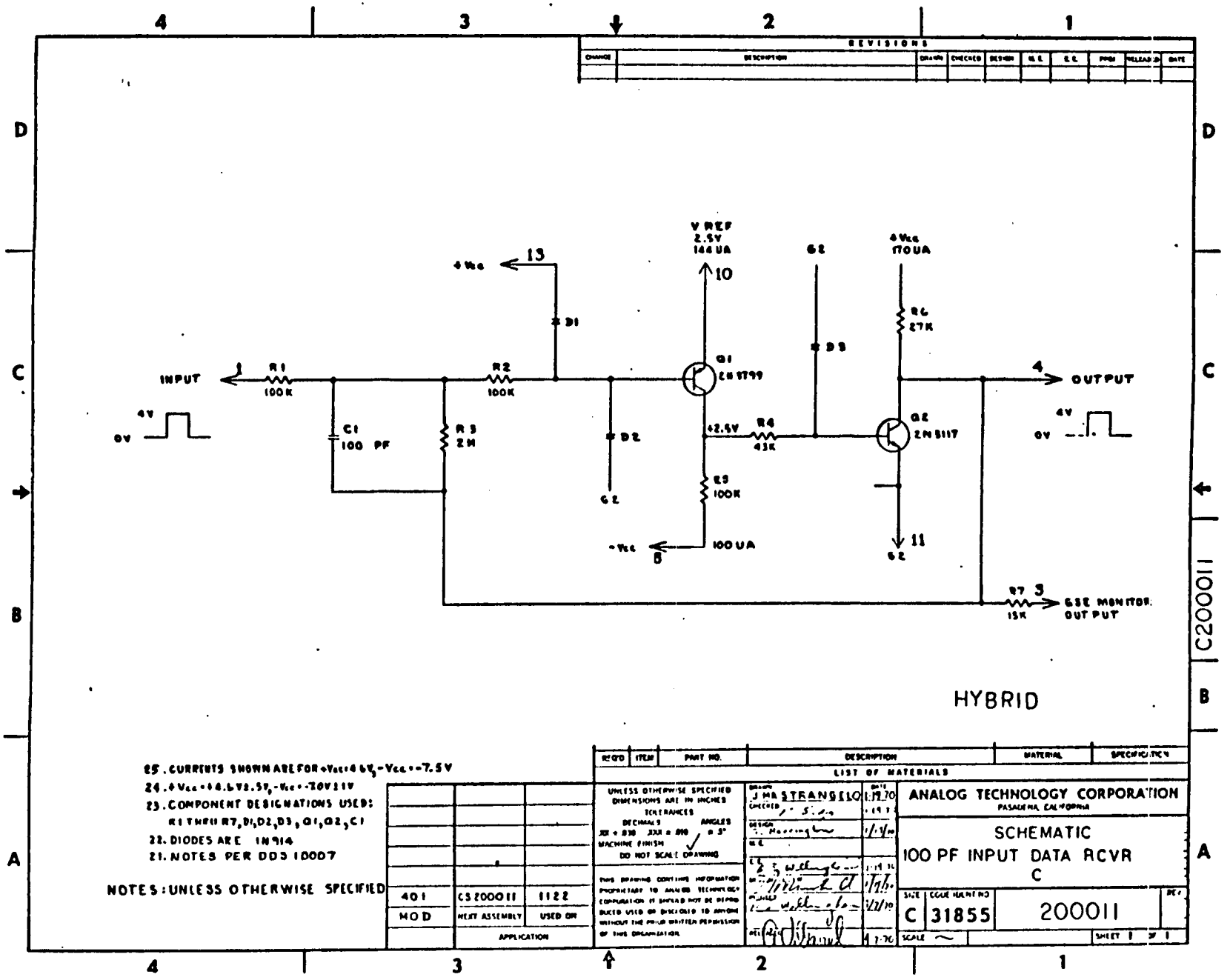
REVISIONS
INPUT
OUTPUT
4V
0V
R1
100K
R2
100K
R3
2M
C1
100 PF
D1
D2
D3
Q1
2N 5799
Q2
2N 5117
R4
43K
R5
100K
R6
27K
R7
15K
13
10
11
8
3
4
+Vcc
-Vcc
VREF
2.5V
144 UA
170UA
100 UA
62.5V
G.S.E. MONITOR OUT PUT
HYBRID
NOTES: UNLESS OTHERWISE SPECIFIED
22. DIODES ARE 1N914
23. COMPONENT DESIGNATIONS USED:
R1 THRU R7, D1, D2, D3, Q1, Q2, C1
24. +Vcc = +6.5V ± 5%, -Vcc = -10V ± 1V
25. CURRENTS SHOWN ARE FOR +Vcc = 6.5V, -Vcc = -7.5V
LIST OF MATERIALS
ANALOG TECHNOLOGY CORPORATION
PASADENA, CALIFORNIA
SCHEMATIC
100 PF INPUT DATA RCVR
C
C 31855
200011
C200011

Figure 3-23

4.0 MECHANICAL DESIGN

The mechanical configuration and dimensions of the XUV Filter Photometer are given in Figure 4-1. The main chassis provides the principal support for the field-of-view limiter and the electronics packages. In the Design Verification Unit, the main chassis was made of plated magnesium; however, later units are milled from aluminum and coated with an appropriate chemical-conversion low-emissivity paint. The instrument cover is a prefabricated aluminum box chemically etched to 0.020 inch thickness. The cover has no load elements attached to it. The field-of-view limiter is a tube constructed of 0.020-inch wall thickness cylinders with inner flanges for strength.

The purge fitting is threaded to allow the fastening of an extender tube for access through the spacecraft wall. A continuous wire fuzz button is used as a filter element in the fitting. It is assumed that the Pioneer Project controls the rate of nitrogen purge gas flow.

Due to the severe weight restrictions, the instrument packaging is very compact. The field-of-view limiter and the logic elements have required the development of new fabrication and manufacturing techniques. With such a tight package, much of the ease of component replacement has been sacrificed and almost any repair process essentially requires the disassembly of the entire instrument.

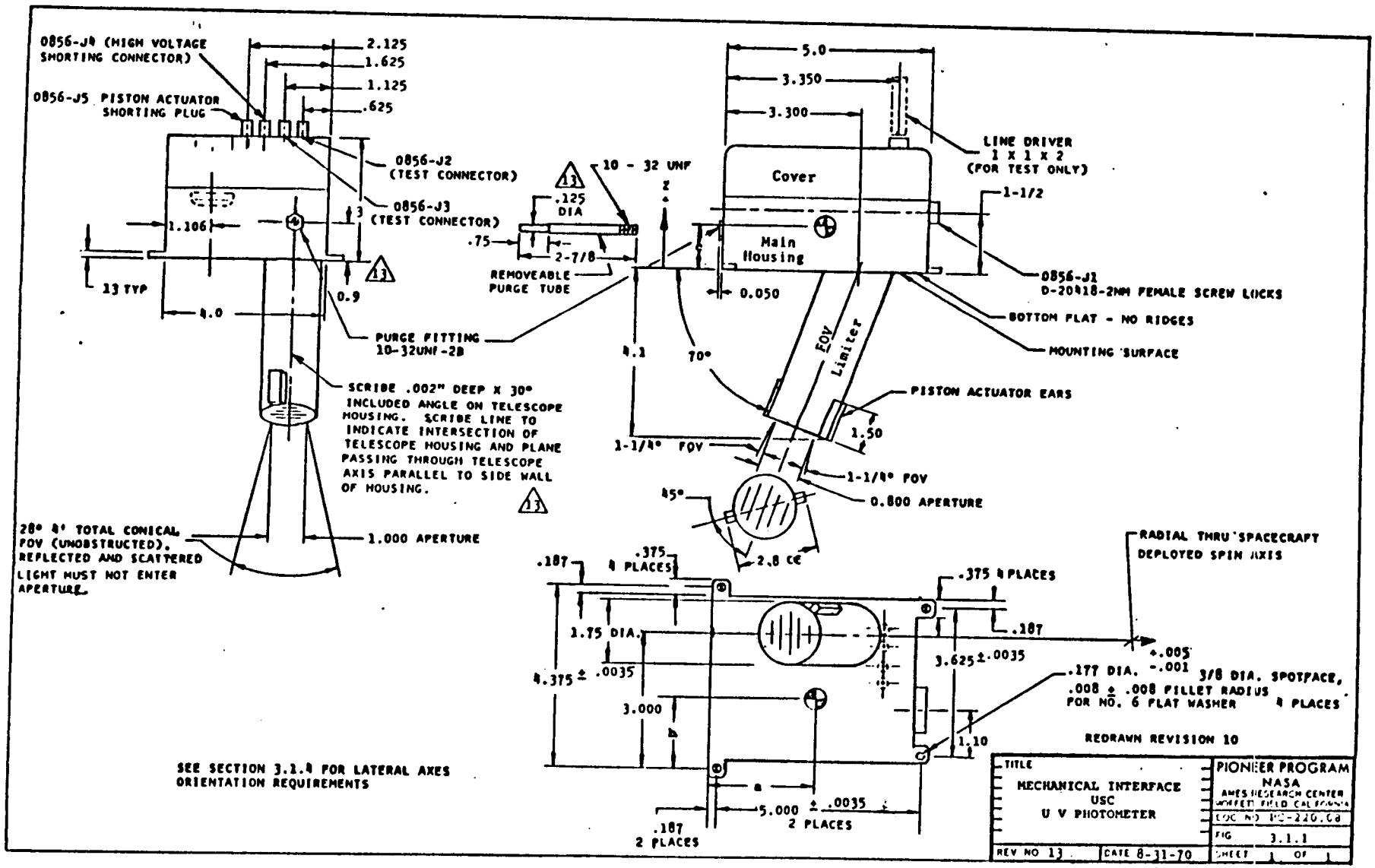
0856-J4 (HIGH VOLTAGE SHORTING CONNECTOR)
0856-J5 PISTON ACTUATOR SHORTING PLUG
2.125
1.625
1.125
.625
0856-J2 (TEST CONNECTOR)
0856-J3 (TEST CONNECTOR)
1.106
.13 TYP
4.0
0.9
PURGE FITTING 10-32UNF-2B
SCRIBE .002" DEEP X 30° INCLUDED ANGLE ON TELESCOPE HOUSING. SCRIBE LINE TO INDICATE INTERSECTION OF TELESCOPE HOUSING AND PLANE PASSING THROUGH TELESCOPE AXIS PARALLEL TO SIDE WALL OF HOUSING.
28° 8' TOTAL CONICAL FOV (UNOBSTRUCTED). REFLECTED AND SCATTERED LIGHT MUST NOT ENTER APERTURE.
1.000 APERTURE
10 - 32 UNF
.125 DIA
.75
2-7/8
REMOVEABLE PURGE TUBE
5.0
3.350
3.300
Cover
Main Housing
LINE DRIVER 1 X 1 X 2 (FOR TEST ONLY)
1-1/2
0.050
0856-J1 D-20818-2NM FEMALE SCREW LOCKS
BOTTOM FLAT - NO RIDGES
MOUNTING SURFACE
4.1
70°
FOV Limiter
PISTON ACTUATOR EARS
1.50
1-1/8° FOV
1-1/8° FOV
0.800 APERTURE
45°
2.8 CE
.187
.375 4 PLACES
.375 4 PLACES
.187
1.75 DIA.
4.375 ± .0035
3.625 ± .0035
3.000
.177 DIA. +.005 -.001 3/8 DIA. SPOTFACE, .008 ± .008 FILLET RADIUS FOR NO. 6 FLAT WASHER 4 PLACES
1.10
5.000 ± .0035
2 PLACES
.187
2 PLACES
RADIAL THRU SPACECRAFT DEPLOYED SPIN AXIS
REDRAWN REVISION 10
SEE SECTION 3.1.4 FOR LATERAL AXES ORIENTATION REQUIREMENTS
TITLE
MECHANICAL INTERFACE
USC
U V PHOTOMETER
PIONEER PROGRAM
NASA
AMES RESEARCH CENTER
MOFFETT FIELD CALIFORNIA
DOC NO PC-220.08
FIG 3.1.1
REV NO 13
DATE 8-31-70
SHEET 1 OF 1

Figure 4-1

A photograph of the Flight 1 Unit with the top cover removed are shown in Figure 4-2. The final assembly drawing is provided in Figure 4-3. As can be seen, there is little excess room. The assembly consists of the several subassemblies which were identified in presenting the discussion of Section 3.

Subassembly 10 contains the field-of-view limiter, the photocathode and the spectral bandpass filter for the channeltrons. Subassemblies 11 and 21 ride piggy back on the field-of-view limiter assembly, and, upon build-up, the entire unit is denoted as subassembly 12. Subassembly 31 is the main motherboard assembly containing the logic, PCU and high-voltage control modules. It is fastened on the main chassis support members, allowing the high-voltage multiplier assembly 303 to be packaged beneath the motherboard. The input subassembly 41 is built directly to the back of the main instrument connector. Other miscellaneous components and the piston actuator circuitry are fastened to the main chassis floor and are denoted as part of subassembly 303.

The interwiring of the various subassemblies is shown in the wiring diagram of Figure 4-4. The pin numbers denoted on this drawing and the other assembly drawings correspond to the connector points indicated in the various circuit schematics. The final assembly drawing, the wiring diagram and the schematics can be used to locate desired signal points within the instrument.

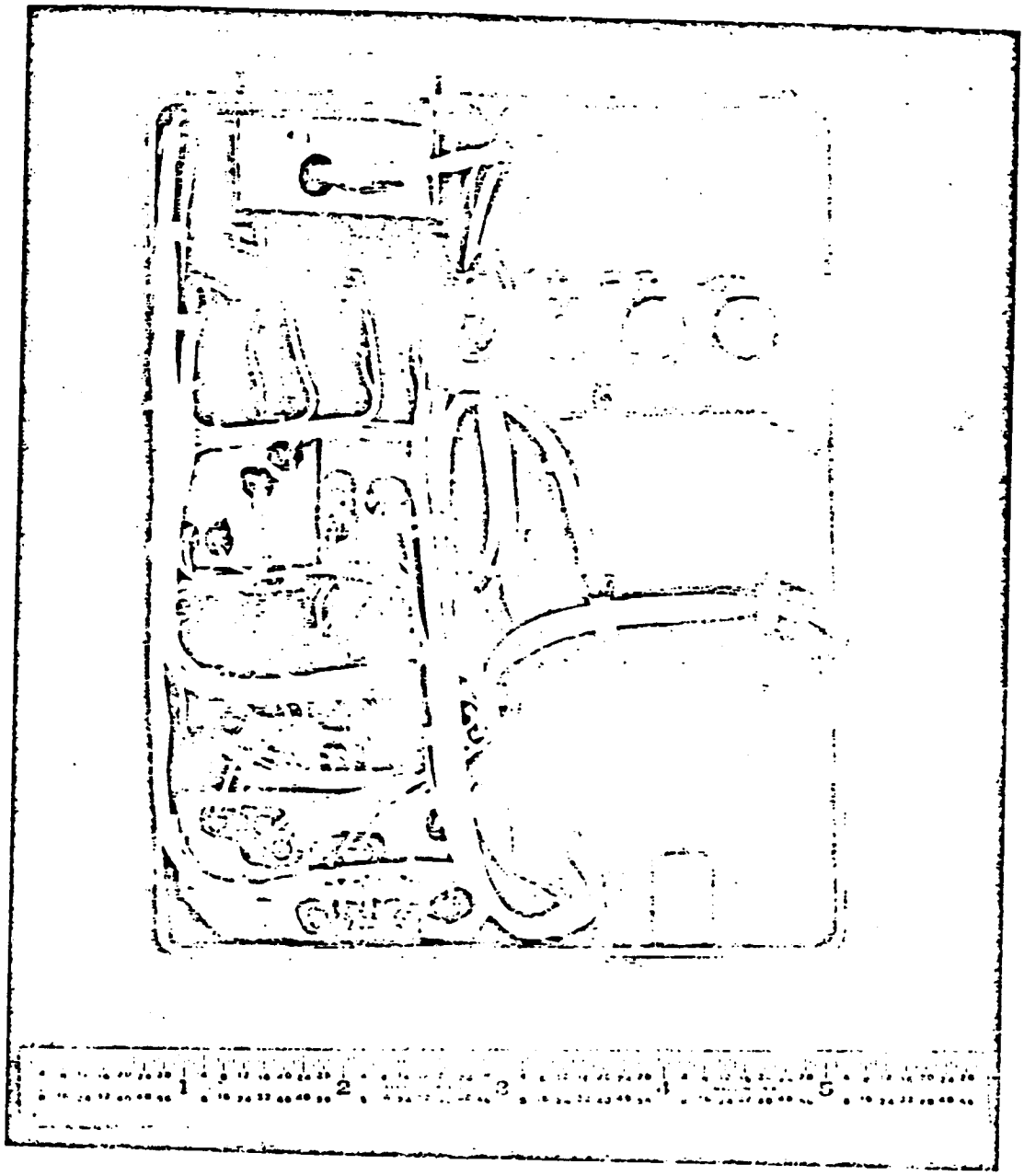

Figure 4-2. Pioneer F & G Extreme Ultraviolet Filter Photometer (Top Cover Removed)

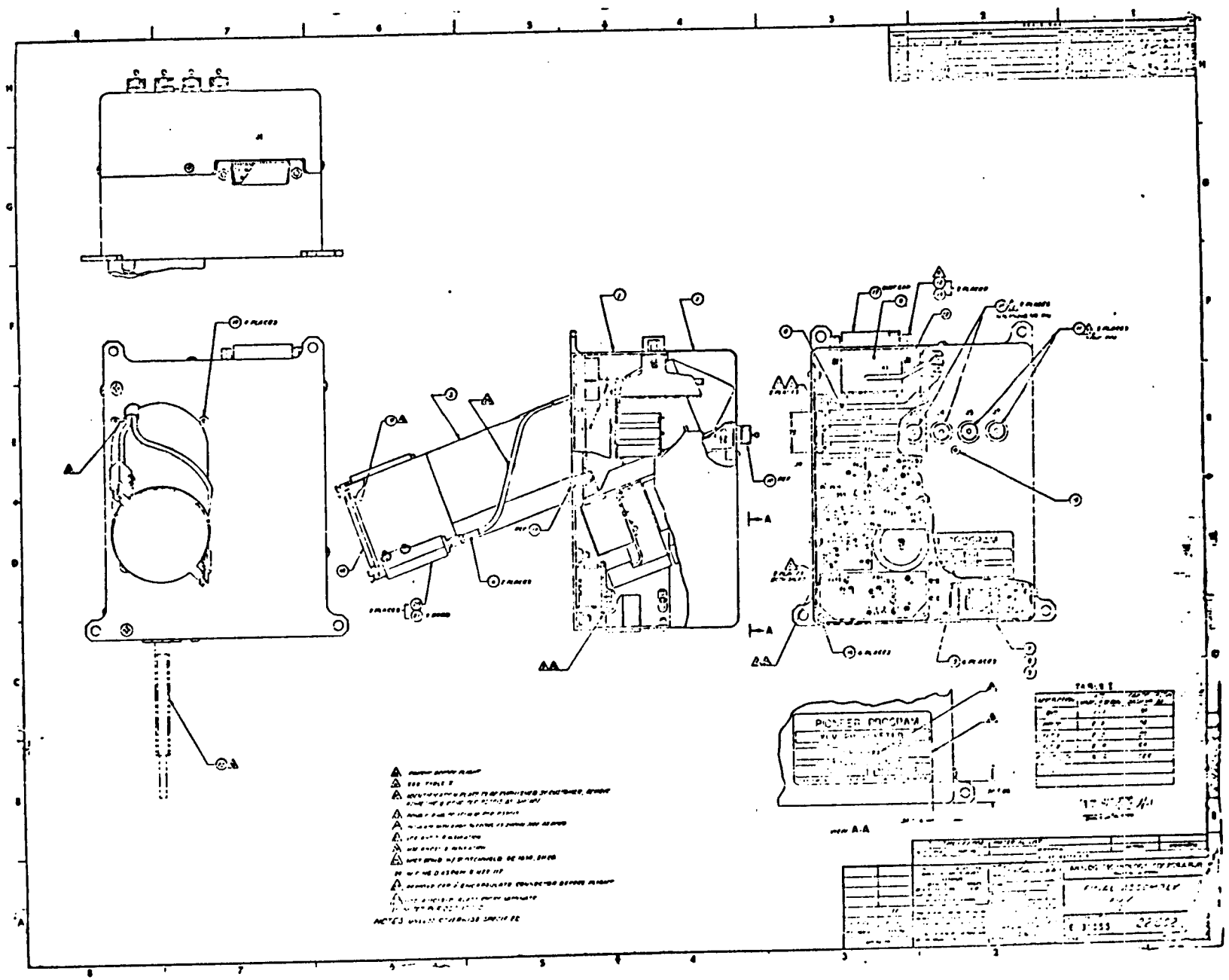

Figure 4 - 3

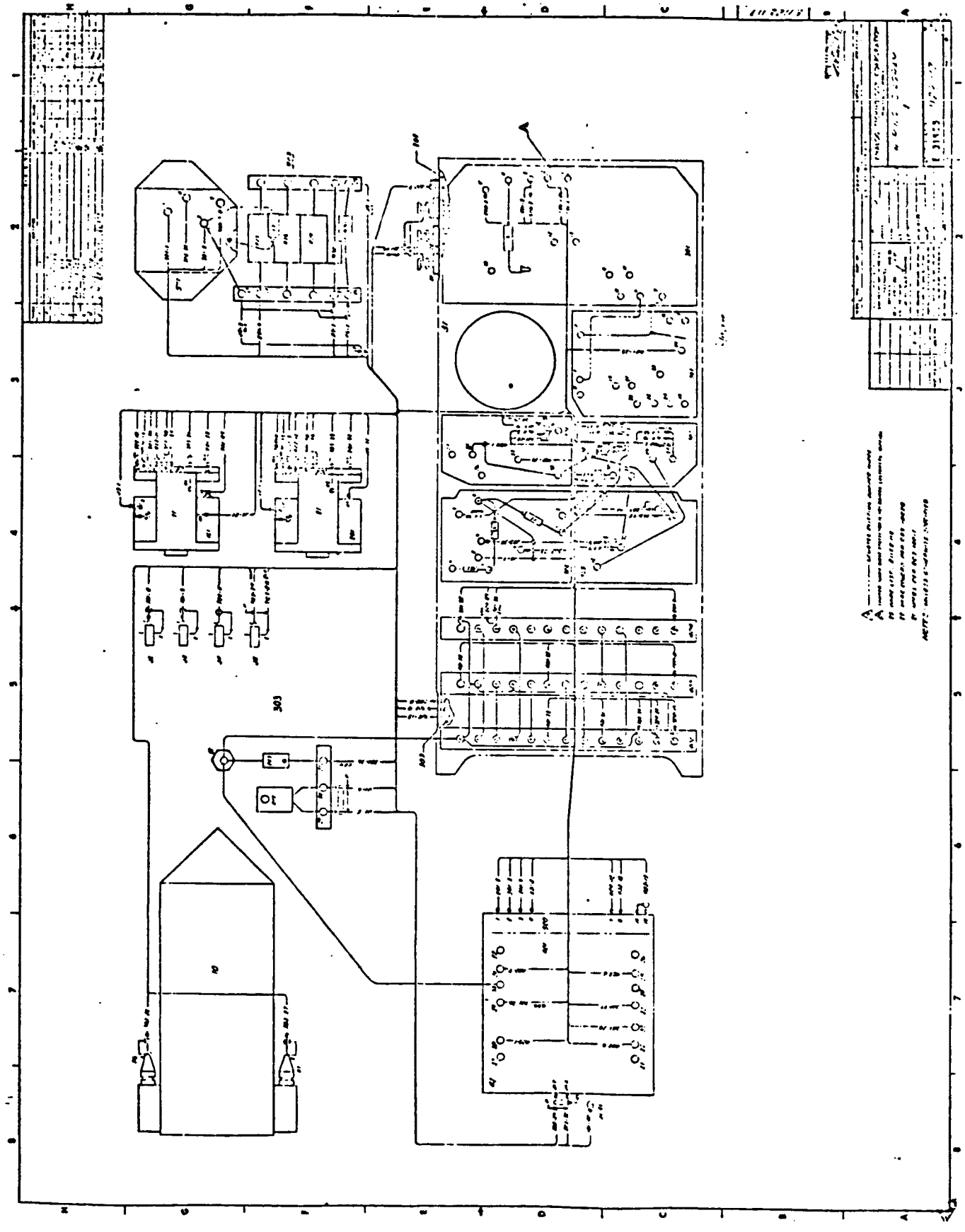

Figure 4 - 4

The major subassembly drawings are provided in Figures 4-5 through 4-11. Comments pertaining to each are given below:

Subassembly 10

The limiter is assembled by using a special tool which utilizes alignment slots that are cut later from the baffle elements. Epoxy is used to hold the elements together and a 2-mil brass wrapping indicated by 1 is used for additional strength.

The filter is cemented to the filter holder, item 2 , and is held between the limiter and photocathode elements.

The photocathode, item 3 , is buffed to a mirror finish internally and receives a lithium-fluoride coating prior to final assembly.

Subassemblies 11 and 21

The assembly drawing shows the details of the channeltron area and the interwiring of the preamplifier and the discriminator denoted by item 1 . Figure 4-7 shows the details of the freestanding high-voltage bias and decoupling components. These components are solidly potted to prevent high-voltage arcing. Their placement and the selection of potting material have been found to be very critical. Incorrect manufacture results in spurious counts being generated at the preamplifier input due to some momentary breakdown phenomenon (not corona or arcing).

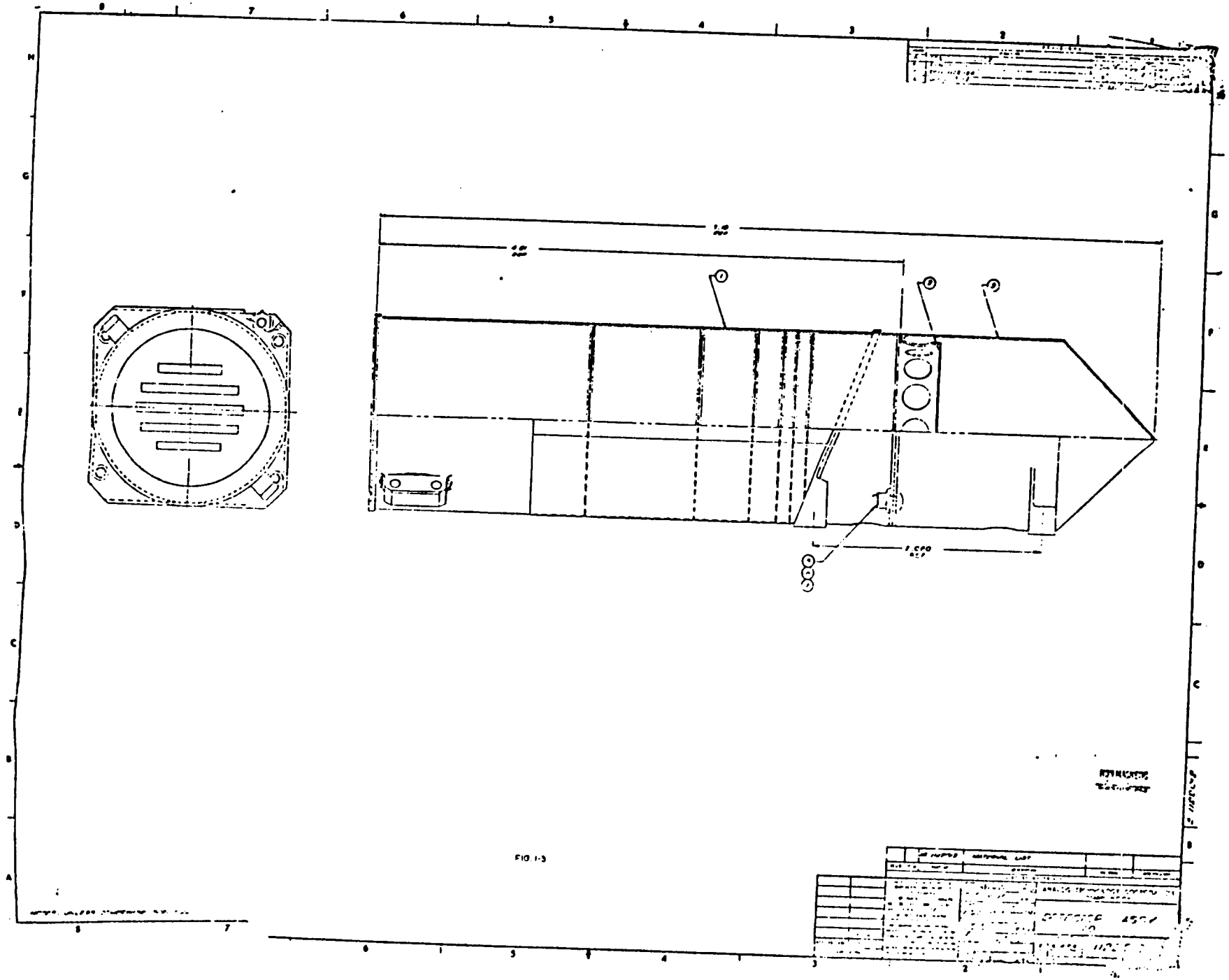

Figure 4 - 5

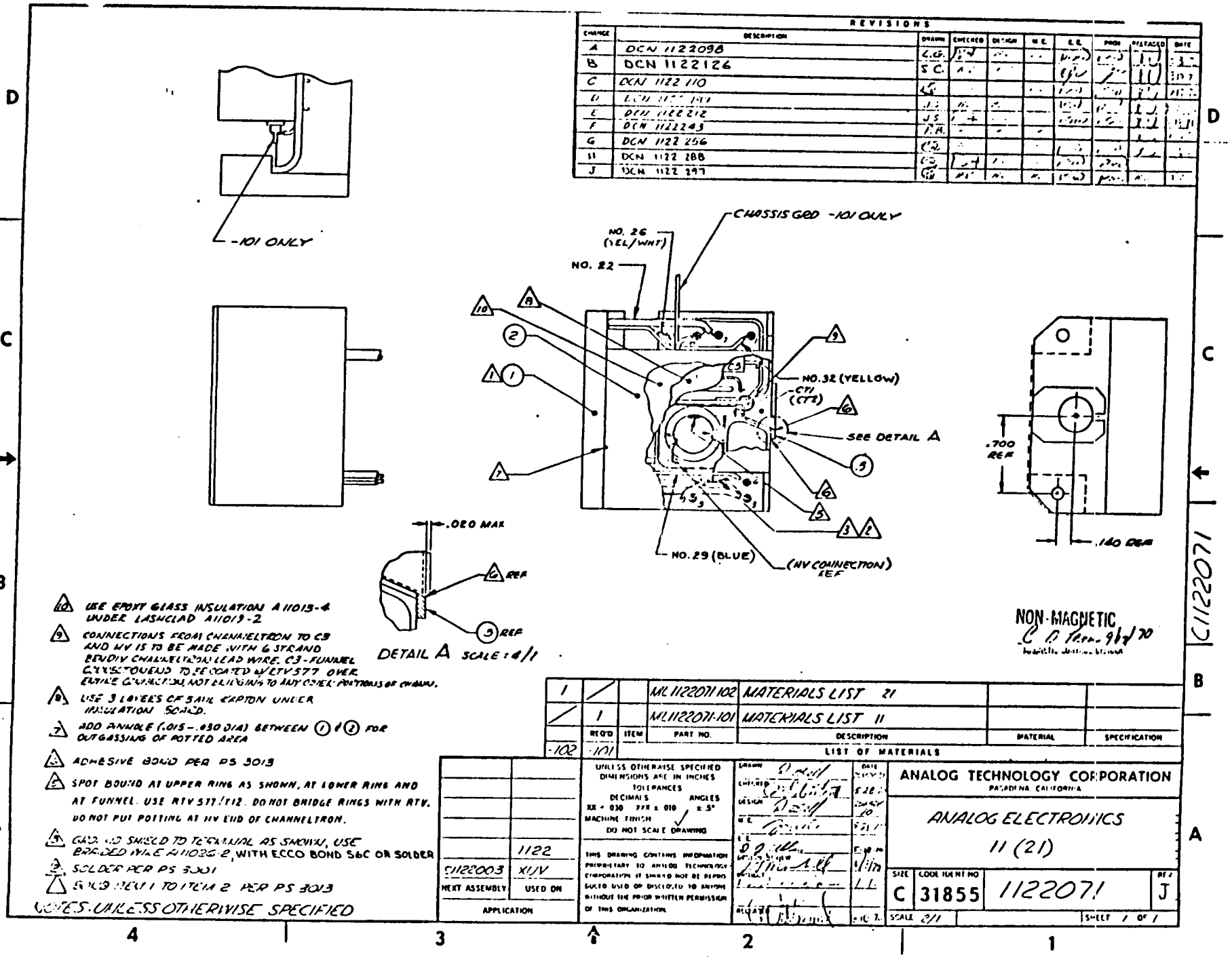
REVISIONS
CHANGE | DESCRIPTION | DRAWN | CHECKED | DESIGN | M.E. | E.E. | PROD | RELEASED | DATE
A | DCN 1122098 | C.G.
B | DCN 1122126 | S.C.
C | DCN 1122 110
F | DCN 1122243 | P.M.
G | DCN 1122 256
H | DCN 1122 288
J | DCN 1122 297
-101 ONLY
CHASSIS GND -101 ONLY
NO. 26 (YEL/WHT)
NO. 22
NO. 32 (YELLOW)
CTI (CTR)
SEE DETAIL A
NO. 29 (BLUE)
(HV CONNECTION) REF
.700 REF
.140 DIA
.060 MAX
DETAIL A SCALE: 4/1
NON-MAGNETIC
1. USE EPOXY GLASS INSULATION A11013-4 UNDER LASHCLAD A11019-2
2. CONNECTIONS FROM CHENNELTRON TO C3 AND HV IS TO BE MADE WITH 6 STRAND BEADIV CHANNELTRON LEAD WIRE. C3-FUNNEL CONNECTION END TO BE COATED W/ LTV 577 OVER ENTIRE CONNECTION, NOT CLINGING TO ANY OTHER PORTIONS OF CHANN.
3. USE 3 LAYERS OF 5 MIL KAPTON UNDER INSULATION BOARD.
4. ADD ANNULE (.015 - .030 DIA) BETWEEN 1 & 2 FOR OUTGASSING OF POTTED AREA
5. ADHESIVE BOND PER PS 3013
6. SPOT BOND AT UPPER RING AS SHOWN, AT LOWER RING AND AT FUNNEL. USE RTV 577/T12. DO NOT BRIDGE RINGS WITH RTV. DO NOT PUT POTTING AT HV END OF CHANNELTRON.
7. GND. TO SHIELD TO TERMINAL AS SHOWN, USE BRAIDED WIRE A11026-2, WITH ECCO BOND 56C OR SOLDER
8. SOLDER PER PS 3001
9. SOLID WIRE 1 TO ITEM 2 PER PS 3013
NOTES: UNLESS OTHERWISE SPECIFIED
1 | | | ML1122071-102 | MATERIALS LIST 21
| 1 | | ML1122071-101 | MATERIALS LIST 11
REQ'D | ITEM | PART NO. | DESCRIPTION | MATERIAL | SPECIFICATION
-102 | -101 | LIST OF MATERIALS
1122
S1122003 | X1V
NEXT ASSEMBLY | USED ON
APPLICATION
UNLESS OTHERWISE SPECIFIED DIMENSIONS ARE IN INCHES TOLERANCES DECIMALS .XX ± .030 .XXX ± .010 ANGLES ± .5° MACHINE FINISH ✓ DO NOT SCALE DRAWING
THIS DRAWING CONTAINS INFORMATION PROPRIETARY TO ANALOG TECHNOLOGY CORPORATION IT SHALL NOT BE REPRODUCED USED OR DISCLOSED TO ANYONE WITHOUT THE PRIOR WRITTEN PERMISSION OF THIS ORGANIZATION
DRAWN | CHECKED | DESIGN | M.E. | E.E. | MATERIALS | RELEASED
ANALOG TECHNOLOGY CORPORATION
PASADENA CALIFORNIA
ANALOG ELECTRONICS
11 (21)
SIZE C | CODE IDENT NO 31855 | 1122071 | REV J
SCALE 2/1 | SHEET 1 OF 1
1122071
4-9

Figure 4-6

REVISIONS									
CHANGE	DESCRIPTION	DRAWN	CHECKED	DESIGN	M.E.	E.E.	TEST	RELEASED	DATE
A	DCN 1122082	[illegible]	[illegible]	[illegible]		[illegible]	[illegible]	[illegible]	[illegible]
B	DCN 1122097	[illegible]	[illegible]	[illegible]		[illegible]	[illegible]	[illegible]	[illegible]
C	DCN 1122116	[illegible]	[illegible]	[illegible]		[illegible]	[illegible]	[illegible]	[illegible]
D	DCN 1122227	[illegible]	[illegible]	[illegible]		[illegible]	[illegible]	[illegible]	[illegible]
E	DCN 1122243	[illegible]	[illegible]	[illegible]		[illegible]	[illegible]	[illegible]	[illegible]
F	DCN 1122253	[illegible]	[illegible]	[illegible]		[illegible]	[illegible]	[illegible]	[illegible]

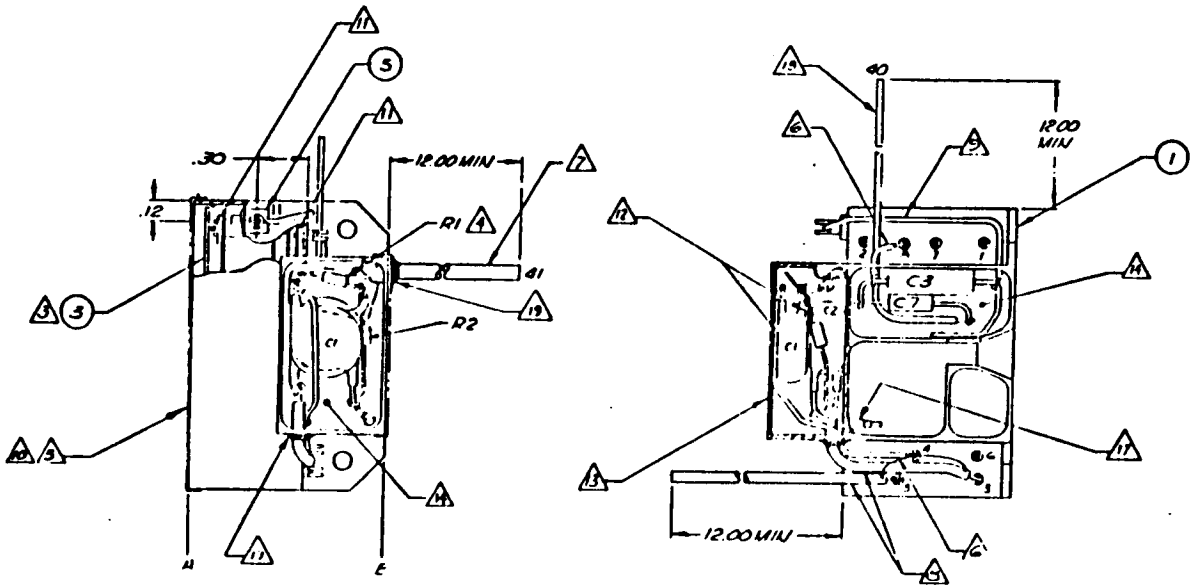

(17) USE ETCHED TEFLON SLEEVING A11010-18 OVER ETCHED TEFLON SLEEVING A11010-22

(14) POT WITH RTV-615 AFTER ELECTRICAL CHECKOUT.

(3) USE EPOXY GLASS INSULATION A11013-4

(5) USE TEFLON INSULATION A11022-5

(11) USE POLYURETHANE FOAM A11035-2

(4) USE LASHCLAD -CP A11019-2

(9) USE INSULATED WIRE A11003-26, WHITE

(6) USE SHIELDED WIRE A11007-26-1

(7) USE H.V. WIRE A11008-26

(6) USE INSULATED WIRE A11005-26, BLACK

(8) SHIELD CAVITIES ON SURFACES A & B PER MS 3018 AFTER ELECTRICAL CHECKOUT

(1) INSULATE R1 FROM LEAD 41 WITH A11022-5

(2) SPOT BOND PER M.I. 1122029

2 [illegible] SHIELDING SHALL BE AS SHOWN. FORM / SOLDER LEADS [illegible] CONNECTION OF LEAD WRAP IS OPTIONAL.

8 FOR SCHEMATIC SEE DWG NO. 1122090

NOTES: UNLESS OTHERWISE SPECIFIED

(19) SPOT BOND PER MS 3012. ETCH SURFACE BEFORE BONDING PER MS 3034.

(10) USE A11026-2 BRAIDED WIRE WITH A11010 ETCHED TEFLON SLEEVING, SIZE AS REQUIRED. SLEEVING MUST ENTER POTTED CAVITY.

NON-MAGNETIC

REQ'D	ITEM	PART NO	DESCRIPTION	MATERIAL	SPECIFICATION
		ML1122029	MATERIALS LIST		

LIST OF MATERIALS

	1122
C1122071	XUV
NEXT ASSEMBLY	USED ON
APPLICATION	

UNLESS OTHERWISE SPECIFIED DIMENSIONS ARE IN INCHES
TOLERANCES
DECIMALS .XX ± .03 .XXX ± .010
ANGLES ± 5°
MACHINE FINISH ✓
DO NOT SCALE DRAWING

THIS DRAWING CONTAINS INFORMATION PROPRIETARY TO ANALOG TECHNOLOGY CORPORATION. IT SHALL NOT BE REPRODUCED OR DISCLOSED TO ANYONE WITHOUT THE PRIOR WRITTEN PERMISSION OF THIS ORGANIZATION

DRAWN [illegible]
CHECKED [illegible]
DESIGN [illegible]
M.E. [illegible]
E.E. [illegible]
PROJECT [illegible]
RELEASED [illegible]

ANALOG TECHNOLOGY CORPORATION
PASADENA, CALIFORNIA

SENSOR, DECOUPLING, PREAMP

101

SIZE	CODE IDENT NO		REV
C	31855	1122029	F

SCALE 2/1 SHEET 1 OF 1

1122029

Figure 4-7

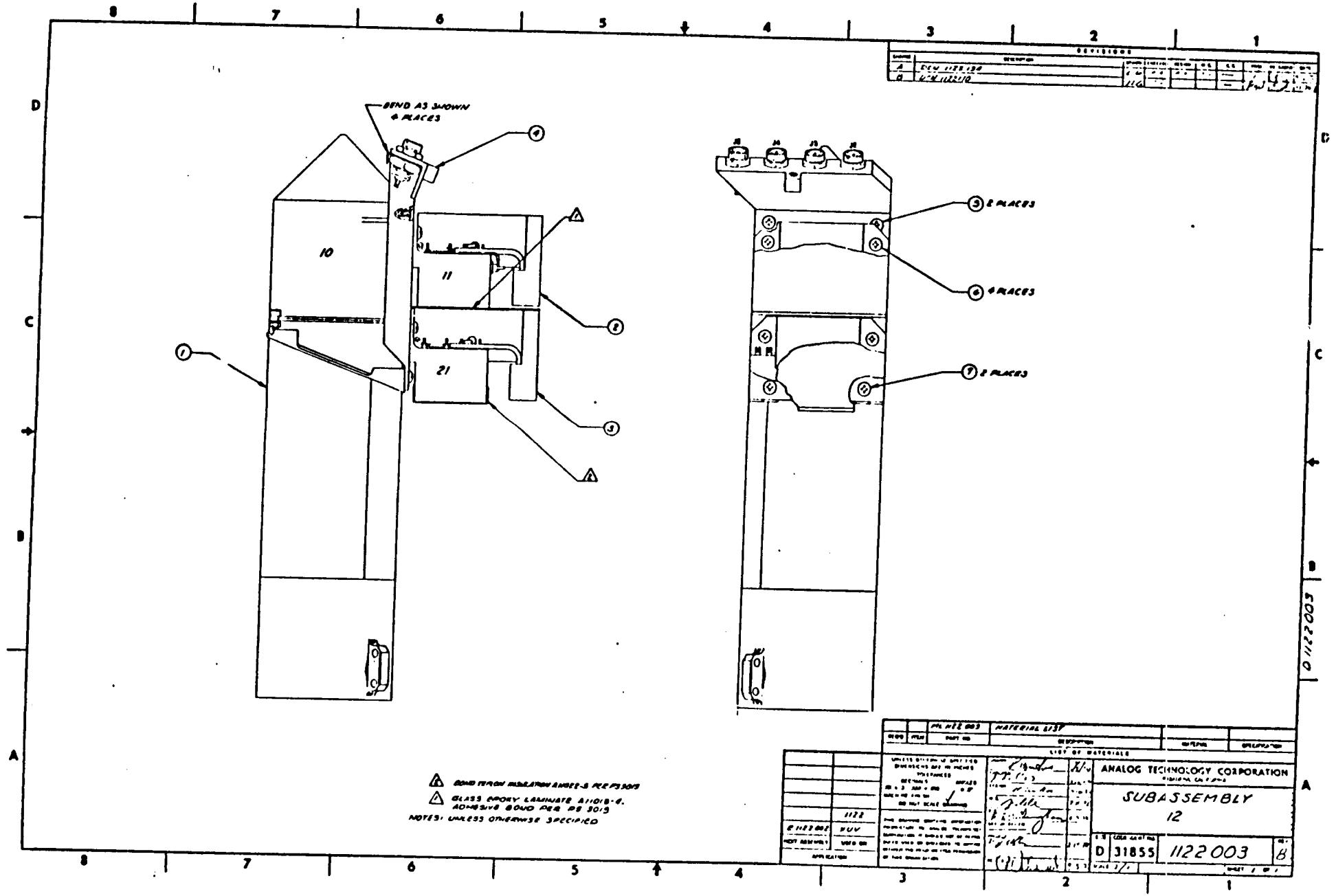
BEND AS SHOWN
4 PLACES
10
11
21
3 2 PLACES
6 4 PLACES
7 2 PLACES
ANALOG TECHNOLOGY CORPORATION
SUBASSEMBLY
12
D 31855 1122003 B

Figure 4-8

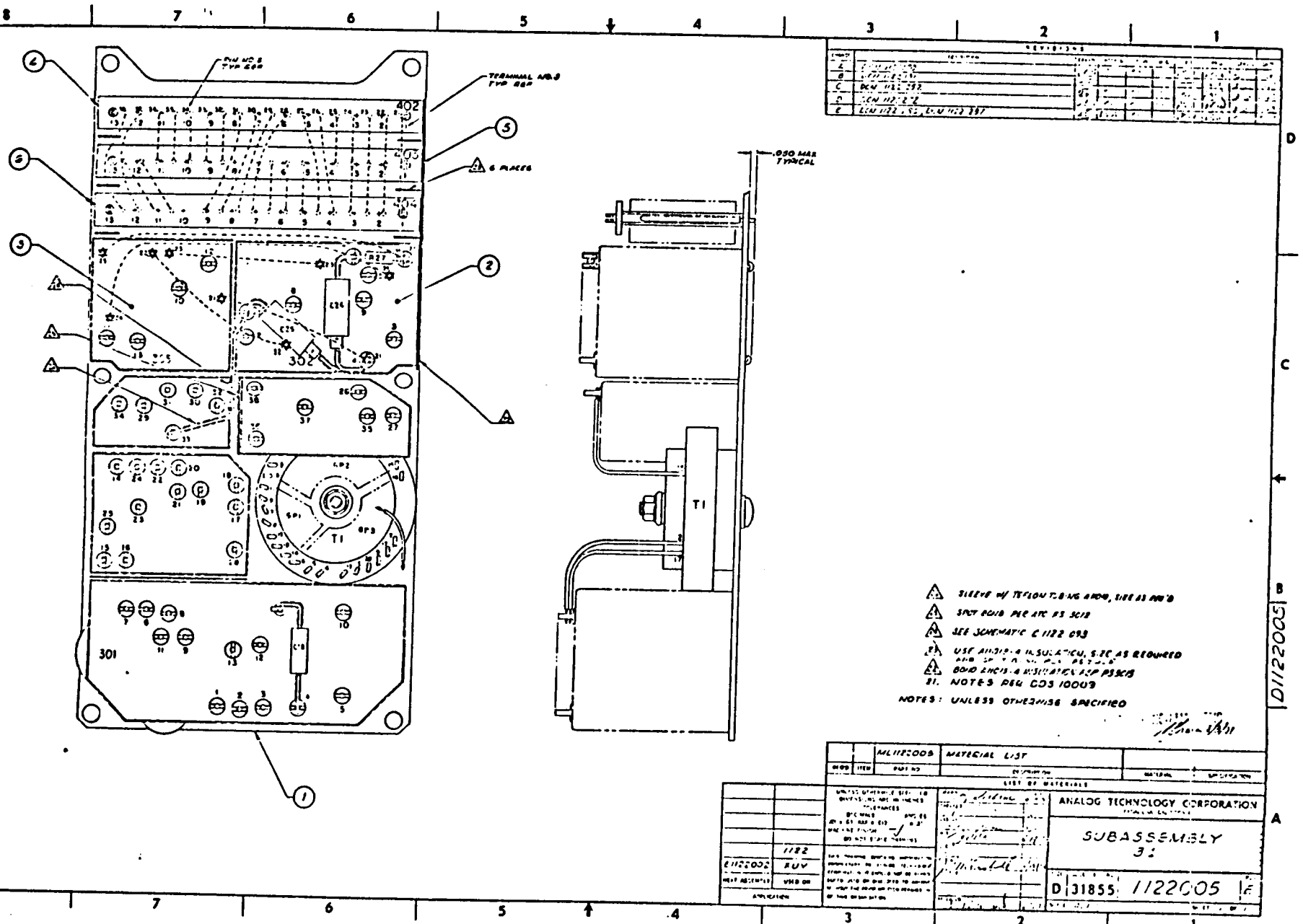
.050 MAX TYPICAL
T1
SUBASSEMBLY 31
ANALOG TECHNOLOGY CORPORATION
D 31855 1122005 E
D1122005

Figure 4 - 9

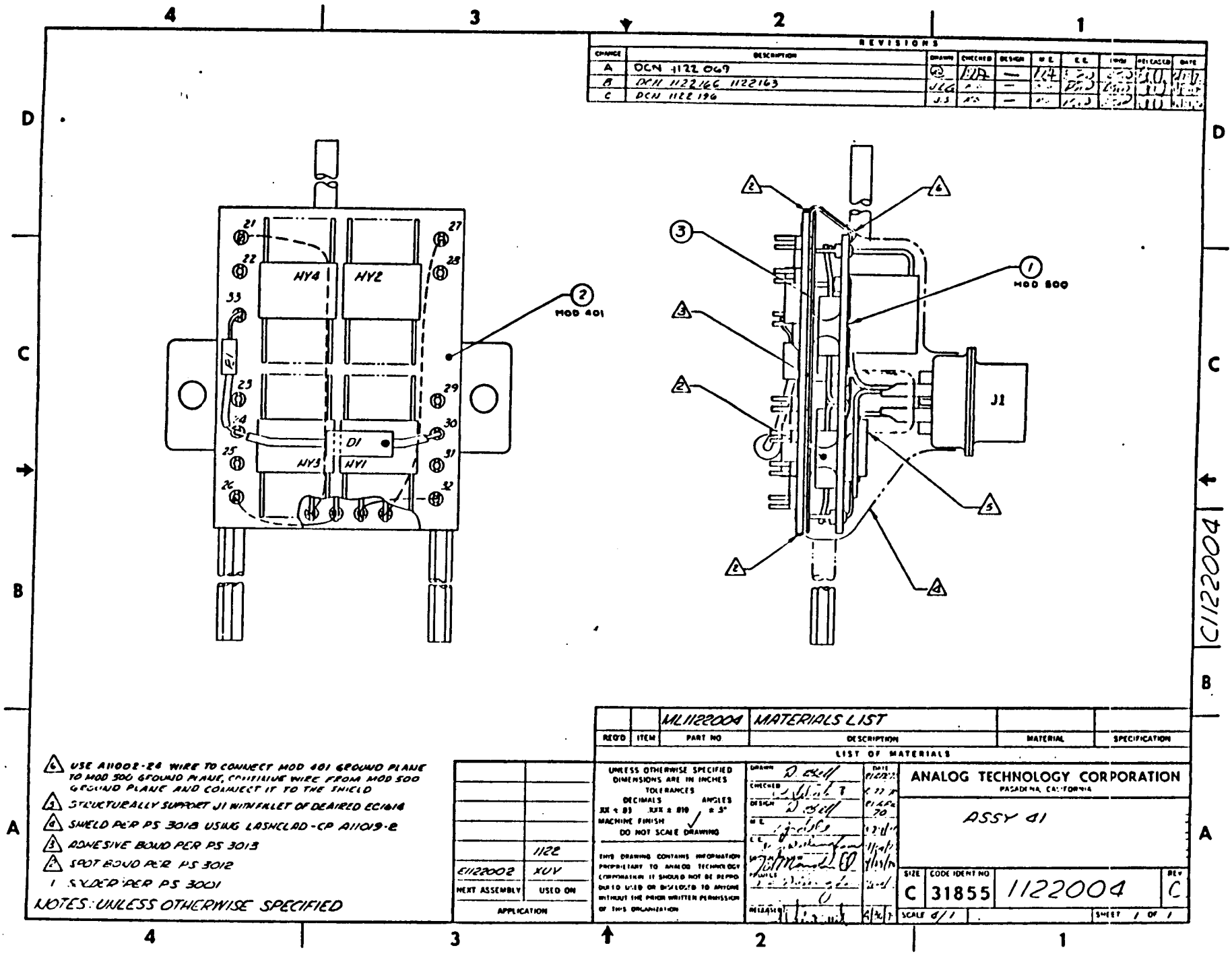
REVISIONS
CHANGE
DESCRIPTION
A
DCN 1122 069
B
DCN 1122166 1122163
C
DCN 11EE 196
HV4
HV2
HV3
HV1
D1
E1
MOD 401
MOD 500
J1
ML1122004
MATERIALS LIST
REQ'D
ITEM
PART NO
DESCRIPTION
MATERIAL
SPECIFICATION
LIST OF MATERIALS
6 USE A11008-24 WIRE TO CONNECT MOD 401 GROUND PLANE TO MOD 500 GROUND PLANE, CONTINUE WIRE FROM MOD 500 GROUND PLANE AND CONNECT IT TO THE SHIELD
5 STRUCTURALLY SUPPORT J1 WITH FILLET OF DEARIED EC1614
4 SHIELD PER PS 3018 USING LASHCLAD-CP A11019-8
3 ADHESIVE BOND PER PS 3013
2 SPOT BOND PER PS 3012
1 SOLDER PER PS 3001
NOTES: UNLESS OTHERWISE SPECIFIED
UNLESS OTHERWISE SPECIFIED DIMENSIONS ARE IN INCHES
TOLERANCES
DECIMALS
ANGLES
MACHINE FINISH
DO NOT SCALE DRAWING
THIS DRAWING CONTAINS INFORMATION PROPRIETARY TO ANALOG TECHNOLOGY CORPORATION. IT SHOULD NOT BE REPRODUCED, USED OR DISCLOSED TO ANYONE WITHOUT THE PRIOR WRITTEN PERMISSION OF THIS ORGANIZATION
DRAWN
CHECKED
DESIGN
M.E.
E.E.
PROJECT
RELEASED
ANALOG TECHNOLOGY CORPORATION
PASADENA, CALIFORNIA
ASSY 01
SIZE
CODE IDENT NO
C
31855
1122004
REV
C
SCALE 4/1
SHEET 1 OF 1
1122
E1122002
XUV
NEXT ASSEMBLY
USED ON
APPLICATION

Figure 4-10

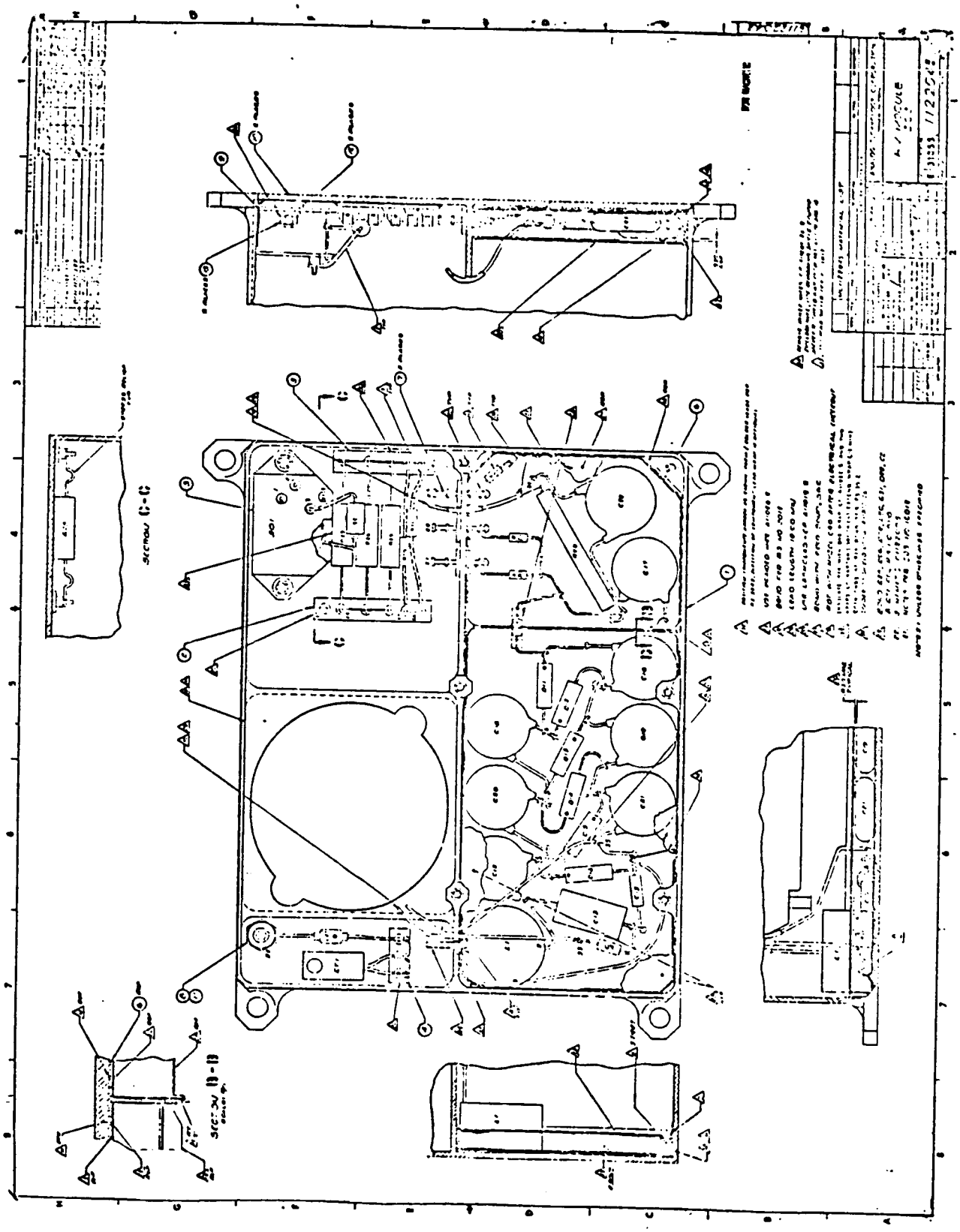

Figure 4 - 11

The same spurious noise effects have been noted upon insertion of the channeltrons. In particular, the spurious counting has been found to be sensitive to the potting material, the housing material, and surface cleanliness. The best results have been obtained by using Vespel housings (modified teflon) and silicone potting materials. The high-voltage lead to the channeltron through the housing wall is sleeved with teflon, and the channeltrons are spot-bonded in such a manner as to not bridge between the helical rings.

Careful cleaning of components and the housing, using 200-proof ethanol as a final step, is conducted prior to component potting. No cleaning is attempted after potting due to residual contamination that almost always results.

The preamplifier modules are of welded cordwood construction. Soldered planar board construction is used for the discriminator hybrid circuits and voltage decoupling elements.

Subassembly 12

No further comments.

Subassembly 31

The main motherboard assembly contains the soldered-cordwood PCU and high-voltage modules. To save weight, the motherboard is used as the base board for the PCU and contains separate ground plane segments and PC board conduction traces for the PCU circuits.

The logic elements are packaged on three sandwich boards. The details of this new packaging technique are given in Figure 4-12. These details are provided as a part of this document primarily because of their newness in design.

Subassembly 41

This assembly is potted directly to the input connector and utilizes stacked soldered planar board construction.

Subassembly 303

The high-voltage elements employ a freestanding, solidly-potted configuration that prevents sharp construction edges and reduces field strengths. Chassis-isolated metal cups are provided for the high-voltage multiplier and output decoupling components. These cups are returned to the local ground point and prevent high-voltage multiplier signals from coupling to the chassis. Soldered-cordwood construction is used for Piston Actuator Module 501.

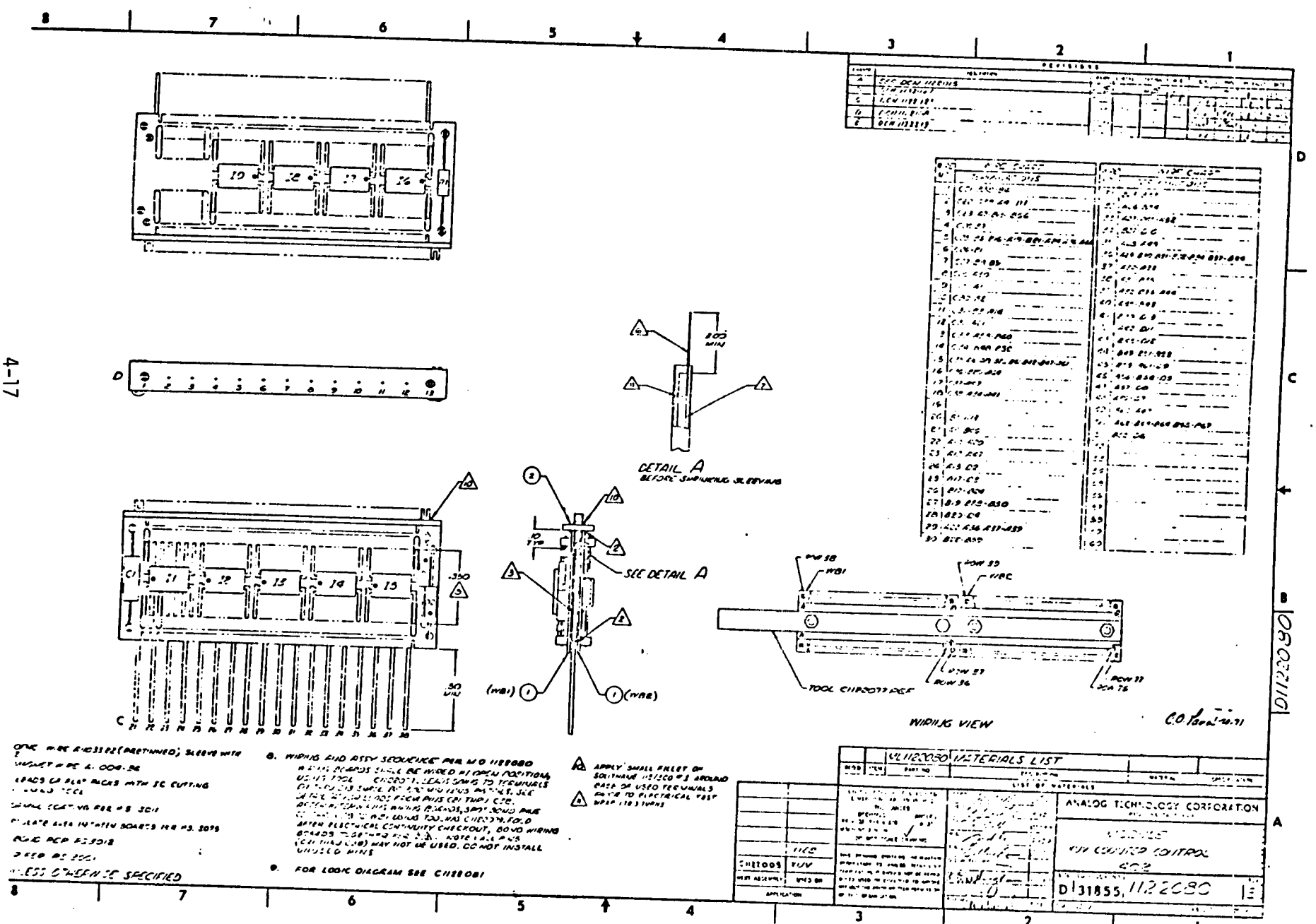
DETAIL A
BEFORE SHRINKING SLEEVING
SEE DETAIL A
WIRING VIEW
MATERIALS LIST
ANALOG TECHNOLOGY CORPORATION
D31855, 1122080

Figure 4 - 12

5.0 GROUND SUPPORT EQUIPMENT

The operation and function of the ground support equipment for the XUV Filter Photometer instrument are described in detail in another volume. For this reason, only a brief description of the GSE is presented here.

The XUV GSE is housed in two containers. The control panel unit is 20" x 20" x 15", and the digital recorder case is 20" x 20" x 9". The units weigh approximately 90 lbs. each.

The GSE operates over an ambient temperature of 0°C to 40°C with a relative humidity of up to 60%. The storage environment is -30°C to +65°C at 80% relative humidity. Power requirements are 115 Vac ±10%, 60 Hz ±1.0 Hz single phase. The GSE requires less than 500 W of power.

5.1 Control Panel

The control panel unit contains everything necessary to simulate the spacecraft interface. It is designed to detect any and all problems that may occur in order to prevent the failure of the XUV experiment in space. The control panel is shown in Figure 5-1.

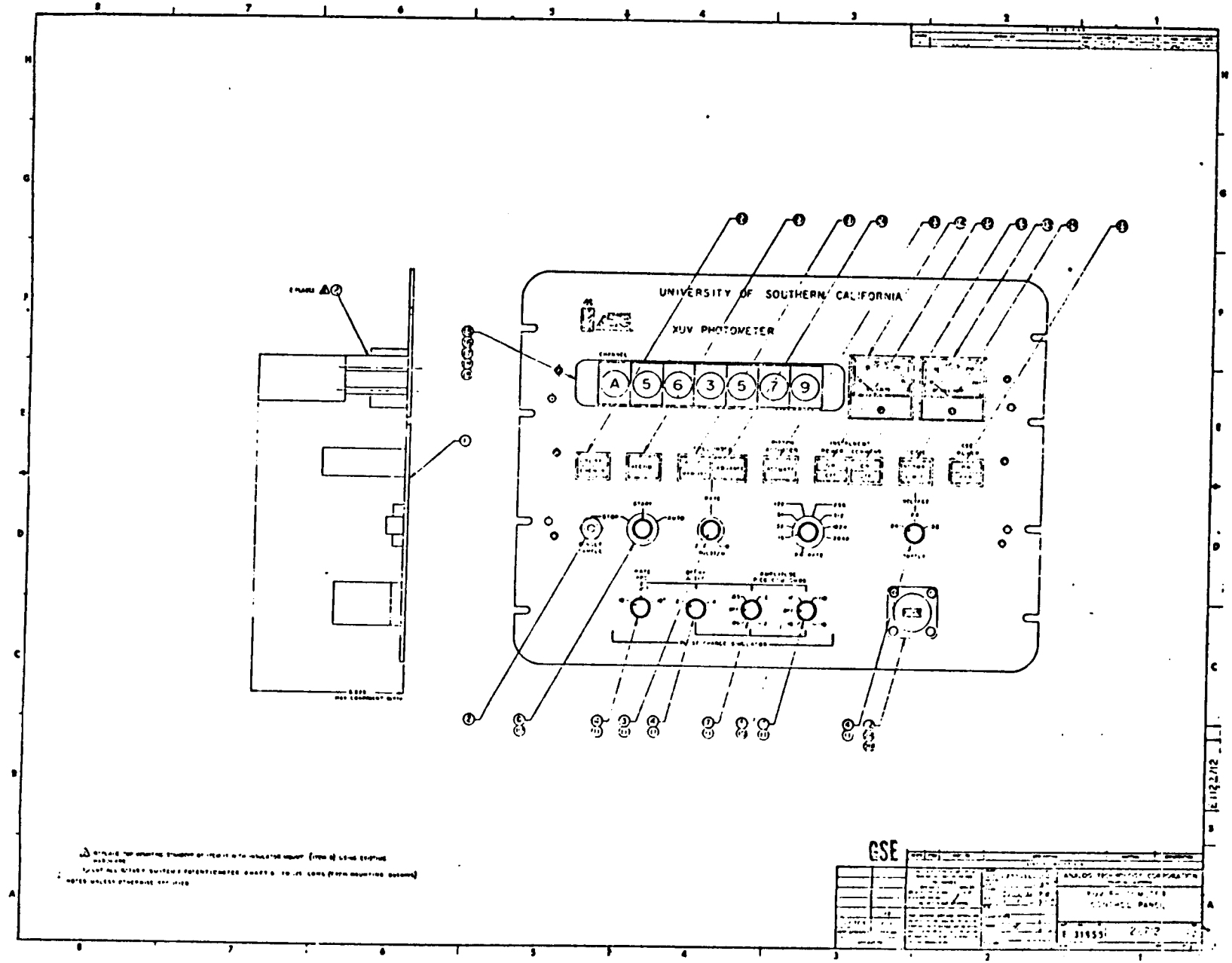
UNIVERSITY OF SOUTHERN CALIFORNIA
XUV PHOTOMETER
A 5 6 3 5 7 9
GSE

Figure 5-1

5.1.1 GSE Power

The GSE supplies the XUV instrument with 24, 28, or 32 V, which can be selected by setting the VOLTAGE-SUPPLY knob on the front panel. The normal operating mode is 28 V, which is monitored by means of the dc voltmeter located above the VOLTAGE-SUPPLY switch. The instrument power is turned on by activating the instrument POWER switch. This power is connected to the instrument but is not activated internally until the INSTRUMENT COMMAND switch is turned on. When the INSTRUMENT COMMAND switch is activated, the dc milliammeter shows the amount of current that the instrument is drawing. A typical amount would be 24 mA. If the instrument draws significantly more than this, the GSE may be immediately turned off by pushing the switch marked GSE POWER that is located on the far right of the panel. The elapsed-time meter, which is in the lower right hand corner, is activated only when the INSTRUMENT COMMAND switch is on. A true indication of the amount of time that the instrument is running is therefore given. Above the VOLTAGE SUPPLY switch is one marked NORMAL and LIMIT. In the NORMAL mode, the digital signals being supplied to the instrument have voltage levels of 4.5 V and 0.2 V. When the switch is in the LIMIT mode, the digital signals to the instrument have voltage levels of +3.5 V and +0.7 V.

5.1.2 Piston Actuator

The PISTON ACTUATOR ACTIVATE switch is a momentary type and works only when the INSTRUMENT COMMAND is off. When the ACTUATE button is pushed, the milliammeter should indicate 250+ mA. This shows that the piston actuator circuitry is working. When the ACTUATE button is released, the current should drop to zero.

5.1.3 Logic Simulator

The GSE performs the logic simulations that will be delivered to the instrument from the DTU. It sends such signals as word gate, phantom word gate, bit shift rate, and roll index. The bit shift rate is variable between 16 pps and 2048 pps in increments of power of two. The BIT RATE switch is located below the instrument power switches. The word gate and phantom word gate are a function of the BIT RATE. The roll index is controlled by three ROLL INDEX switches located in the middle of the panel. In the AUTO mode, the number of pulses per minute are controlled by the RATE knob. In the MANUAL mode, roll index pulses can be generated by pushing the ADVANCE button. If, for some reason, one wishes to advance the roll index while in the automatic mode, that may also be done. The GSE works normally in the CRUISE mode, which is indicated on the

switch located at the middle of the panel on the far left side. In this mode, it simulates format A as described in PC-213. In the ENCOUNTER mode, it simulates formats A and D alternately. Since the XUV Instrument is not interrogated by the spacecraft in Format D, the Encounter mode effectively divides the bit rate by 2.

5.1.4 Pulse Charge Simulator

The Pulse Charge Simulator is designed to send pulses of charge to the instrument so that the channeltron electronics can be tested. The electronics count the number of pulses that exceed threshold and that are not within the instrument dead time. By providing a known number of pulses in a given time period, the functioning of each channel and the corresponding logic can be verified. The PULSE CHARGE SIMULATOR RATE switch allows pulses of charge to be sent at the rate of 10, 1000, and 10,000 pulses per second (pps). The DELAY switch permits a second pulse to be delayed by 2 or 4 μs. When this switch is in the 2-μs position, the second pulse should not be registered since the instrument discriminator has a 3-μs dead time. There are two AMPLITUDE PICO COULOMB switches which control the amplitude of either the leading or delayed pulse. The amplitude of the delayed pulse is set when one of the two switches is in the lower half setting. The leading pulse amplitude is set by one of

the two switches having an upper half setting. The various amplitudes available are 0.05, 0.2, 10, and 110 pc. A calculable answer should be displayed for each combination of switch settings. These answers are listed in Table 5-1. Due to the marginal nature of the charge simulation, large second pulses of 10 and 110 pc sometimes cause second pulse counting when the delay is set both at 2 μs and 4 μs. Therefore, the delay pulse tests should be performed only with large pulses followed by small pulses.

5.1.5 Display

The display section handles the data that is accumulated in the instrument. The information is removed every time the word gate pulse is sent to the instrument. This occurs automatically when the DISPLAY MODE (3 position know) switch is in the AUTO position. The output display consists of six digits with channel A or B indicated to shown which channel is accumulating data. The display is a real number of base 10 and is a conversion of the instrument data per the formula given in Section 3.2. Data can be accumulated in the instrument for as long as desired by turning the MODE switch to STOP, and then pushing the SINGLE SAMPLE button. Rotating the mode switch to START deactivates the single SAMPLE switch to that the accumulation period cannot be accidentally stopped. When the MODE switch is returned to STOP and the SINGLE SAMPLE

Table 5-1a

Simulator Pulse Counts
GSE Pulse Rate, 10,000 pps

SIMULATOR SETTINGS			BIT RATE*	DISPLAY COUNTS	COMMENTS
LEADING PULSE	DELAY	TRAILING PULSE			
0.05 pC	---	OFF	512 bps	0000	Pulse amplitude 1/2 threshold
0.2 pC	---	OFF		3712	Pulse amplitude twice threshold
10 or 110 pC	---	OFF		3712	Full range and overload recovery test
10 to 110 pC	2 μs or 4 μs	0.05 pC		3712	Second pulse below threshold
10 or 110 pC	2 μs	0.2 pC		3712	Second pulse in dead time band and not observed
10 or 110 pC	4 μs	0.2 pC		7424	Second pulse out of dead time band and observed
0.05 pC	2 μs or 4 μs	10 or 110 pC		3712	First pulse below threshold and not observed
0.2 pC	2 μs**	10 or 110 pC		3712-7424	Should be 3712 with perfect simulation, but second pulse still right at threshold level at 3 μs after first pulse
0.2 pC	4 μs	10 or 110 pC		7424	Both pulses observed

* Display counts inversely proportional to bit rate.
** Marginal simulation due to pulse charge simulator.

Table 5-1b

Display Counts at Other
Bit Rates and Pulse Rates (Cruise Mode*)

Bit Rate		GSE-Simulator Pulse Rate** (pps)		
		10	10^3	10^4
Reference Table 5-1a	512	3-4	368	3712
	16	120	11776	118784
	32	60	5888	59392
	64	30	2944	29696
	128	15	1472	14848
	256	7-8	736	7424
	512	3-4	368	3712
	1024	1-2	184-188	1856
	2048	0-1	92-94	928

* Increase number by 2X for encounter mode.
** Increase number by 2X for double-pulse mode.

button is pushed, the data accumulated is read out and displayed. The actual accumulation time is the interval between pushings of the SINGLE SAMPLE button. The ACCUM light comes on only when the MODE switch is in the START position, but in fact, the accumulation begins as soon as the SAMPLE button is pushed.

5.2 Digital Recorder

The digital recorder records the data that is decoded from the instrument in order to verify that the instrument is detecting the correct number of pulses and that the instrument logic is counting in the right manner.

The data is printed out in eight columns, six of which are the number of counts accumulated during a data frame. The other two are for roll status and channel status as shown below.

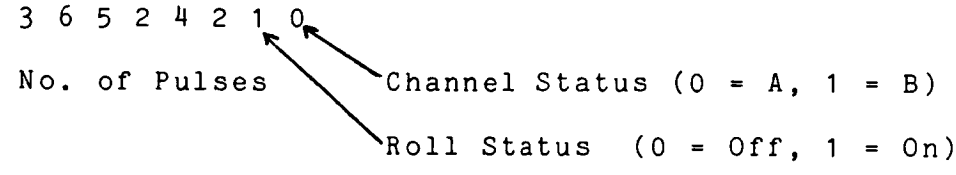

5.3 Cables and Connectors

The rear panel of the GSE has provisions for five connectors. J1 goes to the XUV instrument, J2 runs the pulse charge simulator, J3 is for the internal logic output, J4 is for the data output to the digital recorder, and J5 is the logic input to the GSE. In the normal operating mode, a short jumper cable is attached from J3 to J5. In the BENCH TEST MODE 3 as called out in PC-213, the jumper cable is removed and a cable from the DTU is attached to J5. Two sets of cables are provided. One is 6 feet long and used in the bench test mode. The second is 30 feet long and is for testing the instrument when it is installed in the spacecraft.

6.0 INSTRUMENT OPERATION AND MALFUNCTION DIAGNOSIS

The XUV instrument is essentially a single-connector device. The presence of spacecraft control signals at the spacecraft connector should be verified prior to instrument connection, even though the instrument is fault protected. The connector configuration is shown in Figure 2-3. If the instrument appears to be non operational, the GSE should be connected to the instrument and verification of display parameters should be checked prior to attempting to enter the instrument.

The GSE offers a means of artifically stimulating the entire electronics to provide known channel counts. In addition, current levels can be monitored, logic and supply voltage extremes can be applied, and the high-voltage and piston-actuator functions can be separately controlled.

If the above diagnostic methods indicate an instrument problem, maximum use of the connector information should be made by inserting a connector breakout box in the line. The connector signals are of a dc or digital nature and are easily monitored.

Finally, if the instrument cover must be lifted, the wiring diagram of Figure 4-4 can be used in conjunction with the individual circuit schematics to determine proper waveforms. Each terminal number on the wiring diagram is referenced and principal waveshapes are provided on the individual schematics. In some cases, such as the

discriminator outputs, leads are prewired to a module so that monitoring at the module is impossible. In these cases, the function can be observed at the termination end of the wire.

Because of the compact nature of the instrument and because many connections are embedded in potting material to prevent wire and terminal movement, ATC does not recommend that the customer perform this final diagnostic operation. If there is a malfunction, the instrument will, in all likelihood, be returned to ATC for repair. Thus, since the final diagnosis and extent of failure will have to be determined at ATC anyway, customer entrance into the instrument will be of little value and may well be harmful.

Table 6-1 lists a number of possible failures and how they may be diagnosed without entering the instrument.

Table 6-1.

Malfunction Diagnosis Chart

MALFUNCTION	POSSIBLE INSTRUMENT FAILURE	TEST METHOD
I. No channel A, B switching	Logic = Channel Switching; Input Buffers	1. Send manual Roll Advance commands from GSE. Switching should occur after two advance commands. 2. Monitor Roll Status and Channel Status with breakout box. Observe levels and changes upon applying manual Roll Advance commands. If dc levels are incorrect, logic has failed. If no change, logic or Roll Index buffer have failed.
II. No channel counts upon (out of vacuum) use of GSE stimulus	Analog Amplifier-Discriminator Failure; Logic Failure; PCU Failure; Input Buffer Failure; GSE Failure	1. Test each channel with test pulses from Pulse Charge Converter. If no data from either channel, a logic, buffer, or power failure is indicated. 2. Insure that pulser is operational (see GSE Manual) 3. (See Item IV)
III. No channel counts (in vacuum) with light source applied	Misalignment of Light Source; High-Voltage Failure; Channeltron Failure; Other Instrument Failure	1. Some background counts should occur (many more on channel A) if ion source is placed in chamber. If not, there is a channeltron, HV or other instrument failure. 2. If no counts on either channel, check for HV failure or other instrument failure (see items II, IV, V). 3. If counts only on channel A, make sure that previous data shows channel B counts. See item II. Consult experimenter on how to stimulate channel B.

Table 6-1 (continued)

MALFUNCTION	POSSIBLE INSTRUMENT FAILURE	TEST METHOD
III. (con't.)		4. If counts only on Channel B, channeltron A or channel A electronics has failure. See item II.
IV. Excess current (< 100 mA)	High-Voltage Failure; PCU Failure; Other circuit Failure	1. Install HV dearming connector. Observe for current reduction. 2. If still out of tolerance, there is probably an instrument short in PCU, logic buffers, or analog circuits. (Check items I and II also)
(> 100 mA)	Piston Actuator Circuit On or Input Line Short	1. Monitor Piston Actuate command to ensure it is low. 2. (Optional) Remove Actuator Shorting plug. This will fire the pistons if the Actuator circuit is still on. 3. If firing does not take place and excess current persists, an input line short probably exists.
V. High-voltage malfunction	HV Short, or HV Starting Failure	1. Insert HV dearming connector and note current reduction. Check reduction with previous data. If no reduction and current is less than normal, the HV has not started. 2. If current higher than normal with HV armed, a HV short may exist. (See item IV)

Table 6-1 (continued)

MALFUNCTION	POSSIBLE INSTRUMENT FAILURE	TEST METHOD
VI. No piston actuator firing	Incorrect Operation of GSE; Actuator Circuit Failure; Spent Pistons in place	1. Check to see if Instrument Power Command is off (this allows GSE to command firing). 2. Insert actuator shorting plug and perform firing. If GSE current meter indicates no current, then circuit has failed.

7. CURRENT SCIENTIFIC OBJECTIVES

(1) Extension of the filtered interplanetary hydrogen and helium resonance glow data to 27 A.U.

(2) Extension of the filtered interplanetary hydrogen and helium glow vs. clock angle and A.U.

(3) Re-examination and improvement of the Jovian environment data base with emphasis on the I_o torus data.

(4) a) Cross calibration with Voyager and possible absolute calibration using Star data and Interplanetary data.

b) Variability study of the two stars (δ - Cet and γ - Peg) viewed by both Pioneer 10 and Voyager.

(5) Extension of the star field map for hot stars (B type or hotter).

(6) An extended study of the effects of solar electron and proton heating of the inflowing interstellar gas.

(7) Determination of the radial velocity and spatial density distributions of the interplanetary gas as a base for determining:

a) Rate of absorption of solar lines by the interplanetary gas.

b) Line profiles and the intensity distribution of the scattered radiation along the direction outward of the solar system.

c) Attenuation of solar lines as the radiation

proceeds through interplanetary space.

(8) A review of the interplanetary model assumption that charge exchange produced hydrogen ionization removes, through Doppler shift, hydrogen Ly-α scattering within about 2 A.U. of the Sun.

FINAL REPORT

USC Extreme Ultraviolet Filter Photometer for the Pioneer F&G Spacecraft

NAS-205608, Subcontract 53085

Prepared for

Physics Department
University of Southern California
Los Angeles, California

31 August 1972

Analog Technology Corporation
3410 East Foothill Boulevard
Pasadena, California 91107

Frank L. Schutz
Project Manager

FOREWORD

Analog Technology Corporation is proud to have participated in the Ames Research Center's Pioneer F&G Spacecraft Program through a subcontract with the Physics Department of the University of Southern California.

We wish to thank the USC Principal Investigator, Dr. Darrell Judge, and his co-investigator, Dr. Robert Carlson, for the confidence they expressed in selecting ATC as their subcontractor. We have found them to be cooperative and to always act in the best interest of the instrument program. Mr. Arnold Welch, the USC Project Engineer, has been especially helpful in assisting ATC in environmental testing of the instruments.

We also wish to thank Mr. J. E. Lepetich, the Pioneer Program Scientific Instrument Manager, and Mr. Tom Wong, the XUV Scientific Instrument Manager, for their helpful suggestions and patience during some of the more hectic portions of the instrument development and testing. In particular, we are grateful for their assistance in providing the ARC Environmental Laboratory for our use. Mr. Wong was especially helpful in this regard and volunteered many hours of assistance both during and after the regularly scheduled testing periods.

INTRODUCTION

On August 1, 1969, Analog Technology Corporation (ATC) was selected by the University of Southern California as a subcontractor for the design, development, and fabrication of an Extreme Ultraviolet (XUV) Filter Photometer instrument for the Pioneer F and G missions to Jupiter. The first flight instrument is presently several months into its mission and has met all performance requirements. All contractually deliverable items, with the exception of this report which summarizes ATC's activities in fulfillment of the subcontract, have been prepared and shipped.

ATC is especially proud of its performance on the Pioneer Program since the XUV instrument is one of the few instruments to meet its original weight and power allocations. In fact, it required only 70% of its power allocation of one watt and weighed slightly less than its specified weight of 1.5 pounds.

The following sections briefly describe the purpose of the XUV instrument and provide details on ATC's hardware and financial performance. A later section discusses the special technical problems that were encountered and suggests methods for avoiding these types of problems in the designs of future instruments.

INSTRUMENT OBJECTIVES AND DESCRIPTION

Scientific Objectives

The XUV instrument was designed to measure extreme ultraviolet radiation at heliocentric distances of greater than one A.U. and, in the vicinity of the planet Jupiter, to provide answers to several problems concerning the solar wind, the interplanetary medium, and the atmosphere and magnetosphere of Jupiter. Successful completion of these measurements will enable the radius of the heliosphere (the distance from the sun to the solar wind transition region) to be determined by calculating the distribution of interplanetary hydrogen. The measurements will result from investigating the interaction of hydrogen with the solar wind, which is determined from observation of (1) the He II (303 A) resonance line resulting from the charge exchange reaction

$$He^{++} + H \rightarrow He^{+} (2P) + H^{+}$$

and (2) the strength of Lyman-alpha (Lα) (1216 A) radiation.

The ratio of hydrogen to helium in the Jovian atmosphere is to be determined through measurements of the neutral helium line at 584 A. This information will help to determine the temperature of the upper atmosphere of Jupiter and will further the development of theories pertaining to planetary formation and evolution. Finally, the instrument will determine the existence and location of the Jovian day-side auroral "oval," which will be useful in stating general auroral theories and in learning more about the Jovian magnetosphere.

Functional Description

Photographs of the XUV Filter Photometer are shown in Figure A; its primary specifications are listed in Table I. A functional block diagram of the instrument is presented in Figure B.

Incoming radiation is collimated by a field-of-view limiter and is incident on an aluminum filter with a pass band of 200 to 800 A. Photons passing through the filter are collected by a lithium-fluoride photocathode, which emits photoelectrons. Photoelectrons are also liberated from the front face of the filter by predominant Lyman-alpha radiation. The three spectral lines of interest are measured by two separate channeltron detectors and their associated pulse-handling circuits. In one channel, photoelectrons produced in the photocathode are electrostatically focused into the funnel-shaped cup of a channeltron multiplier. This channel, which monitors radiation in the filter pass band, is used to observe the 584-A and 303-A lines. The other channel, which also uses a channeltron multiplier, monitors photoelectrons released from the leading edge of the aluminum filter.

The charge pulse produced at the anode of each channeltron is amplified and shaped by a charge-sensitive amplifier. The resulting shaped pulse is then sent to a fixed-deadtime discriminator, which is biased to reject noise and to deliver standard pulses to the digital data-handling electronics.

Table I.

XUV FILTER PHOTOMETER INSTRUMENT SPECIFICATIONS

	ACTUAL (FOR THREE UNITS)	SPECIFICATION
Weight	1.5 lb ± 0.15 lb	1.5 lb
Power	0.67 W ± 0.03 W	1.0 W
Dimensions	3" x 4" x 5" (main chassis) with 1-3/4" diameter x 4" tubular collimator protrusion	
Data Storage	19 bits, compressed to 9 bits	
Data Output	9 bits per interrogation, 6-bit resolution	
Sensors	Bendix #4028 channeltrons (2)	
Spectral Sensitivity	Channel A - 1215 A (Lα) Channel B - 200 A to 800 A	
Field of View	1 degree x 14 degrees (FWHM)	
Electronics	Pulse Counting Electronics 3.7 kV high-voltage supply Low-Voltage Power-Conditioning Unit Compression-Storage Logic Piston Actuator-Dust Cover Remover System	

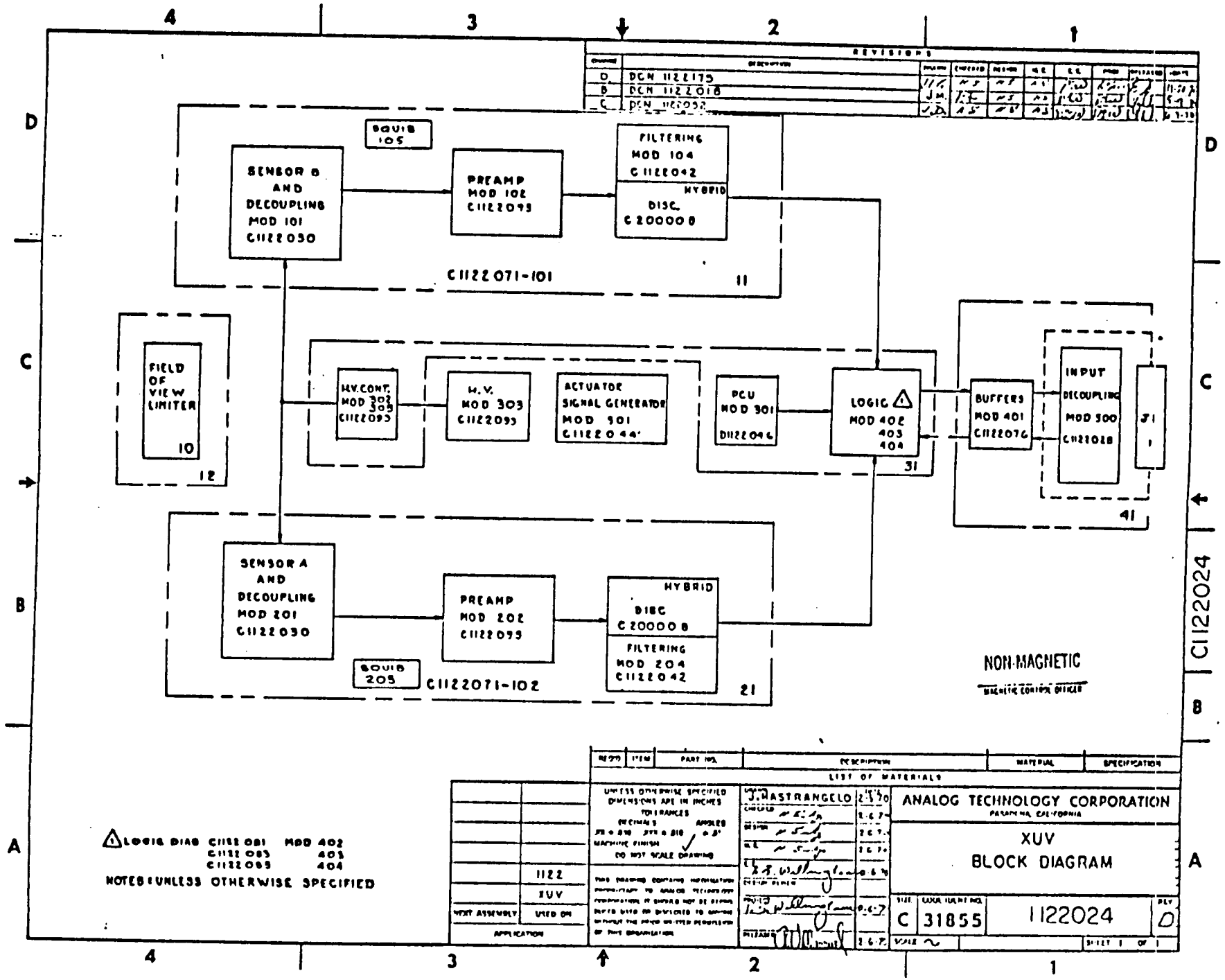
SQUID 105
SENSOR B AND DECOUPLING MOD 101 C1122030
PREAMP MOD 102 C1122095
FILTERING MOD 104 C1122042
HYBRID DISC. C200008
C1122071-101
11
FIELD OF VIEW LIMITER
10
12
H.V. CONT. MOD 302 305 C1122095
H.V. MOD 303 C1122095
ACTUATOR SIGNAL GENERATOR MOD 901 C1122044
PCU MOD 901 D1122046
LOGIC MOD 402 403 404
31
BUFFERS MOD 401 C1122076
INPUT DECOUPLING MOD 500 C1122028
41
SENSOR A AND DECOUPLING MOD 201 C1122030
PREAMP MOD 202 C1122095
HYBRID DISC C200008
FILTERING MOD 204 C1122042
SQUID 205
C1122071-102
21
NON-MAGNETIC
MAGNETIC CONTROL OFFICER
LOGIC DIAG C1122081 MOD 402
C1122083 403
C1122095 404
NOTES: UNLESS OTHERWISE SPECIFIED
REVISIONS
D DCN 1122175
B DCN 1122018
C DCN 1122052
LIST OF MATERIALS
ANALOG TECHNOLOGY CORPORATION
PASADENA, CALIFORNIA
XUV
BLOCK DIAGRAM
C 31855
1122024
D
C1122024

A-5

Figure B

Pulse data from the two channels is commutated into a single data-processing system. The instrument's digital data-processing electronics has as its principal function the compression of 19-bit data (required to linearly count pulses over a 10^5 dynamic range) into a 9-bit word suitable for telemetry transmission. The system used to accomplish this compression is the floating-point accumulator. This device transmits a 4-bit characteristic that describes the position of the most significant bit plus an additional 5 bits describing the second to sixth most significant bits. In this particular version of the floating-point accumulator, where the most significant bit is suppressed, the transmitted word, in effect, provides 6-bit quantizing resolution throughout the 10^5 dynamic range. In addition to the signal-processing electronics, the instrument also contains a programmer, a low-voltage regulated power supply, a high-voltage channeltron power supply, and a piston-actuated cover that protects the optical portions of the instrument until it is permanently released.

OFFICIAL ADDENDUMS

The documents listed in Table II form an official part of this report and represent the major documents previously delivered in performance of the XUV instrument subcontract. However, because of their previous delivery, these documents are not furnished as part of this report.

TABLE II. PREVIOUSLY DELIVERED DOCUMENTS

DOCUMENT	RELEASE DATE
PROPOSAL	
A Proposal for an Extreme Ultraviolet (XUV) Filter Photometer Experiment for Pioneer F&G	23 May 1969
Supplement to a Proposal for an Extreme Ultraviolet (XUV) Filter Photometer Experiment for Pioneer F&G	3 Jul 1969
INSTRUMENT AND GSE MANUALS	
Instrument Description	20 Nov 1970
Revision A	15 Mar 1971
Revision B	31 Mar 1972
Ground Support Equipment Operations Manual	29 Dec 1970
Revision A	15 Mar 1971
Revision B	31 Mar 1972
PRODUCT PLANS AND QUALITY ASSURANCE ANALYSES	
Instrument Development Plan	26 Nov 1969
Product Assurance Plan	10 Dec 1969
Reliability Prediction and Parts Application Analysis	2 Dec 1970
Failure Mode, Effects, and Criticality Analysis	11 May 1971
TESTING REPORTS	
Design Verification Unit Qualification Testing Report	1 Mar 1971
Interim Report, XUV Channeltron Testing Program	2 Apr 1971
Prototype Unit Acceptance Test Report	28 Apr 1971
Flight Unit 1 Acceptance Test Report	1 Sep 1971
Flight Unit 2 Acceptance Test Report	Jun 1972
Refurbished Prototype Acceptance Test Report	Jul 1972
DATA PACKAGES	
Conceptual Design Review Data Package	26 Sep 1969
Preliminary Design Review Data Package	31 Dec 1969
Data Package for Flight Unit 1	7 Sep 1971
Data Package for Flight Unit 2	Jun 1972
Data Package for the Refurbished Prototype	Jul 1972

PERFORMANCE SUMMARY

Project Team

The Project Manager throughout the contract period was Donald E. Willingham. During the design phases and continuing through to the completion of the Design Verification Unit, Mr. David Allen functioned as the Project Engineer. This position was eliminated in December 1970 because of decreased program requirements.

In the design phases additional engineers were active on the project: Mr. Lauren Merritt designed the Power Conditioning Unit (PCU) and the high-voltage circuits; Mr. Willingham and Mr. Allen were responsible for the discriminator and preamplifier designs; Mr. Ted Dillingham designed the logic subsystem; the Ground Support Equipment was designed by Mr. Ross Gorgone under the direction of Mr. Tim Harrington; and Dr. Howard Marshall, Vice President - Technical of ATC, acted as chairman of the ATC Instrument Design Review Committee.

Hardware Performance

Figure C provides a summary graph for the complete XUV program, indicating the major program milestones.

During the design phase, the principal problems

mechanical design of the instrument was delayed slightly because of vendor approval problems that required a change in vendors and in packaging. Also, initial use of a magnesium chassis resulted in corrosion through the special copper-silver-gold plating. This problem was eliminated by converting to aluminum for the chassis.

The design and packaging of a dust cover removal system proved to be more difficult than anticipated. This system had not been originally included (at least to the extent required to solve the problem) in ATC's weight estimate or pricing, but was technically within the contractual requirements.

Compared to the problems mentioned previously, the most annoying problem that developed was noise background counts occurring at the channeltron sensors. This problem was partially resolved through the use of silicone potting materials. Any form of polymer or carbon compound materials was found to be detrimental to the instrument operation; in addition, 200-proof ethyl alcohol had to be used for cleaning. Finally, the housing material was converted to Vespel from fiberglass. However, this conversion did not occur until after the prototype was fabricated, since passable sensor-housing combinations had been found for the DVU.

The prototype acceptance tests indicated that the high voltage was arcing and that there was a system oscillation problem. These two problems were quickly solved and the instrument performed well. However, the acceptance tests for Flight Units 1 and 2 and for the Refurbished Prototype were

not so easily accomplished. A variety of problems in the channeltron sensor areas caused considerable difficulties throughout all of these tests. Details of the problems encountered by each unit can be found in the individual acceptance test reports.

Each instrument passed all the acceptance test criteria as well as exceeding specifications in most areas. The problems that were encountered could, in general, be attributed to the exceptionally tight packaging required by the rigid weight and volume specifications. After completion of the prototype acceptance tests, no significant electrical design changes were required. This indicates the design adequacy of the XUV instruments.

Financial Performance

The initial contract value for the XUV instrument development, design, fabrication, testing, field support, and documentation was $386,230. Through various change-in-scope items, including the Prototype Instrument refurbishment and several design changes, the final in-scope contract value (as of this report) was $487,736. As of July 1, 1972, the estimated final value is at a point in the contract at which all hardward items have been delivered and at which only nominal future support is anticipated.

Table III presents the change proposal values that have been negotiated to date, and Table IV presents a summary of

each change.

The principal sources of overrun in the program were caused by technical problems that would have been difficult to anticipate. These problems are grouped into three main categories:

1. Systems problems due to circuit interactions.
2. Manufacture and repair problems resulting from the extremely tight mechanical packaging configuration.
3. Sensor screening rejection rates and background noise.

The first category caused delays in the completion of the initial acceptance tests in the Prototype and Flight 1 instruments due primarily to the PCU response to input voltage transients. Category 2 then compounded the analysis and repair problems, since each repair attempt resulted in a major dismantling of the instrument. The tight packaging also created several conditions in which high-voltage breakdown occurred after serveral days of thermal vacuum testing. The sensor problems resulted in a 70% rejection ratio during the screening and assembly processes. Some sensors passed initial screening tests, but were found to exhibit background noise problems when installed in the instrument. Considerable time was spent in refining material selection and assembly procedures to reduce the background noise effects. Significantly, it is noted that these noise problems seemed to be especially prominent with the particular type channeltron

TABLE III

NEGOTIATED CHANGE PROPOSAL VALUES VS. CONTRACT COST

Change Proposals		1 thru 4	5 thru 8	9	10 thru 13	14	15 thru 17	21 (10/5/71 letter)	18 (Proto) Refurb)	19 (Accept. Test Supt.at ARC) Add on to Change 13	22 & 23 (Fit & Test Overruns & Overhead Changes)	20 (Additional Piston Actuators)	24 & 25
Original Contract	357,620												
Change In Scope		41,667	6,779	-0-	24,814	-0-	2,159	-0-	13,774	3,068	-0-	2,328	-0-
Fee Increment		3,333	(108)	-0-	1,985	-0-	173	-0-	1,102	246	-0-	186	-0-
Overrun		-0-	-0-	75,579	-0-	62,527	-0-	43,198	-0-	-0-	14,241	-0-	14,125
Change Proposal Total		45,000	6,671	75,579	26,799	62,527	2,332	43,198	14,876	3,314	14,241	2,514	14,125
Total In Scope Value		399,287	406,066	406,066	430,880	430,880	433,039	433,039	446,813	449,881	449,881	452,209	452,209
Total Fee	28,610	31,943	31,835	31,835	33,820	33,820	33,993	33,993	35,095	35,341	35,341	35,527	35,527
Total In Scope Cost + Fee		431,230	437,901	437,901	464,700	464,700	467,032	467,032	481,908	485,222	485,222	487,736	487,736
Total Overrun		-0-	-0-	75,579	75,579	138,106	138,106	181,304	181,304	181,304	195,545	195,545	209,670
Total Contract	386,230	431,230	437,901	513,480	540,279	602,806	605,138	648,336	663,212	666,526	680,767	683,521	697,406
% Overrun		-0-	-0-	14.7%	14%	22.9%	22.8%	28%	27.4%	27.2%	28.7%	28.5%	30%

Table IV. CHANGE PROPOSAL SUMMARY

Change Proposal Number	Type	Description
1	Scope	Additional costs incurred due to extended parts approval cycle.
2	Scope	Untimely disapproval of hybrid circuit vendor, which caused program delays and mechanical redesign.
3	Scope	Revision of Field-of-View Limiter.
4	Non-Fee Bearing	Redesign of piston actuator plug-in assembly.
5	Scope	Addition of purge fitting to instrument.
6	Scope	Increased polishing requirement for photo-cathode.
7	Scope	Incurred costs in locating environmental facilities due to increased testing requirements.
8	Non-Fee Bearing	Modification of GSE containers due to drawing errors.
9	Overrun Anal.	Analysis of breadboard phase overruns and G&A adjustments (reduction).
10	Scope	Procurement of spare piston actuators for dust cover removal system.
11	Scope	Addition of collar ring to field-of-view limiter.
12	Scope	Redesign of PistonActuator Signal Generator Circuit to preclude S/C interface problem.
13	Scope	Additional acceptance testing support required at ARC.
14	Overrun Anal.	Prototype overruns and increased G&A expenses.
15	Scope	Redesign of Piston Actuator Signal Generator Circuit to preclude S/C interface problem (second redesign).
16	Scope	Additional piston actuator procurements.
17	Scope	Additional photographs of the instrument.
18	Scope	Prototype refurbishment.
19	Scope	Modification of Change 13 due to increased testing time.
20	Scope	Additional piston actuator and dust cover purchases.
21	Overrun Anal.	Flight Unit 2 overrun cost analysis.
22	Overrun Anal.	Flight Unit 2 acceptance test overrun analysis.
23	Adjustment	G&A variance billing.
24 & 25	Overrun Anal.	Refurbished prototype acceptance testing modification overrun, and general contract continuation overrun.

used in the XUV instrument. In another ATC program which used essentially identical manufacturing and packaging techniques, and which was in process during the same period as the XUV program, none of these noise behavior problems were encountered. The only difference between the two systems was the type of channeltron used.

Another factor that contributed to the projected overrun was ATC's attempt to present carefully justified change-in-scope estimates. A good example of this is the Prototype Refurbishment. Change No. 18 contained an estimate that the refurbishment cost of the Prototype would be $14,876; this was considered a fair and reasonable estimate for the anticipatd work and the modification was performed as anticipated. However, during the reacceptance testing, sensor failures were encountered. Since the sensors were not even remotely associated with the rework areas, sensor failures were not anticipated. The extensive reword involved in this area is reflected in overrun changes 24 and 25.

Other principal overrun factors were attributable to early developmental phase problems. ATC did not fully anticipate the impact that the dust cover removal system would have on the overall system design with respect to packaging density and cost. Unfortunately, this item was included in the original contract as an ATC responsibility should such a system be required at later date.

Other problems that resulted in modest cost increases included:

1. Magnesium plating problems that forced a late change to an aluminum chassis.
2. Hybrid circuit vendor problems that ultimately required a discrete preamplifier package and a larger discriminator hybrid package than had been anticipated.

These are only a few of the problems that were encountered during the program. However, even with the circuit, chassis, and packaging changes, ATC was able to meet the original weight and power specifications.

TECHNICAL RECOMMENDATIONS

Most of the systems and packaging problems experienced with the XUV instrument were directly associated with the requirements and characteristics of the instrument. This is especially true of the packaging density and the manufacturing problems associated with dense packaging. Consequently, no specific technical design recommendations are made in this area other than the strong recommendation that packaging densities of the order required for the XUV instrument be avoided whenever possible.

With respect to sensor selection and packaging, it is important to note that the Bendix #4028 channeltrons are especially susceptible to noise discharges, a fact that

seemed to be little understood or believed by the manufacturer. There is great variability in noise background from sensor to sensor that appears to be independent of any other parameters (as evidenced by our use of several channeltrons in the same packaging subassembly). Similar noise counting problems have been experienced with other types of channeltrons, but these problems were usually traceable to factors other than the sensors themselves. In this regard, we have found that the coupling and high-voltage filtering elements must be potted in non-polymeric materials such as the silicone derivative potting compounds. We found also that the housing for both these elements and the channeltron should be made of a teflon type material. We used Vespel for the XUV channeltron-filtering housings, which worked quite well. The problem with Vespel, however, is that there is a plating problem involving adherence of the plating to the Vespel material. We also found that minimum potting should be used around the sensors and that cleaning them with anything but 200-proof ethyl alcohol resulted in excessive counting problems. It should be noted, that although severe problems were encountered in handling the sensors, each of the XUV instruments eventually performed with noise counting rates of less than 0.1 counts/second, a performance level clearly within the instrument's design constraints.

Other programs at ATC have used the Bendix No. 1141 channeltron very successfully without encountering the severe noise problems that were evidenced with the XUV instrument.

INSTRUMENT PERFORMANCE

The first XUV Flight Unit was launched on the Pioneer 10 spacecraft on March 1, 1972 and is functioning as designed. In the interplanetary portion of the mission, the hydrogen channel data is of principal value. As the spacecraft spins, the instrument field-of-view rotates in and out of the plane of the ecliptic, viewing the neutral hydrogen flux from its position in space and moving in a generally outward direction from the sun. Peaks in hydrogen flux were expected as the instrument rotated through the ecliptic plane. Two ecliptic plane viewing directions are achieved as the spacecraft moves the instrument field-of-view through its cycle. These view were selected by the experimenters such that the flux measured in one would be much greater than that measured in the other.

As shown in Figure D, the Pioneer 10 XUV data yield one large peak per spacecraft revolution. Upon close inspection of the data, one can imagine a smaller peak centered between the two large peaks shown, but without adequate statistical data it would be difficult to fit an accurate curve to these data.

The instrument is performing as designed, and ATC expects that the insrument will provide valuable data throughout the Pioneer 10 Mission.

The second instrument has been installed on the Pioneer G spacecraft, which will be launched in 1973.

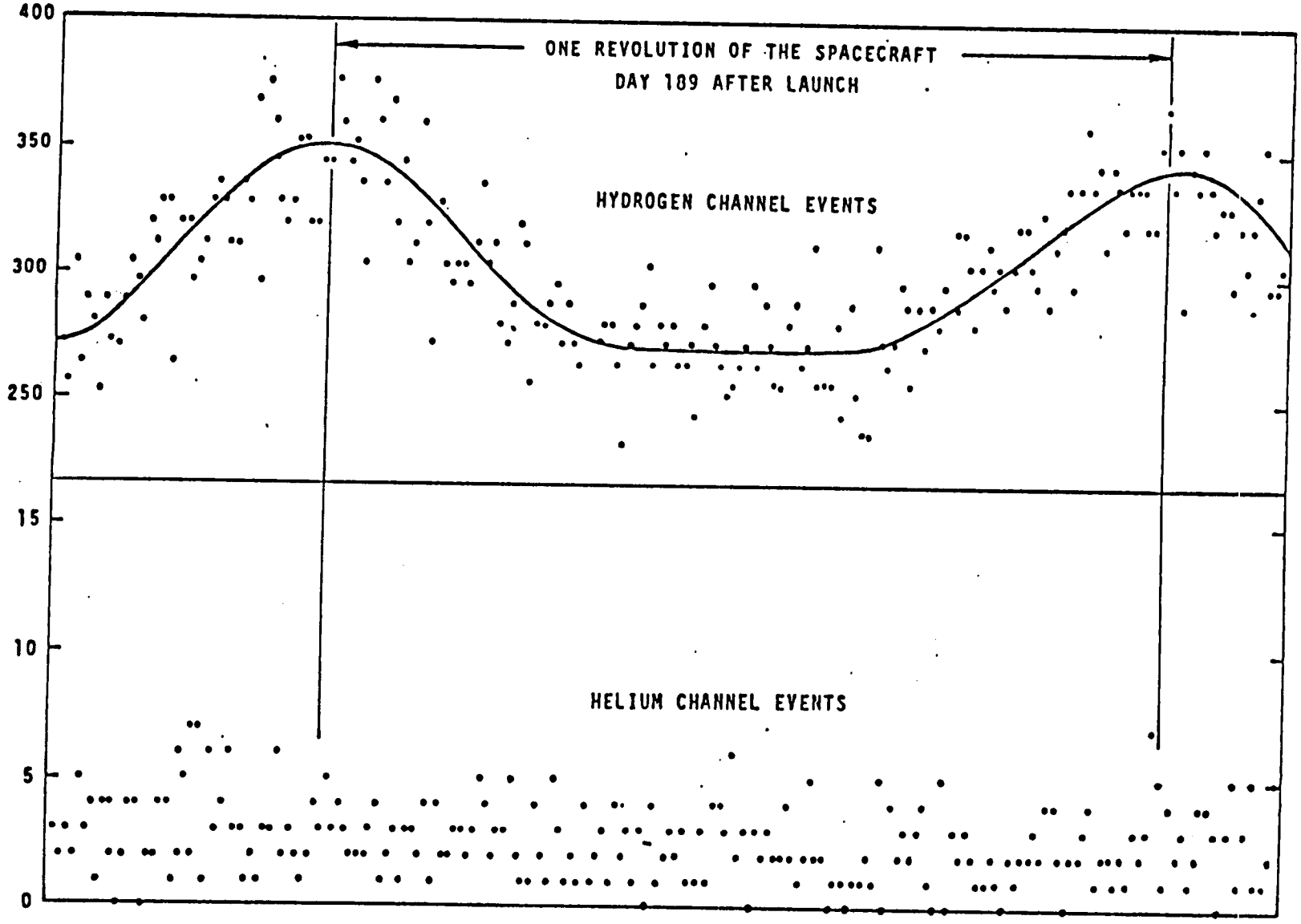

Figure D. Data from Pioneer 10 Filter Photometer